RADalrymple

NUMERICAL MODELS FOR THE PREDICTION OF WAVE SET-UP AND NEARSHORE CIRCULATION

by
William A. Birkemeier
and
Robert A. Dalrymple

Technical Report No. 1
Contract No. N0014-76-C-0342
with the OFFICE OF NAVAL RESEARCH GEOGRAPHY PROGRAMS

Ocean Engineering Report No. 3

January 1976

Department of Civil Engineering
University of Delaware
Newark, Delaware

NUMERICAL MODELS FOR THE PREDICTION OF WAVE SET-UP AND NEARSHORE CIRCULATION

BY

William A. Birkemeier

and

Robert A. Dalrymple

OCEAN ENGINEERING TECHNICAL REPORT NO. 3

Supported by ONR Contract Number N0014-76-C-0342

ONR Geography Programs

January, 1976

TABLE OF CONTENTS

LIST OF FIGURES

KEY TO SYMBOLS AND ABBREVIATIONS

a	wave amplitude
$a(m)$	slope dependent quantity defined Equation 2.70
A	Wave height variation amplitude Equation 4.2
A	Amplitude of bottom variation Equation 4.3
$A_{i,j}$	Quantity defined Equation 2.44
b	wave breaking parameter; bottom parameter
$b(m)$	Slope dependent quantity defined Equation 2.71
$B_{i,j}$	Quantity defined Equation 3.13
BBC	Bottom Boundary Condition
C	Wave celerity
C_g	Wave group velocity
C_f	Bottom Friction Coefficient
D	Total depth
$\overline{D}$	Average depth between two grids
E	Wave energy
$f(k)$	A function of the wave number
$f'(k)$	Derivative of $f(k)$
FTFS	Forward Time Forward Space Differencing
g	Acceleration of gravity
h	Depth from MWL to bottom
H	Wave height
H_o	Deepwater wave height

Key to Symbols and Abbreviations (continued)

H_s	Starting wave height
i	Grid index x direction
$\hat{i}$	Unit vector x direction
j	Grid index y direction
$\hat{j}$	Unit vector y direction
k	Time step index
k	Wave number
$\vec{k}$	Wave number vector
$\hat{k}$	Unit vector z direction
K	Van Dorn wind stress coefficient
KFSBC	Kinematic Free Surface Boundary Condition
ℓ	Length of the basin
L	Wave length
L.H.S.	Left hand side of equation
m	Beach slope
M	Number of grids in x direction
MWL	Mean water level
M_x	Mass flux due to waves x direction
M_y	Mass flux due to waves y direction
$\tilde{M}_x$	Mean total mass flux, x direction
$\tilde{M}_y$	Mean total mass flux, y direction
n	Integer; ratio of wave celerity to group velocity
$\vec{n}$	Unit vector perpendicular to the bottom
N	Number of grids in y direction

Key to Symbols and Abbreviations (continued)

P	Pressure
Q	Quantity defined by Equation 3.22; arbitrary quantity
R.H.S.	Right hand side of equation
S_{xx}, S_{xy}, S_{yy}	Directional radiation stresses
t	Time
T	Wave period
T_s	Seich period
T_g	Period of wave group
u	Instantaneous velocity x direction
$\vec{u}$	General velocity vector
$\overline{u}$	Time average velocity, x direction
u'	Fluctuating velocity due to the waves, x direction
U	Mass transport velocity, x direction
v	Instantaneous velocity, y direction
$\overline{v}$	Time average velocity, y direction
v'	Fluctuating velocity, due to the wave, y direction
V	Mean transport velocity, y direction
w	Instantaneous velocity, z direction
W	Wind speed
x, y, z	Coordinate directions
α	Wind angle

Key to Symbols and Abbreviations (continued)

β	Angle of channel to beach normal, Equation 4.3
Δx	Grid length, x direction
Δy	Grid length, y direction
Δt	Time step length
η	Instantaneous water level elevation
$\bar{\eta}$	Mean water level set-up or set-down
θ	Wave direction
λ	Periodic beach length
ρ	Density of water
σ	non-wave-current interactive wave frequency
$\bar{\sigma}$	Wave frequency field with wave-current interaction
$\bar{\sigma}_{xx}$	$= \frac{S_{xx}}{E}$
$\bar{\sigma}_{xy}$	$= \frac{S_{xy}}{E}$
$\bar{\sigma}_{yy}$	$= \frac{S_{yy}}{E}$
$\bar{\tau}$	Quantity defined Equation 2.53
τ_{xx}, τ_{xy}, τ_{yy}	Directional shear stresses
$\bar{\tau}_{sx}$, $\bar{\tau}_{sy}$	Mean surface stress, x and y directions
$\bar{\tau}_{bx}$, $\bar{\tau}_{by}$	Mean bottom stress, x and y directions
ϕ	Wave phase

ABSTRACT

An explicit finite difference model for predicting time-dependent, wave-induced nearshore circulation is discussed. The formulation includes wave refraction, wave-current interaction, an anisotropic bottom friction, wave set-up, wind effects and coastal flooding. In addition to the explicit scheme, a one-dimensional implicit scheme was developed to determine the importance of the convective acceleration terms in the equation of motion. Results are shown for three cases including: set-up in a wave channel due to steady waves and wave groups, circulation in a rectangular wave tank under oblique wave attack, and for wave and wind induced circulation on a longshore periodic beach. In all three cases comparison is made to experimental data. Important results are that tuned wave groups can incite seiching in an enclosed basin and harbors and that rip currents will be induced or maintained by the presence of surf zone channels.

CHAPTER I

INTRODUCTION

Although man has throughout his history studied the open sea, it is only in the last hundred years that he has turned his attention to the ocean's shoreline. As use of this narrow strip separating land and sea increases, it is highly desirable to be able to predict its changes. The problem is not a small one for, though the effects of winds, currents and waves may be somewhat understood individually, the total picture containing these processes and their interactions is too complex to handle analytically. For this reason, the coastal engineer is starting to utilize the power of the computer in trying to unravel the complexities of the coastal environment.

This thesis concerns a numerical model that was developed to predict the circulation that a wind and wave climate would have on a particular stretch of coastline.

1.1 PURPOSE OF A NUMERICAL MODEL

The three basic means used to study coastal processes are field studies, hydraulic modelling, and numerical modelling. Since one is ultimately interested in predicting actual events, accurate field observations are very important. Unfortunately, due to the many variables involved, it is often difficult to isolate the effect of any one variable.

For this reason the hydraulic model is popular, for by scaling down the actual study area, it is possible to bring it into the controlled environment of a laboratory. There the important variables may be isolated and carefully measured. There are disadvantages, notably the reliability of the results after they are scaled up to the prototype, and the difficulty in modelling loose bed materials like sand. Cost may also be a factor, as large-scale models are expensive, both to build and operate.

Though the numerical model is a relatively new tool, it is becoming very popular. Before a numerical model can be undertaken, two requirements must be met. The governing equations must be known and field or hydraulic data must be available for calibration purposes. Some of the advantages of a numerical model are:

1. Equations too complex for an analytic solution can be solved.
2. Once formulated, many different cases can be studied very quickly.
3. Though computer time is costly, an extensive numerical model should be cheaper than a similar hydraulic one.
4. Since the prototype is modeled directly, there are no scaling problems as in the hydraulic model.

Though the model may be somewhat limited by the capabilities of the computer used, its main limitation is the accuracy and completeness of the formulation itself. For this reason the creation-stage of a model may be quite long, but once completed and tested, the researcher is provided with a very powerful tool.

1.2 THE IMPORTANCE OF COASTAL CIRCULATION MODELS

When waves enter shallow coastal waters, they undergo rapid changes controlled by local winds, beach structures and the bottom topography. Energy, momentum and mass are carried toward shore where the wave eventually breaks. Energy is dissipated through bottom friction and breaking and input by winds.

One component of the excess momentum flux due to the waves which reaches the shore drives the longshore current, with another component causing a set-up of the water level. The picture becomes even more complicated if the various processes are allowed to interact and vary in magnitude.

Since the response of the beach in terms of erosion and flooding depends on this complicated process, it is highly desirable to be able to predict it. It is for this reason that the effort reported here was undertaken. There has been a great deal of analytical work done in this area, but the complexity of the full equations prohibit general solutions, allowing only simple cases to be treated. The goal then was to develop a general program that would, through finite difference approximations, solve the complete equations. There are many uses for such a model. Some of the major ones are:

1. Prediction of storm set-up and low land flooding for any storm, and also determine "worst" storm parameters.

2. From velocity predictions, estimation of erosion and locating erosion problem spots.

3. Studying and predicting the occurrence and magnitude of rip currents.

4. As a design tool to study effects of new coastal structures by revealing areas of high scour, shoaling, energy reflection, etc.

5. An aid in taking both field and hydraulic model data by revealing areas of interest.

It was desired that the model be able to handle any combination of wind and wave fields and be adaptable to any beach topography. As a first cut toward modeling wave spectra, it was also desired to vary in time the incoming wave height. With this information as input, the program would generate values of set-up, current magnitude and direction, and wave heights.

1.3 REVIEW OF LITERATURE

One of the first significant numerical models was developed by Reid and Bodine (1968) to calculate storm surge in Galveston Bay. It utilized the vertically-integrated equations of motion and continuity which were simplified, neglecting Coriolis terms and convective accelerations. Bottom and surface stresses were included using quadratic approximations. Coastal flooding was also allowed. Their program predicted simply the water elevation changes in time ignoring entirely the details of the wave field. The model was calibrated with astronomical tide data and data from Hurricane Carla. Good agreement was then obtained by comparing predicted results to actual data for Hurricane Cindy.

Following this work, there have been a number of similar models created for different areas, for example, Pearce (1972) and Hess and White (1974). Gordon and Spaulding (1974) have compiled a bibliography listing a number of these tidal models and various other coastal and estuary models.

There are few models that deal specifically with coastal circulation. Two of the more notable ones were done by Noda et.al. (1974) and Liu and Mei (1974). Noda developed an extensive program for nearshore circulation on a periodic regular beach. The governing equations used were the time-averaged, depth-integrated long wave equations of motion as first derived by Longuet-Higgins and summarized by Phillips (1966). Convective acceleration terms were neglected and a quasi-quadratic bottom friction formulation was used. In order to simplify the calculations, a steady state solution was obtained once every three hours of real time. In this manner changes over a tidal cycle would be revealed in four calculations. Wave refraction and shoaling was calculated through a relaxation technique that included the effects of wave-current interaction. They were, however, unable to achieve more than 50 percent wave-current interaction and still arrive at a solution. Coastal flooding and water level set-up were not included.

A model by Liu and Mei (1974) considers the effects of an off-shore or shore-connected breakwater on the nearshore circulation over a plane beach. Again the time-averaged, depth-integrated equations of motion were used. Convective acceleration terms were neglected and steady state was assumed. In addition to refraction effects, the diffraction caused by the breakwater was also included. Wind effects, flooding and wave-current interaction were not included though wave-induced set-up was.

The first extensive data of wave-induced set-up was obtained by Saville (1961) on a study of maximum runup on sloping shore structures. Longuet-Higgins and Stewart (1963) used this data to check their theoretical solution. Good agreement was obtained inshore of the breaker line where a linear variation in set-up was predicted.

Because Saville (1961) was primarily interested in runup and overtopping, Bowen et.al. (1968) performed a series of experiments to accurately measure set-up and set-down on a plane beach. They were able to verify the linear set-up relationship of Longuet-Higgins and Stewart (1963) and also predicted the set-down in water level occurring from the breaker line offshore. They were, however, unable to include the change from set-down to set-up occurring at the break point.

Hwang and Divoky (1970) examined wave set-up and set-down on gentle slopes using cnoidal wave theory which is a better approximation in shallow water than the linear wave theory used previously. This affects both the shape of the wave and its behavior after breaking, and it was found that the resulting set-up profile was not linear but always convex upward. They did agree with the previous studies in finding that the magnitude of the set-up was of the same order as the wave height.

Although it is common practice to use wave basins to model coastal hydraulics, the wave-induced circulations resulting from the basin walls is sometimes overlooked. This problem was realized by Galvin (1965) and Brebner and Kamphuis (1963) who attempted in their longshore current studies to eliminate this problem by allowing the longshore current to exit from their basin.

More recently this problem was studied by Dalrymple et.al. (as yet unpublished, 1975), who analytically and experimentally investigated the circulation in three different basin configurations. Testing was done in a small 4' x 8' x 6" wave tank with a plane sloping beach constructed at an angle of 15° to the flap wavemaker. Velocities were measured by timing the travel distance of paper circle indicators. Streamlines were also found from time lapse photographs of these indicators over the entire basin. The results of the fully-enclosed basin, shown in Figure 1, were used to calibrate the model described in this report and are discussed further in Chapter 4.

1.4 SUMMARY

The purpose of this study was to develop a more complete coastal circulation model than previous investigators. To facilitate development, the refraction program of Noda et.al. (1974) was used to determine wave heights, wave angles and the effects of wave-current interaction. Although there are other refraction programs available, this one was chosen because of the important interaction effects and because computationally it is very fast.

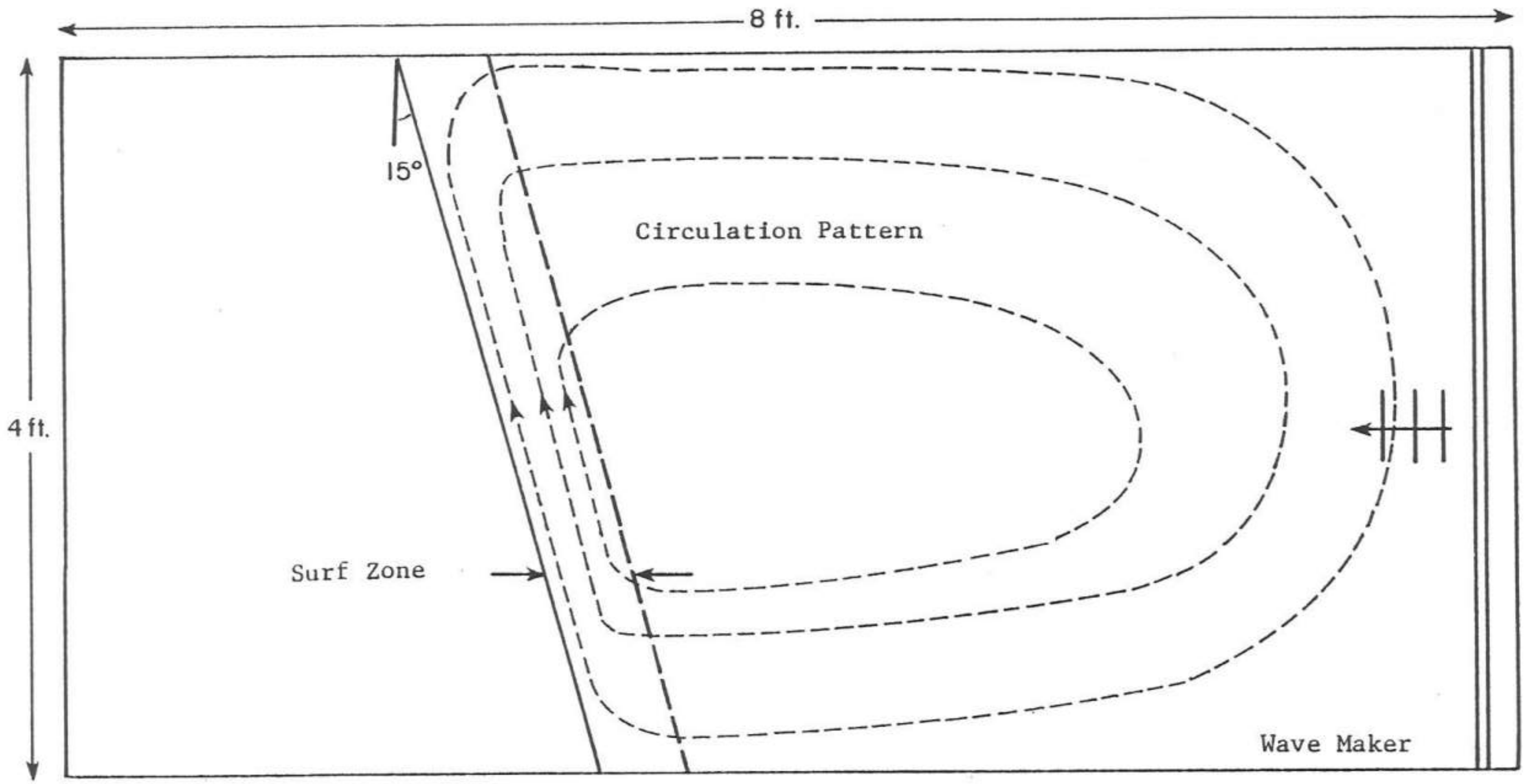

Figure 1 Experimental Set-up for Testing Circulation in a Shallow Rectangular Wave Basin (Dalrymple, et.al., 1975)

In the discussion of their results, Noda et.al. (1974) suggested a number of areas for further study including:

1. Further examination of the breaking criteria. They employed a variation of the Miche formula;

$$\left(\frac{H}{L}\right)_b = .12 \tanh 2\pi \left(\frac{D}{L}\right)_b \tag{1.1}$$

   where H_b = breaking wave height
   D_b = breaking depth
   L_b = wave length at breaking

   in the determination of the break point and to calculate the wave heights after breaking. Since this controls the magnitude of the longshore velocity, the set-up, and the set-down, it is an important factor.

2. The inclusion of wave-induced set-up which would affect the depths inshore of the breaker line and consequently the magnitude of the longshore velocity.

3. A more accurate evaluation of the bottom friction and its dependence on wave-induced orbital motions and mean currents.

4. Take into account the fact that waves are usually random in nature having different heights, directions, lengths and periods.

The first three of these considerations have been incorporated into this model. An attempt has been made to include the fourth one by allowing the incoming wave height to vary with time. Though this is not a complete picture of a random wave field, it is a start at understanding a very complex process. Coastline flooding and wind effects have also been included. In order to study the transient nature of the various processes involved and to include the wave height time dependence, steady state was not assumed. Since actual running times were relatively short, tidal variations in water level were not included but could be if desired.

The governing equations are the depth-integrated, time-averaged (over a wave period) equations of motion and continuity. The effect of convective terms are shown to be small for some cases and have been neglected, as are the lateral mixing terms. It has also been assumed that the use of linear wave theory is valid for all depths. An anisotropic quasi-quadratic bottom friction depending strongly on wave orbital velocities is employed as is a quadratic wind stress. A complete analysis of the governing equations is given in the next chapter.

Three different configurations were tested: A one-dimensional wave channel approximating the Bowen et.al. (1968) experiment, a two-dimensional wave basin similar to that used by Dalrymple et.al. (1975), and a periodic beach with a regular bottom topography as used by Noda et.al., (1974). The validity of neglecting the convective accelerations was tested by including them in an implicit-type formulation in the wave channel model. Time dependent wave heights were also tested in this model.

Once assured that the model was working properly, the more realistic regular beach was tested and the results compared to those reported by Noda et.al. (1974). Wind effects were also examined. The results obtained from this testing, are discussed in Chapter 4. Chapter 2 examines the governing equations in detail and Chapter 3 explains the workings of the program.

CHAPTER II

GOVERNING EQUATIONS

Although most of the equations used are fairly well known, their derivations are repeated here for completeness. The procedure in the derivation of both the continuity equation and the equations of motion are similar. The general 3-dimensional equation is integrated over depth, and after substituting for the velocity:

$$\begin{aligned} u &= \overline{u} + u' \\ v &= \overline{v} + v' \end{aligned} \tag{2.1}$$

the entire equation is time-averaged over a wave period. This substitution replaces the instantaneous velocities, u,v, with the sum of a time-averaged current velocity, $\overline{u},\overline{v}$, and a velocity due to the fluctuations of the wave, u',v'. The coordinate system and important parameters are shown in Figure 2. Since Leibnitz Rule of Integration is used several times to remove a derivative from within an integral, it is given below

$$\begin{aligned} \int_{\alpha(x)}^{\beta(x)} \frac{\partial f(x,y)}{\partial x}\, dy = \frac{\partial}{\partial x} \int_{\alpha(x)}^{\beta(x)} f(x,y)dy - f(\beta,y)\, \frac{\partial \beta(x)}{\partial x} \\ + f(\alpha,y)\, \frac{\partial \alpha(x)}{\partial x} \end{aligned} \tag{2.2}$$

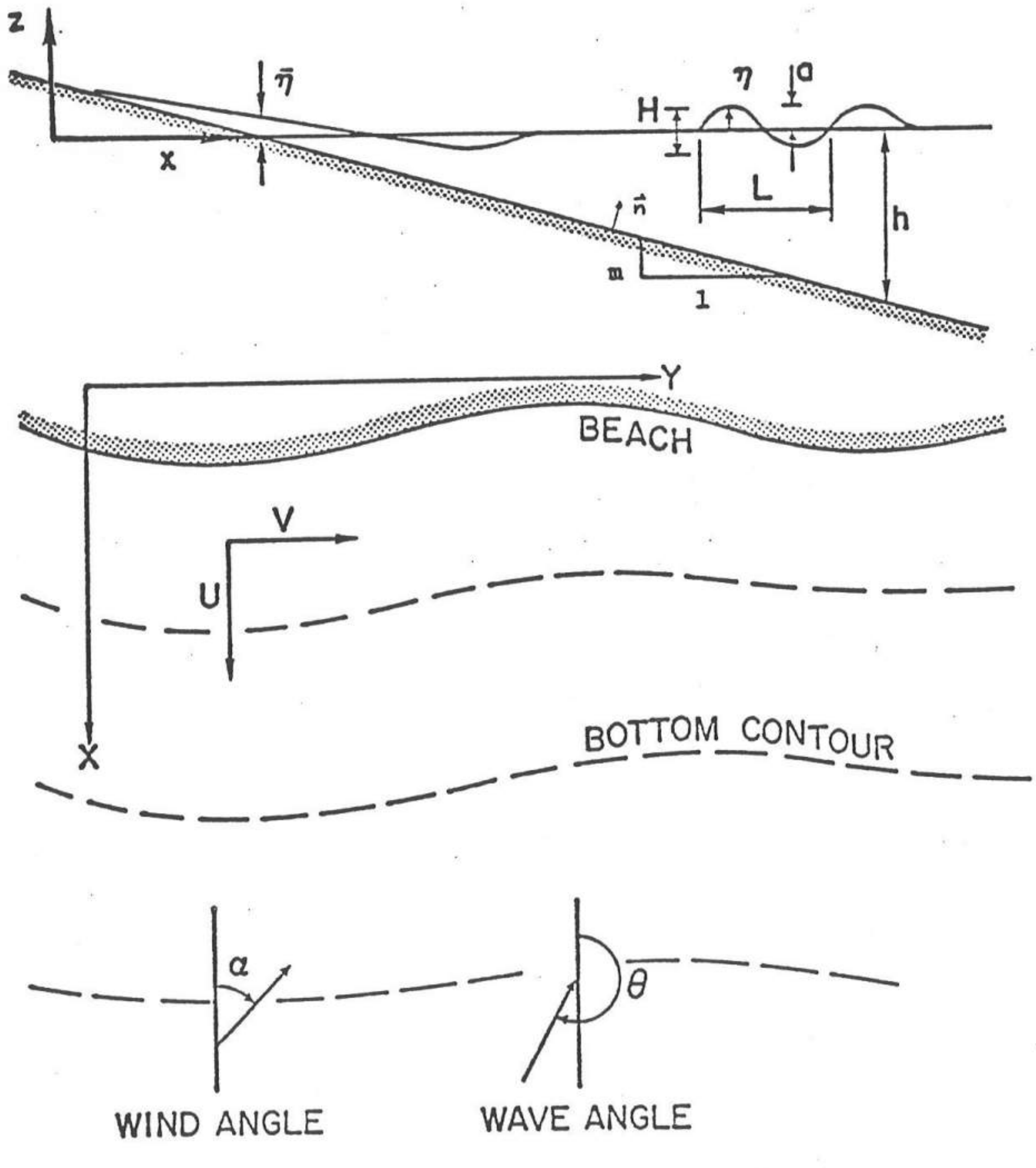

Figure 2 Section and Plan Definition Sketches

2.1 BOUNDARY CONDITIONS

At the bottom, $z = -h$, a no-flow boundary condition exists. In vector form

$$\vec{u} \cdot \vec{n} = 0$$

with

$$\vec{u} = u\hat{i} + v\hat{j} + w\hat{k}$$

$$\vec{n} = \left(\frac{\partial h}{\partial x}\hat{i} + \frac{\partial h}{\partial y}\hat{j} + \hat{k}\right) / \sqrt{\left(\frac{\partial h}{\partial x}\right)^2 + \left(\frac{\partial h}{\partial y}\right)^2 + 1}$$

$\hat{i}$, $\hat{j}$, $\hat{k}$ unit vectors in the x, y, z directions
$\vec{n}$ = unit vector normal to the bottom

making the bottom boundary condition (BBC)

$$u\frac{\partial h}{\partial x} + v\frac{\partial h}{\partial y} + w = 0 \qquad (z = -h) \tag{2.3}$$

At the free surface, the vertical velocity (w) must account for the changes in the instantaneous water surface elevation (η),

$$w = \frac{D\eta}{Dt} = \frac{\partial \eta}{\partial t} + u\frac{\partial \eta}{\partial x} + v\frac{\partial \eta}{\partial y} \qquad (z = \eta) \tag{2.4}$$

where $\frac{D}{Dt}$ denotes the total derivative, and η is a function of x,y,t. This is known as the kinematic free surface boundary condition (KFSBC).

2.2 CONTINUITY EQUATION

The three-dimensional general form of the continuity equation is:

$$\frac{\partial \rho}{\partial t} + \frac{\partial \rho u}{\partial x} + \frac{\partial \rho v}{\partial y} + \frac{\partial \rho w}{\partial z} = 0 \tag{2.5}$$

Integrating this with respect to the depth (z) from -h to η, and imposing Leibnitz Rule this becomes:

$$\frac{\partial}{\partial t}\int_{-h}^{\eta} \rho dz - \rho_{\eta}\frac{\partial \eta}{\partial t} - \rho_{-h}\frac{\partial h}{\partial t} + \frac{\partial}{\partial x}\int_{-h}^{\eta} \rho u dz - (\rho u)_{\eta}\frac{\partial \eta}{\partial x} - (\rho u)_{-h}\frac{\partial h}{\partial x}$$

$$+ \frac{\partial}{\partial y}\int_{-h}^{\eta} \rho v dz - (\rho v)_{\eta}\frac{\partial \eta}{\partial y} - (\rho v)_{-h}\frac{\partial h}{\partial y} + (\rho w)_{\eta} - (\rho w)_{-h} = 0$$

Invoking the BBC and KFSBC, this simplifies to:

$$\frac{\partial}{\partial t}\int_{-h}^{\eta} \rho dz - \rho_{-h}\frac{\partial h}{\partial t} + \frac{\partial}{\partial x}\int_{-h}^{\eta} \rho u dz + \frac{\partial}{\partial y}\int_{-h}^{\eta} \rho v dz = 0$$

Assuming that the bottom is constant with time, and substituting

$$u = \overline{u} + u'$$

$$v = \overline{v} + v'$$

as defined above, the above equation expands to

$$\frac{\partial}{\partial t}\int_{-h}^{\eta} \rho dz + \frac{\partial}{\partial x}\int_{-h}^{\eta} \rho \overline{u} dz + \frac{\partial}{\partial y}\int_{-h}^{\eta} \rho \overline{v} dz + \frac{\partial}{\partial x}\int_{-h}^{\eta} \rho u' dz$$

$$+ \frac{\partial}{\partial y}\int_{-h}^{\eta} \rho v' dz = 0 \qquad (2.6)$$

Defining time average as

$$\overline{F} = \frac{1}{T}\int_{0}^{T} F\, dt \quad ; \quad T = \text{wave period}$$

and time averaging Equation 2.6, one obtains after performing the integration,

$$\frac{\partial}{\partial t}\rho(h+\overline{\eta}) + \frac{\partial}{\partial x}\rho(h+\overline{\eta})\ \overline{u} + \frac{\partial}{\partial y}\rho(h+\overline{\eta})\ \overline{v} + \frac{\partial}{\partial x}\overline{\int_{-h}^{\eta}\rho u'dz}$$

$$+ \frac{\partial}{\partial y}\overline{\int_{-h}^{\eta}\rho v'dz} = 0 \tag{2.7}$$

Notice that this is in terms of time-averaged $\overline{\eta}$, $\overline{u}$ and $\overline{v}$. Also unlike turbulent fluctuations, the time average of the wave-induced fluctuations is not zero. Following the definitions of Phillips (1966) for the mean total mass flux $\tilde{M}_x$ and $\tilde{M}_y$,

$$\tilde{M}_x = \rho\overline{u}\ (h+\overline{\eta}) + M_x \tag{2.8}$$

$$\tilde{M}_y = \rho\overline{v}\ (h+\overline{\eta}) + M_y \tag{2.9}$$

with M_x, M_y the mass flux due to the waves

$$M_x = \overline{\int_{-h}^{\eta}\rho u'dz} \tag{2.10}$$

$$M_y = \overline{\int_{-h}^{\eta}\rho\ v'dz} \tag{2.11}$$

and his definitions of mean transport velocity,

$$U = \frac{\tilde{M}_x}{\rho\ (h+\overline{\eta})} \qquad V = \frac{\tilde{M}_y}{\rho\ (h+\overline{\eta})} \tag{2.12}$$

Equation 2.7 becomes

$$\frac{\partial}{\partial t}\,[\rho(h+\bar{\eta})] + \frac{\partial}{\partial x}\,(\tilde{M}_x) + \frac{\partial}{\partial y}\,(\tilde{M}_y) = 0$$

Utilizing the definitions of Equations 2.12 this reduces to a form similar to Equation 2.5

$$\frac{\partial\bar{\eta}}{\partial t} + \frac{\partial}{\partial x}\,[U(h+\bar{\eta})] + \frac{\partial}{\partial y}\,[V(h+\bar{\eta})] = 0 \qquad (2.13)$$

except that it involves only the total mean transport velocity and the total depth $(h + \bar{\eta})$.

2.3 EQUATIONS OF MOTION

In the x direction, the general form of the equation of motion is,

$$\frac{\partial u}{\partial t} + \frac{\partial u^2}{\partial x} + \frac{\partial uv}{\partial y} + \frac{\partial uw}{\partial z} = -\frac{1}{\rho}\frac{\partial P}{\partial x} + \frac{1}{\rho}\left[\frac{\partial\tau_{xx}}{\partial x} + \frac{\partial\tau_{xy}}{\partial y} + \frac{\partial\tau_{xz}}{\partial z}\right] \qquad (2.14)$$

with P = pressure and τ_{xx}, τ_{xy}, τ_{xz}, are the directional shear stresses. To avoid confusion, and since the derivation is exactly similar in the y direction, only the x direction will be treated here.

Multiplying Equation 2.14 by ρ and integrating over the depth gives, term by term:

Left Hand Side (L.H.S.)

$$\int_{-h}^{\eta} \frac{\partial\rho u}{\partial t}\,dz = \frac{\partial}{\partial t}\int_{-h}^{\eta} \rho u dz - (\rho u)_{\eta}\,\frac{\partial\eta}{\partial t} - (\rho u)_{-h}\,\frac{\partial h}{\partial t}$$

$$\int_{-h}^{\eta} \frac{\partial}{\partial x} (\rho u^2) dz = \frac{\partial}{\partial x} \int_{-h}^{\eta} \rho u^2 dz - (\rho u^2)_{\eta} \frac{\partial \eta}{\partial x} - (\rho u^2)_{-h} \frac{\partial h}{\partial x}$$

$$\int_{-h}^{\eta} \frac{\partial}{\partial y} (\rho uv) dz = \frac{\partial}{\partial y} \int_{-h}^{\eta} \rho uv\, dz - \rho (uv)_{\eta} \frac{\partial \eta}{\partial y} - \rho (uv)_{-h} \frac{\partial h}{\partial y}$$

$$\int_{-h}^{\eta} \frac{\partial}{\partial z} (\rho uw) dz = \rho (uw)_{\eta} - \rho (uw)_{-h}$$

Again assuming that the bottom is constant in time and invoking the KFSBC and the BBC the L.H.S. simplifies to

$$\frac{\partial}{\partial t} \int_{-h}^{\eta} \rho u dz + \frac{\partial}{\partial x} \int_{-h}^{\eta} \rho u^2 dz + \frac{\partial}{\partial y} \int_{-h}^{\eta} \rho uv dz = \text{R.H.S.} \tag{2.15}$$

Integrating the right hand side

$$\text{R.H.S.} = \int_{-h}^{\eta} \frac{\partial}{\partial x} (-P) dz + \int_{-h}^{\eta} \left[\frac{\partial \tau_{xx}}{\partial x} + \frac{\partial \tau_{xy}}{\partial y} + \frac{\partial \tau_{xz}}{\partial z} \right] dz$$

If lateral mixing is neglected and the integration performed, this becomes

$$\text{R.H.S.} = \frac{\partial}{\partial x} \int_{-h}^{\eta} -P dz + P_{-h} \frac{\partial h}{\partial x} + P_{\eta} \frac{\partial \eta}{\partial x} + \tau_{xz_{\eta}} - \tau_{xz_{-h}} \tag{2.16}$$

with $\tau_{xz_{\eta}} = \tau_{sx}$ = surface stress x direction

$\tau_{xz_{-h}} = \tau_{bx}$ = bottom stress x direction

Again making the substitution

$$u = \overline{u} + u'$$

$$v = \overline{v} + v'$$

and time averaging, the complete equation becomes, term by term

L.H.S.

$$\frac{\partial}{\partial t}\overline{\int_{-h}^{\eta} \rho u dz} = \frac{\partial}{\partial t}\int_{-h}^{\eta} \rho\overline{u} dz + \frac{\partial}{\partial t}\overline{\int_{-h}^{\eta} \rho u' dz}$$

$$\frac{\partial}{\partial x}\overline{\int_{-h}^{\eta} \rho u^2 dz} = \frac{\partial}{\partial x}\int_{-h}^{\eta} (\rho\overline{u}^2) dz + \frac{\partial}{\partial x}\overline{\int_{-h}^{\eta} \rho u'^2 dz} + 2\frac{\partial}{\partial x}\overline{\int_{-h}^{\eta} \rho\overline{u}u' dz}$$

$$\frac{\partial}{\partial y}\overline{\int_{-h}^{\eta} \rho uv dz} = \frac{\partial}{\partial y}\int_{-h}^{\eta} \rho\overline{uv} dz + \frac{\partial}{\partial y}\overline{\int_{-h}^{\eta} \rho u'v' dz} + \frac{\partial}{\partial y}\overline{\int_{-h}^{\eta} u'\overline{v} dz}$$

$$+ \frac{\partial}{\partial y}\overline{\int_{-h}^{\eta} \rho\overline{u}v' dz}$$

R.H.S.

$$= -\frac{\partial}{\partial x}\overline{\int_{-h}^{\eta} P dz} + \overline{P}_{\eta}\frac{\partial\overline{\eta}}{\partial x} + \overline{P}_{-h}\frac{\partial h}{\partial x} + \overline{\tau}_{sx} - \overline{\tau}_{bx}$$

Examining the pressure terms, at the surface, $P_{\eta} = P_{atm} = 0$ and at the bottom, $z = -h$, the pressure is considered as hydrostatic. Defining the mean dynamic pressure as,

$$P = \overline{P}_{-h} - \rho g(h+\overline{\eta})$$

and solving for $\overline{P}_{-h} \frac{\partial h}{\partial x}$,

$$\overline{P}_{-h} \frac{\partial h}{\partial x} = \frac{P\partial h}{\partial x} + \frac{1}{2} \frac{\partial}{\partial x} \rho g \ (\overline{\eta}+h)^2 - \rho g \ (h+\overline{\eta}) \ \frac{\partial \overline{\eta}}{\partial x}$$

Combining and performing the integration for the pressure

$$\frac{\partial}{\partial t} \ [\rho\overline{u}(h+\overline{\eta}) + \overline{\int_{-h}^{\eta} \rho u' dz}] + \frac{\partial}{\partial x} \ [\rho\overline{u}^2(h+\overline{\eta}) + \overline{\int_{-h}^{\eta} \rho u'^2 dz} + \overline{u}\overline{\int_{-h}^{\eta} 2\rho u' dz}$$

$$+ \overline{\int_{-h}^{\eta} P dz} - \frac{1}{2} \rho g (h+\overline{\eta})^2] + \frac{\partial}{\partial y} \ [\rho\overline{u}\overline{v}(h+\overline{\eta}) + \overline{\int_{-h}^{\eta} \rho u'v' dz} + \overline{v}\overline{\int_{-h}^{\eta} \rho u' dz}$$

$$+\overline{u}\int_{-h}^{\eta} \rho v' dz] = \frac{P\partial h}{\partial x} - \rho g(h+\overline{\eta}) \ \frac{\partial \overline{\eta}}{\partial x} + \overline{\tau}_{sx} - \overline{\tau}_{bx} \tag{2.17}$$

Assuming that $\frac{\partial h}{\partial x}$ is small, then $\frac{P\partial h}{\partial x} \cong 0$.

With $\widetilde{M}$ and U as before (Equation 2.8, 2.12) and defining the "radiation stresses" S_{xx}, S_{xy} as

$$S_{xx} = \overline{\int_{-h}^{\eta} [P+\rho u'^2] dz} - \frac{\rho g}{2} \ (h+\overline{\eta})^2 - \frac{\overline{\int_{-h}^{\eta} (\rho u' dz)^2}}{\rho (h+\overline{\eta})} \tag{2.18}$$

$$S_{xy} = \overline{\int_{-h}^{\eta} \rho u'v' dz} - \frac{\overline{\int_{-h}^{\eta} \rho v' dz} \ \overline{\int_{-h}^{\eta} \rho u' dz}}{\rho (h+\overline{\eta})} \tag{2.19}$$

it is a simple procedure to reduce Equation 2.17 to the following form

$$\frac{\partial \widetilde{M}_x}{\partial t} + \frac{\partial}{\partial x} \ (U \ \widetilde{M}_x + S_{xx}) + \frac{\partial}{\partial y} \ (U \ \widetilde{M}_y + S_{xy}) = - \rho g(h+\overline{\eta}) \ \frac{\partial \overline{\eta}}{\partial x} + \overline{\tau}_{sx} - \overline{\tau}_{bx}$$

The radiation stresses are important, for they represent the momentum flux attributed to the wave motion. Using Equation 2.12, this can be reduced to

$$\frac{\partial}{\partial t}[U\rho(h+\bar{\eta})] + \frac{\partial}{\partial x}[U^2\rho(h+\bar{\eta}) + S_{xx}] + \frac{\partial}{\partial y}[UV\rho(h+\bar{\eta}) + S_{xy}] =$$

$$-\rho g\ (h+\bar{\eta})\frac{\partial\bar{\eta}}{\partial x} + \bar{\tau}_{sx} - \bar{\tau}_{bx}$$

When this is expanded and simplified with the continuity Equation (2.13), it becomes

$$\frac{\partial U}{\partial t} + \frac{U\partial U}{\partial x} + \frac{V\partial U}{\partial y} = -g\frac{\partial\bar{\eta}}{\partial x} - \frac{1}{\rho(h+\bar{\eta})}\left[\frac{\partial S_{xx}}{\partial x} + \frac{\partial S_{xy}}{\partial y} - \bar{\tau}_{sx} + \bar{\tau}_{bx}\right] \qquad (2.20)$$

For the purpose of this thesis, the convective acceleration terms will be dropped to simplify computation. This appears to be a valid procedure for small currents and will be somewhat justified in Chapter 3. The equation then simplifies to

$$\frac{\partial U}{\partial t} = -g\frac{\partial\bar{\eta}}{\partial x} - \frac{1}{\rho(h+\bar{\eta})}\left[\frac{\partial S_{xx}}{\partial x} + \frac{\partial S_{xy}}{\partial y} - \bar{\tau}_{sx} + \bar{\tau}_{bx}\right] \qquad (2.21)$$

The corresponding equation in the y direction is:

$$\frac{\partial V}{\partial t} = -g\frac{\partial\bar{\eta}}{\partial y} - \frac{1}{\rho(h+\bar{\eta})}\left[\frac{\partial S_{yx}}{\partial x} + \frac{\partial S_{yy}}{\partial y} - \bar{\tau}_{sy} + \bar{\tau}_{by}\right] \qquad (2.22)$$

It is of interest to note that these equations and the continuity equation (2.13) are written entirely in terms of time and depth average quantities.

2.4 RADIATION STRESSES

It is difficult to use the general form of the radiation stress as expressed in Equations 2.18 and 2.19. They can, however, be simplified, and it has been shown that to second order the radiation stresses due to a single progressive wave train can be approximated by, written in Cartesian coordinates,

$$S_{xx} = E[(2n-1/2)\cos^2\theta + (n-1/2)\sin^2\theta] \tag{2.23}$$

$$S_{yy} = E[(2n-1/2)\sin^2\theta + (n-1/2)\cos^2\theta] \tag{2.24}$$

$$S_{xy} = S_{yx} = \frac{E}{2} n \sin(2\theta) \tag{2.25}$$

where E is the wave energy, θ is the wave angle, and n = ratio of group velocity (C_g), to wave celerity (C). This is the form used by Noda et.al. (1974).

$$E = \frac{1}{8} \rho g H^2 \tag{2.26}$$

$$n = \frac{C_g}{C} = \frac{1}{2} [1 + \frac{2kh}{\sinh(2kh)}] \tag{2.27}$$

k = wave number ($= \frac{2\pi}{L}$)
h = depth
L = wave length
H = wave height

This form is arrived at if turbulent Reynolds stresses and the mass transport terms,

$$\frac{\overline{\left[\int_{-h}^{\eta} \rho u' dz\right]^2}}{\rho(h+\overline{\eta})} \quad \text{and} \quad \frac{\overline{\int_{-h}^{\eta} \rho v' dz} \; \overline{\int_{-h}^{\eta} \rho u' dz}}{\rho(h+\overline{\eta})}$$

of Equations 2.18 and 2.19 are neglected as they are of order $O(ka)^4$ for waves of small amplitude (a).

2.5 WAVE REFRACTION

The following discussion on wave refraction follows that given by Noda et.al. (1974) as their procedure was adapted for use here. For a more detailed derivation, the reader is directed to the original paper.

Classical wave refraction in the absence of currents and diffraction effects is fairly well understood; Munk and Arthur (1952), and a number of numerical programs, such as those by Wilson (1966), Dobson (1967), and Skovgaard et.al. (1975), have been developed. Noda included the effects of wave-current interactions and devised a scheme that would calculate wave angles and heights at specific points instead of along a wave ray.

Starting from the equation of a progressive gravity wave field of phase ϕ, moving in the ξ direction,

$$\eta(\vec{\xi},t) = a(\vec{\xi},t)\cos\phi$$

$$\phi = 2\pi\left(\frac{\vec{\xi}}{L} - \frac{t}{T}\right)$$

T = wave period

$a(\vec{\xi},t)$ = wave amplitude = $\dfrac{H(\vec{\xi},t)}{2}$,

a wave number field can be defined

$$\vec{k} = \nabla\phi \tag{2.28}$$

along with a scalar frequency field

$$\bar{\sigma} = -\frac{\partial\phi}{\partial t} \tag{2.29}$$

From the fact that the curl of a gradient is identically zero, it is easily seen that the wave number field is irrotational

$$\nabla x \nabla\phi = \nabla x \vec{k} = 0 \tag{2.30}$$

If ϕ is continuous then the order of differentiation can be interchanged.

$$\frac{\partial}{\partial t}(\nabla\phi) = \nabla\left(\frac{\partial\phi}{\partial t}\right)$$

Substituting in Equations 2.28 and 2.29, this becomes

$$\frac{\partial\vec{k}}{\partial t} + \nabla\bar{\sigma} = 0 \tag{2.31}$$

which is commonly known as the conservation of waves equation; the change in the number of waves being balanced by the convergence of $\bar{\sigma}$, the flux of the waves. In the presence of a current $\vec{u}$ in the ξ direction, to account for the moving coordinate system,

$$\bar{\sigma} = \sigma + \vec{k} \cdot \vec{u} \tag{2.32}$$

where σ is the wave frequency with respect to the current system.

If it is assumed that h and $\vec{u}$ are slowly varying, then the classic wave celerity equation will remain valid under interaction and

$$C^2 = \frac{g}{k} \tanh kh = \left(\frac{\sigma}{k}\right)^2 \tag{2.33}$$

where C is the velocity of the wave with respect to the current $(\vec{u})$.

Substituting Equations 2.32 into 2.31 and assuming a steady wave number field, then

$$\nabla(\sigma + \vec{k} \cdot \vec{u}) = 0 \tag{2.34}$$

requiring

$$\sigma + \vec{k} \cdot \vec{u} = \text{constant} \tag{2.35}$$

This constant can be evaluated in a region where $\vec{u} = 0$ giving

$$\sigma = \text{constant} = \frac{2\pi}{T}$$

the non-interactive wave frequency. Expanding 2.34 in Cartesian coordinates and utilizing Equation 2.33, Equation 2.35 becomes;

$$[gk \tanh (kh)]^{1/2} + U(x,y)\ k \cos\theta + V(x,y)\ k \sin\theta = \frac{2\pi}{T} \tag{2.36}$$

In similar coordinates, Equation 2.30 becomes

$$\nabla x \vec{k} = 0 = \frac{\partial k \cos\theta}{\partial y} - \frac{\partial k \sin\theta}{\partial x} \tag{2.37}$$

Expanding,

$$\cos\theta \frac{\partial\theta}{\partial x} + \sin\theta \frac{\partial\theta}{\partial y} = \cos\theta \frac{1}{k}\frac{\partial k}{\partial y} - \sin\theta \frac{1}{k}\frac{\partial k}{\partial x} \tag{2.38}$$

The coordinate system is shown in Figure 2.

Equation 2.36 can be used to determine the wave number, k, for a given current velocity, wave angle and depth. If k is known, then Equation 2.38 can be used to find the wave direction (θ). Noda et.al. (1974) checked this equation by showing that without wave-current interaction, it reduced to the classic wave ray equation of Munk and Arthur (1952).

Equation 2.38 requires $\frac{\partial k}{\partial y}$, $\frac{\partial k}{\partial x}$ which can be found from Equation 2.36.

$$\frac{\partial k}{\partial x} = \{k \frac{\partial \theta}{\partial x} (U \sin\theta - V \cos\theta) - k (\cos\theta \frac{\partial U}{\partial x} + \sin\theta \frac{\partial V}{\partial x}) - \frac{gk^2 \text{sech}^2(kh)}{2[gk \tanh(kh)]^{1/2}}$$

$$\frac{\partial h}{\partial x}\} \div \{U \cos\theta + V \sin\theta + \frac{g[kh \text{ sech}^2(kh) + \tanh(kh)]}{2[gk \tanh(kh)]^{1/2}}\} \tag{2.39}$$

$$\frac{\partial k}{\partial y} = \{k \frac{\partial \theta}{\partial y} (U \sin\theta - V \cos\theta) - k(\cos\theta \frac{\partial U}{\partial y} - \sin\theta \frac{\partial V}{\partial y}) - \frac{gk^2 \text{sech}^2(kh)}{2[gk \tanh(kh)]^{1/2}}$$

$$\frac{\partial h}{\partial y}\} \div \{U \cos\theta + V \sin\theta + \frac{g[kh \text{ sech}^2(kh) + \tanh(kh)]}{2[gk \tanh(kh)]^{1/2}}\} \tag{2.40}$$

Rewriting Equation 2.38 as

$$\cos\theta \left[\frac{\partial \theta}{\partial x} - \frac{1}{k}\frac{\partial k}{\partial y}\right] + \sin\theta \left[\frac{\partial \theta}{\partial y} + \frac{1}{k}\frac{\partial k}{\partial x}\right] = 0 \tag{2.41}$$

shows that it is desirable to determine $\frac{1}{k}\frac{\partial k}{\partial y}$, $\frac{1}{k}\frac{\partial k}{\partial x}$.

Using Equations 2.39 and 2.40 and after some manipulation including the use of the identity

$$\mathrm{sech}^2 kh = \frac{2 \tanh kh}{\sinh 2kh}$$

the following equations result:

$$\frac{1}{k}\frac{\partial k}{\partial x} = \frac{\partial \theta}{\partial x}\left[\frac{U \sin\theta - V \cos\theta}{A}\right] + \overline{\frac{1}{k}\frac{\partial k}{\partial x}} \tag{2.42}$$

$$\frac{1}{k}\frac{\partial k}{\partial y} = \frac{\partial \theta}{\partial y}\left[\frac{U \sin\theta - V \cos\theta}{A}\right] + \overline{\frac{1}{k}\frac{\partial k}{\partial y}} \tag{2.43}$$

with

$$A = U \cos\theta + V \sin\theta + \frac{1}{2}\left[1 + \frac{2kh}{\sinh(2kh)}\right]\left[\frac{\sigma}{k} - U \cos\theta - V \sin\theta\right] \tag{2.44}$$

and

$$\overline{\frac{1}{k}\frac{\partial k}{\partial x}} = \frac{-\left[\cos\theta \frac{\partial U}{\partial x} + \sin\theta \frac{\partial V}{\partial x}\right] - \left[\frac{\sigma - Uk \cos\theta - Vk \sin\theta}{\sinh(2kh)}\right]\frac{\partial h}{\partial x}}{A} \tag{2.45}$$

$$\overline{\frac{1}{k}\frac{\partial k}{\partial y}} = \frac{-\left[\cos\theta \frac{\partial U}{\partial x} + \sin\theta \frac{\partial V}{\partial x}\right] - \left[\frac{\sigma - Uk \cos\theta - Vk \sin\theta}{\sinh(2kh)}\right]\frac{\partial h}{\partial y}}{A} \tag{2.46}$$

Substituting 2.42 and 2.43 into 2.41, the following final equation is arrived at.

$$\frac{\partial \theta}{\partial x}\left[\cos\theta + \frac{\sin\theta\ (U \sin\theta - V \cos\theta)}{A}\right] + \frac{\partial \theta}{\partial y}\left[\sin\theta - \frac{\cos\theta (U \sin\theta - V \cos\theta)}{A}\right] = \overline{\frac{1}{k}\frac{\partial k}{\partial y}} \cos\theta - \overline{\frac{1}{k}\frac{\partial k}{\partial x}} \sin\theta \tag{2.47}$$

As will be shown in the next chapter, this form of Equation 2.38, and Equation 2.36 are used to calculate the wave number, and the refraction angle.

2.6 WAVE HEIGHTS

Since in linear wave theory, the energy of a wave is related to the wave height squared, an energy balance is used to determine the wave height (H). The derivation of the governing equation follows a procedure similar to that for the equations of motion given before, and results in

$$\frac{\partial E}{\partial t} + \frac{\partial}{\partial x}\left[E(U + C_{g_x})\right] + \frac{\partial}{\partial y}\left[E(V + C_{g_y})\right] + S_{xx}\frac{\partial U}{\partial x} + S_{xy}\frac{\partial U}{\partial y} + S_{yy}\frac{\partial V}{\partial y} + S_{yx}\frac{\partial V}{\partial y} = 0 \tag{2.48}$$

The derivation of this equation can be found in Phillips (1966), pages 45-50 and the above form is his Equation 3.6.21. Equation 2.48 represents that part of the total energy balance due to the fluctuating motion of the waves and assumes negligible dissipation. Expanding in Cartesian coordinates,

$$\frac{1}{E}\frac{\partial E}{\partial t} + (U+C_g \cos\theta)\frac{1}{E}\frac{\partial E}{\partial x} + (V+C_g \sin\theta)\frac{1}{E}\frac{\partial E}{\partial y} + \frac{\partial}{\partial x}(U+C_g \cos\theta) + \frac{\partial}{\partial y}(V+C_g \sin\theta) + \left[\bar{\sigma}_{xx}\frac{\partial U}{\partial x} + \bar{\sigma}_{yx}\frac{\partial U}{\partial y} + \bar{\sigma}_{xy}\frac{\partial V}{\partial x} + \bar{\sigma}_{yy}\frac{\partial V}{\partial y}\right] = 0 \tag{2.49}$$

with

$$\bar{\sigma}_{xx} = \frac{S_{xx}}{E} \tag{2.50}$$

$$\bar{\sigma}_{yy} = \frac{S_{yy}}{E} \tag{2.51}$$

$$\bar{\sigma}_{xy} = \bar{\sigma}_{yx} = \frac{S_{xy}}{E} \tag{2.52}$$

defining

$$\bar{\tau} = [\bar{\sigma}_{xx} \frac{\partial U}{\partial x} + \bar{\sigma}_{yx} \frac{\partial U}{\partial y} + \bar{\sigma}_{xy} \frac{\partial V}{\partial x} + \bar{\sigma}_{yy} \frac{\partial V}{\partial y}] \tag{2.53}$$

and using Equation 2.26, Equation 2.49 becomes

$$\frac{2}{H}\frac{\partial H}{\partial t} + (U+C_g \cos\theta)\frac{2}{H}\frac{\partial H}{\partial x} + (V+C_g \sin\theta)\frac{2}{H}\frac{\partial H}{\partial y} + \frac{\partial U}{\partial x} + \frac{\partial V}{\partial y} - C_g \sin\theta \frac{\partial \theta}{\partial x}$$

$$+ \cos\theta \frac{\partial C_g}{\partial x} + C_g \cos\theta \frac{\partial \theta}{\partial y} + \sin\theta \frac{\partial C_g}{\partial y} + \bar{\tau} = 0 \tag{2.54}$$

Thus if θ, C_g, U and V are known, the wave height can be found numerically. Equation 2.54 can be simplified through the following substitutions.

$$C = (\frac{g}{k} \tanh kh)^{1/2} \tag{2.55}$$

$$C_g = \frac{C}{2} [1 + \frac{2kh}{\sinh (2kh)}] \tag{2.56}$$

taking derivatives,

$$\frac{\partial C_g}{\partial x} = \frac{C[k\frac{\partial h}{\partial x} + h\frac{\partial k}{\partial x}]\cdot[\sinh(2kh) - 2kh \cosh(2kh)]}{\sinh^2(2kh)} +$$

$$\frac{1}{2} [1 + \frac{2kh}{\sinh (2kh)}] \frac{\partial C}{\partial x} \tag{2.57}$$

$$\frac{\partial C}{\partial x} = \frac{g}{2k^2 C} [k \ \mathrm{sech}^2(kh)(k \frac{\partial h}{\partial x} + h \frac{\partial k}{\partial x}) - \tanh(kh) \frac{\partial k}{\partial x}] \quad (2.58)$$

$$\frac{\partial C_g}{\partial y} = \frac{C[k\frac{\partial h}{\partial y} + h\frac{\partial k}{\partial y}]\cdot[\sinh 2kh - 2kh \cosh 2kh]}{\sinh^2(2kh)} + \frac{1}{2} [1 + \frac{2kh}{\sinh(2kh)}] \frac{\partial C}{\partial y} \quad (2.59)$$

$$\frac{\partial C}{\partial y} = \frac{g}{2k^2 C} [k \ \mathrm{sech}^2 kh \ (k\frac{\partial h}{\partial y} + h\frac{\partial k}{\partial y}) - \tanh(kh) \frac{\partial k}{\partial y}] \quad (2.60)$$

Equations 2.54 to 2.60 allow the wave height to be calculated and include wave-current interaction. Noda et.al. (1974) showed that these equations reduce to the classical wave shoaling equations in the case of no interaction under a steady state assumption, $\frac{\partial H}{\partial t} = 0$.

2.7 WIND STRESS

Although other methods exist for computing the surface stress due to the wind, see Wu (1968), the one suggested in the Shore Protection Manual (1974) was utilized. This form was first developed by Van Dorn and gives a fairly good fit to the experimental data, see Figure 3. The form of the surface stress is quadratic in the wind speed and is given by

$$\overline{\tau}_{sx} = \rho K|W|W_x \quad (2.61)$$

$$\overline{\tau}_{sy} = \rho K|W|W_y \quad (2.62)$$

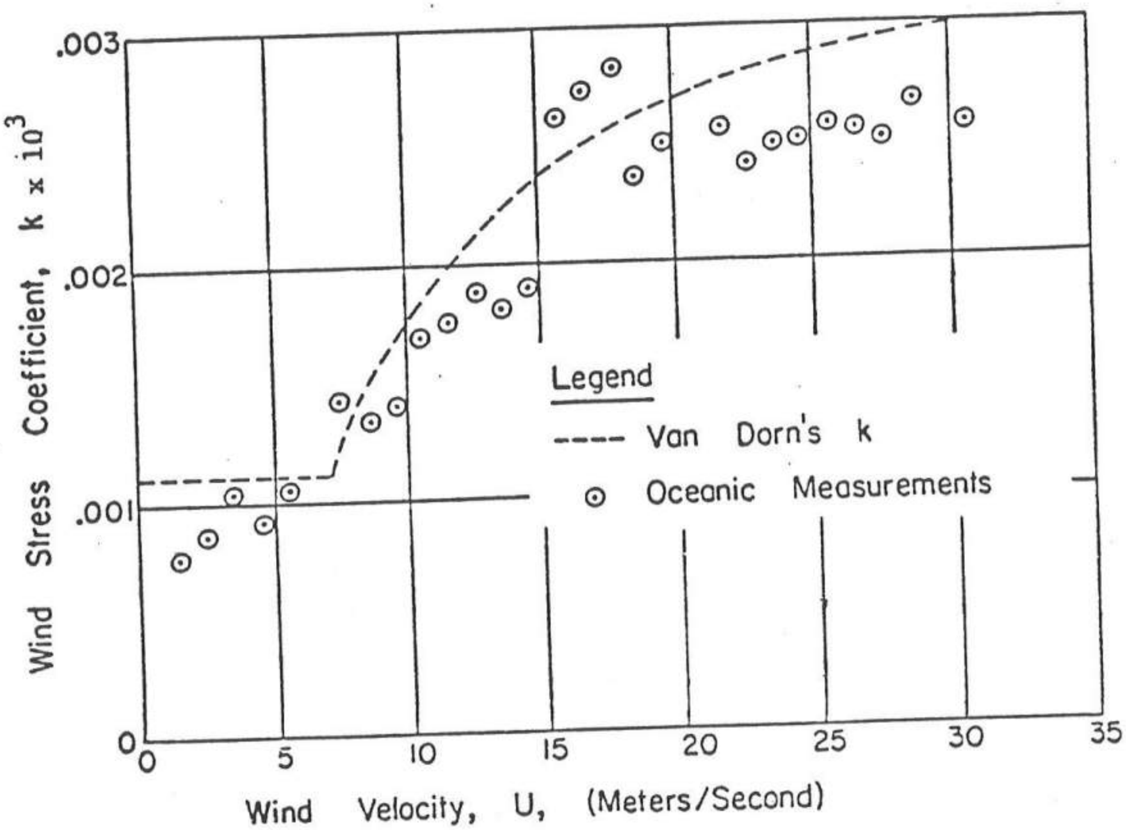

Figure 3 Comparison of Van Dorn Wind Stress Coefficient and Experimental Data [from Pearce (1972)]

where W is the wind speed, and W_x, W_y are wind velocity components in the x and y directions, as determined by the wind angle, α.

The wind stress coefficient K is determined empirically to be dependent on the magnitude of the wind velocity such that

$$K = \begin{cases} K_1 & W < W_{cr} \\ K_1 + K_2\,(1 + W_{cr}/W)^2 & , W > W_{cr} \end{cases} \tag{2.63}$$

and $$K_1 = 1.1 \times 10^{-6} \quad ; \quad K_2 = 2.5 \times 10^{-6}$$

$$W_{cr} = 14 \text{ knots}$$

2.8 BOTTOM SHEAR STRESS

The problem of a correct formulation of the bottom shear stress is one of some debate and is one of the areas for further study suggested by Noda et.al. (1974). It is generally assumed that it is of the basic form of

$$\tau_b = \rho C_f |u| u$$

where u is the instantaneous velocity vector at the bottom. Longuet-Higgins (1970) showed that u is actually the total velocity vector due to the combined effect of the wave orbital velocity and the mean drift velocity. LeBlond and Tang (1974) state that for waves predominantly in the x direction, the bottom stress is actually anisotropic with

$$\overline{\tau}_{bx} = \frac{4\rho C_f}{\pi} U_{max} U \tag{2.64}$$

$$\overline{\tau}_{by} = \frac{2\rho C_f}{\pi} U_{max} V \tag{2.65}$$

where

$$U_{max} = \frac{\pi H}{T \sinh(kh)} \tag{2.66}$$

and is the maximum wave orbital velocity from linear wave theory, U and V are as previously defined and C_f is a friction coefficient dependent on the type of bottom, but shown by Longuet-Higgins (1970) to have a value of about .01.

Since the derivation of Equations 2.64 and 2.65 are not widely known and of some interest, it is given in Appendix A.

2.9 BREAKING CRITERIA

Since Equation 2.48 is applicable only in determining the wave heights of nonbreaking waves, some method is needed to determine the point of breaking and the wave heights after breaking. Though a number of formulas for doing this have been developed, there is not as yet one which is universally applicable or accepted. The choice of a breaking criteria, although somewhat arbitrary, must be made with care since it determines the width of the surf zone and thus controls the set-up. The simplest breaking criteria is that predicted by solitary wave theory.

$$\left(\frac{H}{D}\right)_b = \text{constant} = .78 \tag{2.67}$$

where the subscript, b, denotes the value at breaking. There is, however, considerable evidence (Weggel, 1972) that this is an oversimplification.

Noda et.al. (1974) used a modified version of the Miche formula

$$\left(\frac{H}{L}\right)_b = .12 \tanh \left(\frac{D}{L}\right)_b \qquad (2.68)$$

both to predict the point of breaking and the decay of the wave after breaking. This was done by calculating both a wave height from Equation 2.48 and a breaking height from Equation 2.68. When the point was reached where the wave height was equal to or greater than the breaking height, the wave was considered to have broken and the wave height from Equation 2.68 was used.

It was found in the course of this study that the above criteria predicted too wide a surf zone. Better results were obtained with the criteria proposed by Weggel (1972).

$$\left(\frac{H}{D}\right)_b = b(m) - a(m)\,\frac{H_b}{T^2} \qquad (2.69)$$

where

$$a(m) = 1.36(1-e^{-19m}) \qquad (2.70)$$

$$b(m) = \frac{1.56}{1 + e^{-19.5m}}\ \sec^2/\mathrm{ft} \qquad (2.71)$$

$$m = \text{slope}$$

This criteria has one serious drawback in that the breaking height goes to zero for deepwater. It, therefore, cannot be used in a similar procedure as the Miche formula which goes to infinity as the depth gets deeper. For this reason, though it was found to give better results, it was only used in the one-dimensional wave channel case. For the other cases, Equation 2.68 was used.

CHAPTER III

NUMERICAL FORMULATION

In order to formulate the numerical model, the basic framework of the computer program must be established. This includes a grid scheme, flow chart, finite difference forms of the equations, and a set of boundary conditions.

In order to approximate true beach contours, a specific area is divided into a series of grids with a characteristic depth, and an area of $\Delta x \Delta y$. It is, therefore, easy to vary the accuracy of the bottom representation by adjusting the grid dimensions. The grid system used is illustrated in Figure 4. The x-axis runs perpendicular from the beach a distance of M grids, with the y-axis parallel to the shore consisting of nN+2 blocks, where n is an integer. The purpose of the extra grids will be discussed later in this chapter. Figure 5 illustrates block (i,j): all major quantities $(H, \theta, k, \bar{\eta}, S_{xx}, S_{xy}$, etc.) are calculated at the grid center, with velocities (U,V) calculated at the edges. Central velocities are found by averaging U or V across the grid.

Since they will be used later, the basic finite difference approximations are given below. If the values of a variable (A) are known for all the grid points, then there are three ways to express $\frac{\partial A_{i,j}}{\partial x}$:

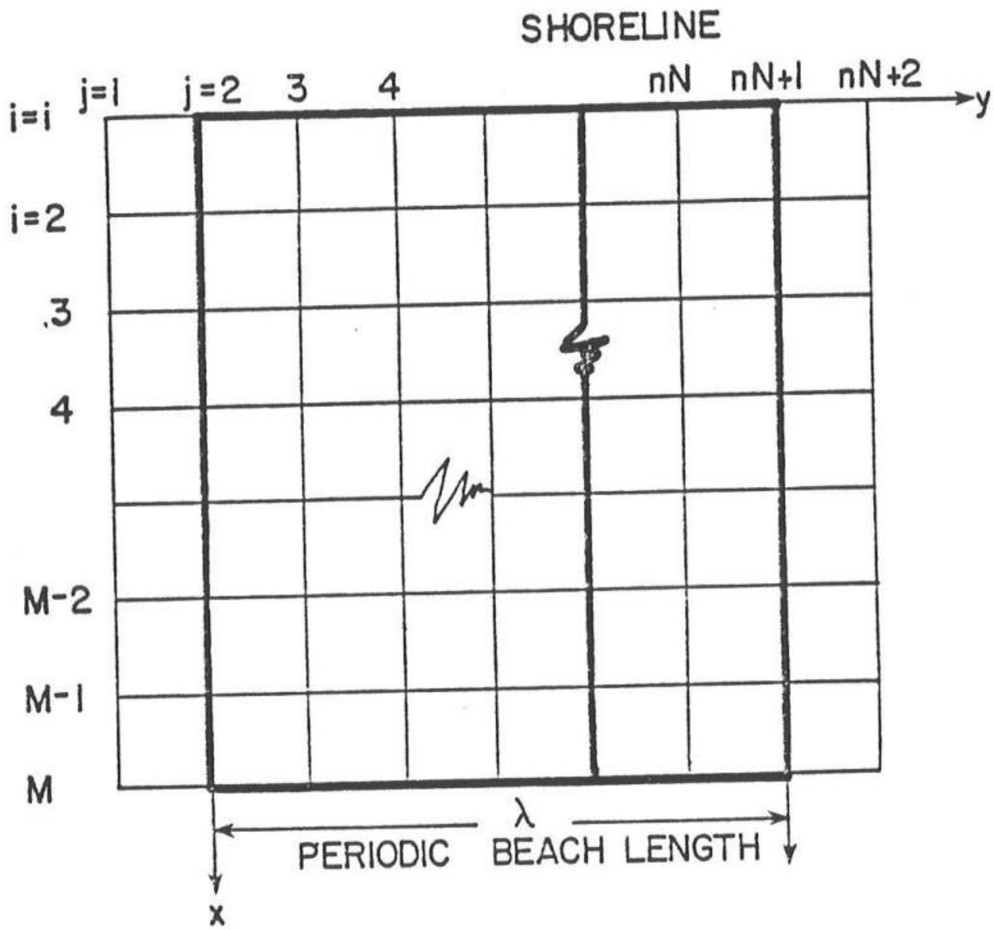

Figure 4 Grid Scheme [After Noda et.al. (1974)]

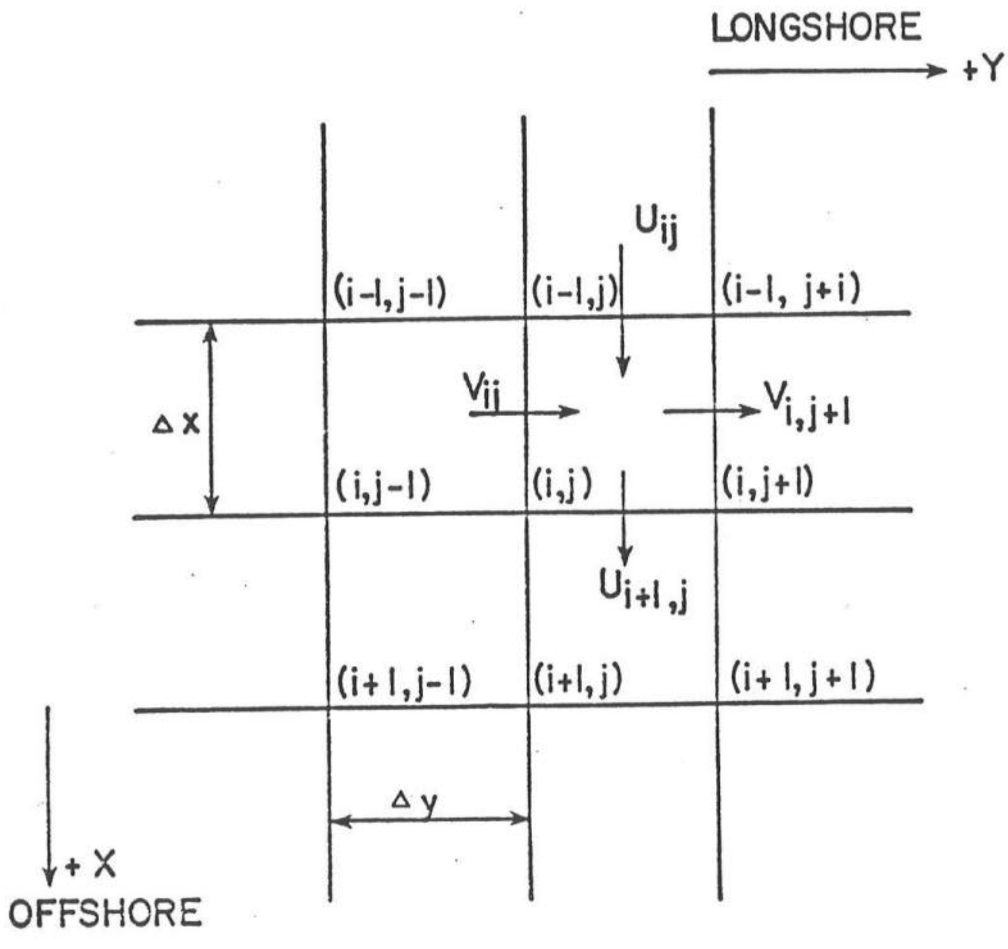

Figure 5 Velocity Components for Grid Block (i,j). All Other Variables (D, S_{xx}, S_{xy}, H, etc.) are Determined at Grid Center.

$$\text{Forward Difference, } \frac{\partial A_{i,j}}{\partial x} = \frac{A_{i+1,j} - A_{i,j}}{\Delta x} + 0(\Delta x), \tag{3.1}$$

$$\text{Central Difference, } \frac{\partial A_{i,j}}{\partial x} = \frac{A_{i+1,j} - A_{i-1,j}}{2\Delta x} + 0(\Delta x^2), \tag{3.2}$$

$$\text{Backward Difference, } \frac{\partial A_{i,j}}{\partial x} = \frac{A_{i,j} - A_{i-1,j}}{\Delta x} + 0(\Delta x), \tag{3.3}$$

where $0(\Delta x)$ refers to additional terms "of the order Δx" and is an indication of the error involved in the approximation. Note that the j index does not change as it refers to the y direction. It is easily seen from these equations, that the accuracy of the approximation depends on the size of the grid (Δx) and also on the amount of change in (A) from one grid to the next.

There are two numerical schemes that may be used to represent differential equations, the explicit or implicit, each having some advantages. Though only a brief discussion will be given here, the interested reader is directed to Roache (1972) or Abbott and Ionescu (1967) for a more rigorous analysis.

The explicit formulation is commonly used as it is the easiest for computer programming. In this scheme, during one iteration in time (Δt), the old value of a variable is updated to find the new value, using other variables from the past iteration. Stability of this type of procedure for hydraulic models depends on whether or not the criteria,

$$\frac{\Delta x}{\Delta t} \geq \sqrt{gh} \text{ , 1-dimensional problem} \tag{3.4}$$

$$\frac{\Delta x}{\Delta t} \geq \sqrt{2gh} \text{ , 2-dimensional problem} \tag{3.5}$$

are satisfied. The left side of these equations can be interpreted as the "solution velocity" and the right side as the maximum shallow water wave celerity. When the above criteria is not satisfied, the solution becomes unstable. Inspection of Equations 3.4 and 3.5 reveal that in an explicit operation, it is impossible to have both long time steps that reduce computer costs, and small grids that increase the accuracy of the calculations.

The implicit formulation differs from the explicit in that by updating several variables at once, a computationally stable scheme is achieved. This, therefore, allows longer time steps to be taken without the loss of detail.

In this work, an explicit scheme was used in both the one and two-dimensional cases. A one-dimensional implicit solution that included the convective acceleration terms of Equation 2.20 was employed in order to verify the explicit solution and reveal the importance of the neglected terms. This implicit scheme is discussed in Appendix B.

3.1 FINITE DIFFERENCE FORMS OF EQUATIONS

In this section, the finite difference forms of the governing equations of Chapter II are derived using Equations 3.1, 3.2 and 3.3. The continuity equation was approximated using a forward time, forward space (FTFS) scheme. Through finite differencing, Equation 2.13 becomes by term,

$$\frac{\partial \bar{\eta}}{\partial t} = \frac{\bar{\eta}^{k+1}_{i,j} - \bar{\eta}^{k}_{i,j}}{\Delta t} \qquad k \text{ denotes a step in time}$$

$$\frac{\partial}{\partial x}[U(h+\bar{\eta})] = \left[\frac{U_{i+1,j}\left(\frac{D_{i,j}+D_{i+1,j}}{2}\right) - U_{i,j}\left(\frac{D_{i,j}+D_{i-1,j}}{2}\right)}{\Delta x}\right]^{k}$$

$$\frac{\partial}{\partial y}[V(h+\bar{\eta})] = \left[\frac{V_{i,j+1}\left(\frac{D_{i,j+1}+D_{i,j}}{2}\right) - V_{i,j}\left(\frac{D_{i,j-1}+D_{i,j}}{2}\right)}{\Delta y}\right]^{k}$$

where

$$D_{i,j} = (h+\bar{\eta})_{i,j} \tag{3.6}$$

is the total depth and is averaged across the grid sides where U,V are known. Combining and solving for $\bar{\eta}^{k+1}_{i,j}$ a final form is obtained.

$$\begin{aligned} \bar{\eta}^{k+1}_{i,j} = \bar{\eta}^{k}_{i,j} + \Delta t \Big\{ & \frac{1}{2\Delta x}[U_{i,j}(D_{i,j}+D_{i-1,j}) - U_{i+1,j}(D_{i,j}+D_{i+1,j})] \\ & + \frac{1}{2\Delta x}[V_{i,j}(D_{i,j-1}+D_{i,j}) - V_{i,j+1}(D_{i,j+1}+D_{i,j})]\Big\}^{k} \end{aligned} \tag{3.7}$$

Values of U,V are found from Equations 2.21 and 2.22, which rewritten are

$$x: \quad \frac{\partial U}{\partial t} = -g\frac{\partial \bar{\eta}}{\partial x} - \frac{1}{\rho(h+\bar{\eta})}\left[\frac{\partial S_{xx}}{\partial x} + \frac{\partial S_{xy}}{\partial y} - \bar{\tau}_{sx} + \bar{\tau}_{bx}\right] \tag{3.8}$$

$$y: \quad \frac{\partial V}{\partial t} = -g\frac{\partial \bar{\eta}}{\partial y} - \frac{1}{\rho(h+\bar{\eta})}\left[\frac{\partial S_{yx}}{\partial x} + \frac{\partial S_{yy}}{\partial y} - \bar{\tau}_{sy} + \bar{\tau}_{by}\right] \tag{3.9}$$

Recalling again from Figure 5 that velocities are calculated on the grid sides, these equations are differenced forward in time and backwards in space (FTBS). Defining,

$$\overline{D} = \frac{1}{2}(D_{i,j}+D_{i-1,j})^{k},$$

Equation 3.8 becomes,

$$\frac{U^{k+1}_{i,j} - U^{k}_{i,j}}{\Delta t} = -g[\frac{\overline{\eta}_{i,j}-\overline{\eta}_{i-1,j}}{\Delta x}]^{k} - \frac{1}{\rho\overline{D}}\left\{\frac{S^{k}_{xx_{i,j}} - S^{k}_{xx_{i-1,j}}}{\Delta x} + \right.$$

$$\frac{1}{2}[\frac{S^{k}_{xy_{i,j+1}} - S^{k}_{xy_{i,j-1}}}{2\Delta y} + \frac{S^{k}_{xy_{i-1,j}} - S^{k}_{xy_{i-1,j-1}}}{2\Delta y}] -$$

$$\left.\frac{\overline{\tau}^{k}_{sx_{i,j}} + \overline{\tau}^{k}_{sx_{i-1,j}}}{2} + \frac{\overline{\tau}^{k}_{bx_{i,j}} + \overline{\tau}^{k}_{bx_{i-1,j}}}{2}\right\}$$

Note that in arriving at the above form, central differences were used in S_{xy} and then averaged to get $\frac{\partial S_{xy}}{\partial y}$ at the grid side. For a similar reason, the shear stresses are averaged between grids (i,j) and (i-1,j). Solving for $U^{k+1}_{i,j}$, the final form is obtained.

$$U^{k+1}_{i,j} = U^{k}_{i,j} + \Delta t\left\{\frac{g}{\Delta x}(\overline{\eta}_{i-1,j}-\overline{\eta}_{i,j}) + \frac{1}{\rho\overline{D}}[\frac{1}{\Delta x}(S_{xx_{i-1,j}}-S_{xx_{i,j}})\right. \tag{3.10}$$

$$-\frac{1}{4\Delta y}(S_{xy_{i,j+1}}-S_{xy_{i,j-1}}+S_{xy_{i-1,j}}-S_{xy_{i-1,j-1}}) + \frac{1}{2}(\overline{\tau}_{sx_{i,j}}+\overline{\tau}_{sx_{i-1,j}})$$

$$\left.-\frac{1}{2}(\overline{\tau}_{bx_{i,j}}+\overline{\tau}_{bx_{i-1,j}})]\right\}^{k}$$

In the y direction, Equation 3.9 becomes,

$$V^{k+1}_{i,j} = V^{k}_{i,j} + \Delta t\left\{ \frac{g}{\Delta y} (\bar{\eta}_{i,j-1} - \bar{\eta}_{i,j}) + \frac{1}{\rho \bar{D}} [\frac{1}{4\Delta x}(S_{xy_{i-1,j-1}} - S_{xy_{i+1,j-1}} \right. \tag{3.11}$$

$$+ S_{xy_{i-1,j}} - S_{xy_{i+1,j}}) + \frac{1}{\Delta y}(S_{yy_{i,j-1}} - S_{yy_{i,j}}) + \frac{1}{2}(\bar{\tau}_{sy_{i,j}} + \bar{\tau}_{sy_{i,j-1}}) -$$

$$\left. \frac{1}{2} (\bar{\tau}_{by_{i,j}} + \bar{\tau}_{by_{i,j-1}})] \right\}^{k}$$

where $\bar{D} = \frac{1}{2}(D_{i,j} + D_{i,j-1})^{k}$

The major equations governing the refraction part of the program are: wave height (2.54), wave number (2.36) and wave angle (2.47). The solution procedure is to determine the refraction angle over the entire grid field, and then to solve for the wave height. New values of k are determined after every updating of H or θ. Rewriting Equation 2.47,

$$\frac{\partial\theta}{\partial x} \cos\theta + \frac{\sin\theta\ (U \sin\theta - V \cos\theta)}{A} + \frac{\partial\theta}{\partial y} \sin\theta - \frac{\cos\theta (U \sin\theta - V \cos\theta)}{A} =$$

$$\overline{\frac{1}{k}\frac{\partial k}{\partial y}} \cos\theta - \overline{\frac{1}{k}\frac{\partial k}{\partial x}} \sin\theta$$

Finite differencing this by using a forward difference in x, and a backwards difference in y, and solving for $\theta_{i,j}$, the following equation was found by Noda <u>et.al</u>. (1974).

$$\theta_{i,j} = \frac{1}{B_{i,j}}\left\{ \overline{\frac{1}{k}\frac{\partial k}{\partial y}} \cos\theta_{i,j} - \overline{\frac{1}{k}\frac{\partial k}{\partial x}} \sin\theta_{i,j} + \right.$$

$$\frac{\theta_{i,j-1}}{\partial y} [\sin\theta_{i,j} - \frac{\cos\theta_{i,j}}{A_{i,j}} (U \sin\theta_{i,j} - V \cos\theta_{i,j})] - \tag{3.12}$$

$$\left. \frac{\theta_{i+1,j}}{\Delta x} [\cos\theta_{i,j} (U \sin\theta_{i,j} - V \cos\theta_{i,j})] \right\}$$

with

$$B_{i,j} = \frac{\sin\theta_{i,j}}{\Delta x} - \frac{\cos\theta_{i,j}}{\Delta y} - \frac{1}{A_{i,j}} (U\sin\theta_{i,j} - V\cos\theta_{i,j})(\frac{\cos\theta_{i,j}}{\Delta y} + \frac{\sin\theta_{i,j}}{\Delta x}) \tag{3.13}$$

where $A_{i,j}$ - as defined in Equation 2.44

$\overline{\frac{1}{k}\frac{\partial k}{\partial x}}$, $\overline{\frac{1}{k}\frac{\partial k}{\partial y}}$ - as defined in Equations 2.45 and 2.46

V,U,k - values taken at i,j

Values of $\cos\theta_{i,j}$ and $\sin\theta_{i,j}$ are determined using an average of these quantities from four surrounding grid blocks approximated to second order in a Taylor series.

$$\sin\theta_{i,j} = \frac{1}{4} (\sin\theta_{i+1,j} + \sin\theta_{i-1,j} + \sin\theta_{i,j+1} + \sin\theta_{i,j-1}) + \frac{1}{8} [(\theta_{i+1,j} - \theta_{i-1,j})(\cos\theta_{i-1,j} - \cos\theta_{i+1,j}) + (\theta_{i,j+1} - \theta_{i,j-1})(\cos\theta_{i,j-1} - \cos\theta_{i,j+1})] \tag{3.14}$$

$$\cos\theta_{i,j} = \frac{1}{4} (\cos\theta_{i+1,j} + \cos\theta_{i-1,j} + \cos\theta_{i,j+1} + \cos\theta_{i,j-1}) + \frac{1}{8}[(\theta_{i+1,j} - \theta_{i-1,j})(\sin\theta_{i+1,j} - \sin\theta_{i-1,j}) + (\theta_{i,j+1} - \theta_{i-1,j})(\sin\theta_{i,j+1} - \sin\theta_{i,j-1})] \tag{3.15}$$

Using Equations 3.12 to 3.15, the angle, θ, is updated through iteration, until every grid point is within an acceptable error of itself. In this study as in Noda <u>et.al.</u> (1974), the criterion was,

$$|\theta_{new} - \theta_{old}| \leq .001|\theta_{new}| \tag{3.16}$$

Convergence is usually very fast being obtained in 2 to 4 iterations.

The wave number Equation 2.36,

$$[gk \tanh(kh)]^{1/2} + Uk \cos\theta + Vk \sin\theta = \frac{2\pi}{T}$$

is solved through a Newton iterative technique defined as;

$$k_{new} = k_{old} - \frac{f(k_{old})}{f'(k_{old})} \tag{3.17}$$

where $f'(k)$ is the first derivative of $f(k)$. Defining:

$$f(k) = gk \tanh kh - [\frac{2\pi}{T} - Uk \cos\theta - Vk \sin\theta]^2 \tag{3.18}$$

$$f'(k) = g[kh \operatorname{sech}^2(kh) + \tanh(kh)] + 2[U \cos\theta + V \sin\theta] \cdot [\frac{2\pi}{T} - Uk \cos\theta - Vk \sin\theta] \tag{3.19}$$

Equation 3.17 is iterated until

$$|k_{new} - k_{old}| \leq .001|k_{new}| \tag{3.20}$$

Rearranging the wave height Equation 2.54, it becomes,

$$\frac{\partial H}{\partial t} + (U+C_g \cos\theta) \frac{\partial H}{\partial x} + (V+C_g \sin\theta) \frac{\partial H}{\partial y} = \frac{H}{2} Q \tag{3.21}$$

with

$$Q = \{C_g \sin\theta \frac{\partial\theta}{\partial x} - C_g \cos\theta \frac{\partial\theta}{\partial y} - [\frac{\partial U}{\partial x} + \frac{\partial V}{\partial y}] - \cos\theta \frac{\partial C_g}{\partial x} - \sin\theta \frac{\partial C_g}{\partial y} - \overline{\tau}\} \tag{3.22}$$

When this is finite differenced forward in time and x, backwards in y, and is solved for $H^k_{i,j}$, the following form is arrived at,

$$H^{k+1}_{i,j} = \frac{\frac{H^k_{i,j}}{\Delta t} - \frac{H^k_{i+1,j}}{\Delta x}(U+C_g \cos\theta)^k + \frac{H^k_{i,j-1}}{\Delta y}(V+C_g \sin\theta)^k}{\frac{1}{\Delta t} + \frac{1}{\Delta y}(V+C_g \sin\theta)^k - \frac{1}{\Delta x}(U+C_g \cos\theta)^k \frac{Q^k_{i,j}}{2}} \tag{3.23}$$

This is the finite difference equation used in the calculation of time dependent input wave height. If steady state is assumed, the terms containing Δt drop out and Equation 3.23 reduces to the form used by Noda et.al. (1974).

Taking central differences for $\frac{\partial\theta}{\partial x}$, $\frac{\partial\theta}{\partial y}$ and using Equations 2.53 to 2.60 given in Chapter II, the steady state form of Equation 3.23 can be solved through a row by row relaxation technique that begins in deepwater and progresses onshore. Again the iteration is continued until an accuracy criterion is satisfied and,

$$|H_{new} - H_{old}| \leq .001|H_{new}| \tag{3.24}$$

3.2 COMPUTER PROGRAM

Since the complete flow chart of the program is very complex, a highly simplified version is outlined in Figure 6. To facilitate

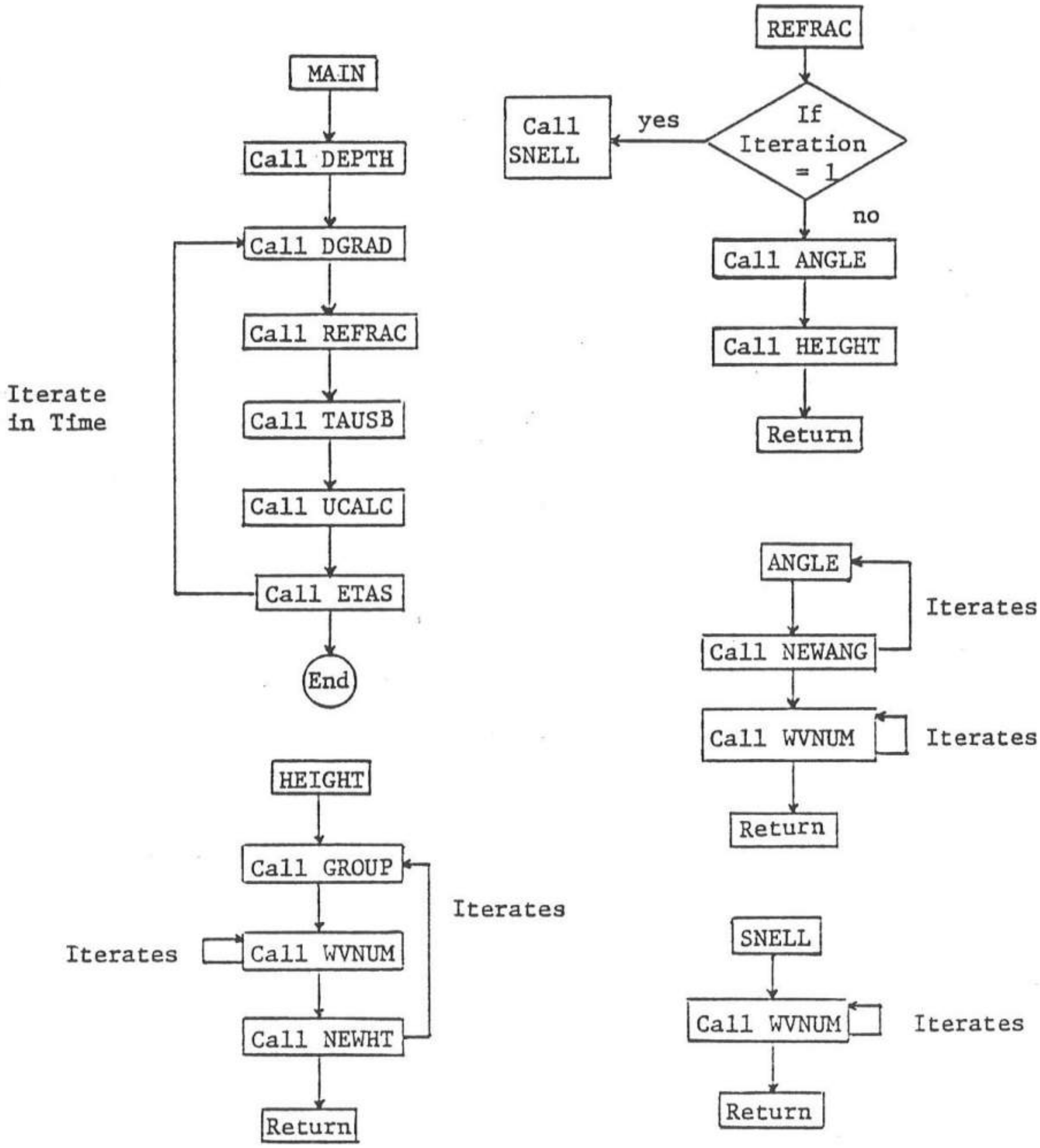

Figure 6 Simplified Flow Chart

understanding, it is written in subroutines which are explained below:

MAIN - not actually a subroutine, this part of the program handles all input and output functions, and ties the subroutines together.

DEPTH - determines the initial depth (h) at each grid. Changes in bottom topography are easily accommodated by changing DEPTH only.

DGRAD - after each updating of the total depth ($D=h+\bar{\eta}$), this routine calculates

$$\frac{\partial D}{\partial x}, \frac{\partial D}{\partial y}$$

REFRAC - this routine ties all refraction subroutines together.

SNELL - called once only, this generates a starting value for the refraction program by calculating Snell's law at each grid. This routine also shoals in deepwater wave height to grid system.

WVNUM - updates values of k using values of U, V, D and θ, Equation 3.17.

ANGLE - solves for θ by relaxation, Equation 3.12.

NEWANG - updates values of θ including wave-current interaction.

HEIGHT - calculates H through row by row relaxation, including wave-current interaction, also calculates radiation stresses, Equation 3.23.

NEWHT - updates H, checks for breaking, Equation 2.68 or 2.69.

TAUSB - calculates bottom and surface stresses, Equations 2.61, 2.62, 2.64 and 2.65.

UCALC - calculates U and V, Equations 3.10 and 3.11.

ETAS - updates grid depth by calculating $\overline{\eta}$. Also allows beach flooding, Equation 3.7.

GROUP - calculates values of C, C_g and their spatial derivatives, Equations 2.55 to 2.60.

3.3 BOUNDARY CONDITIONS

In order to satisfy the equations at the sides of the grid system, extra grid columns are added at i=1, j=nN+2. Calculations are performed from j=2 to j=nN+1 with values at these side grids set internally. No flow conditions are imposed at the beach, i=1 and at the offshore row i=M, but the location of the beach boundary is allowed to fluctuate through flooding.

For the open coast case, the boundary conditions are satisfied by requiring a beach, of periodic length nN(Δy), where n is an integer. Values at side grids can then be established using the following criteria

$$\begin{aligned} Q_{i,1} &= Q_{i,N} \\ Q_{i,N+2} &= Q_{i,3} \\ Q_{i,2} &= Q_{i,N+1} \end{aligned} \tag{3.25}$$

where Q is some quantity (H,U,V,etc.). These boundary conditions were also used for the wave channel problem, with the addition that flow was constrained to the x-direction (V=0).

The two-dimensional wave basin required that the periodic boundary condition be modified to include walls at j=2, j=N+1, where a no-flow condition was established,

$$V_{i,j} = 0 \begin{cases} i = 1 \text{ to } M \\ j = 2,\ N+1 \end{cases}$$

To accommodate this condition, a reflection boundary condition was used as shown in Figure 7 with

$$Q_{i,j} = Q_{i,2}$$

$$Q_{i,N+2} = Q_{i,N+1}$$

While in theory this is a valid criterion, some unrealistic results were obtained due to central differences taken across the side walls. To avoid this problem and still retain the general finite difference Equations 3.7, 3.10, and 3.11, backwards differences were employed at the wall boundary. The effected quantities were $\frac{\partial S_{xy}}{\partial x}$, $\frac{\partial S_{xy}}{\partial y}$. The backwards differences were obtained by making the following substitution for the value of the quantity at the edge boundaries (j=1,j=N+2)

$$\begin{aligned} Q_{i,1} &= 2Q_{i,2} - Q_{i,3} \\ Q_{i,N+2} &= 2Q_{i,N+1} - Q_{i,N} \end{aligned} \tag{3.26}$$

It is a simple procedure to show that these equations reduce the central difference

$$\frac{\partial Q_{i,2}}{\partial y} = \frac{Q_{i,3} - Q_{i,1}}{2\Delta y} \tag{3.27}$$

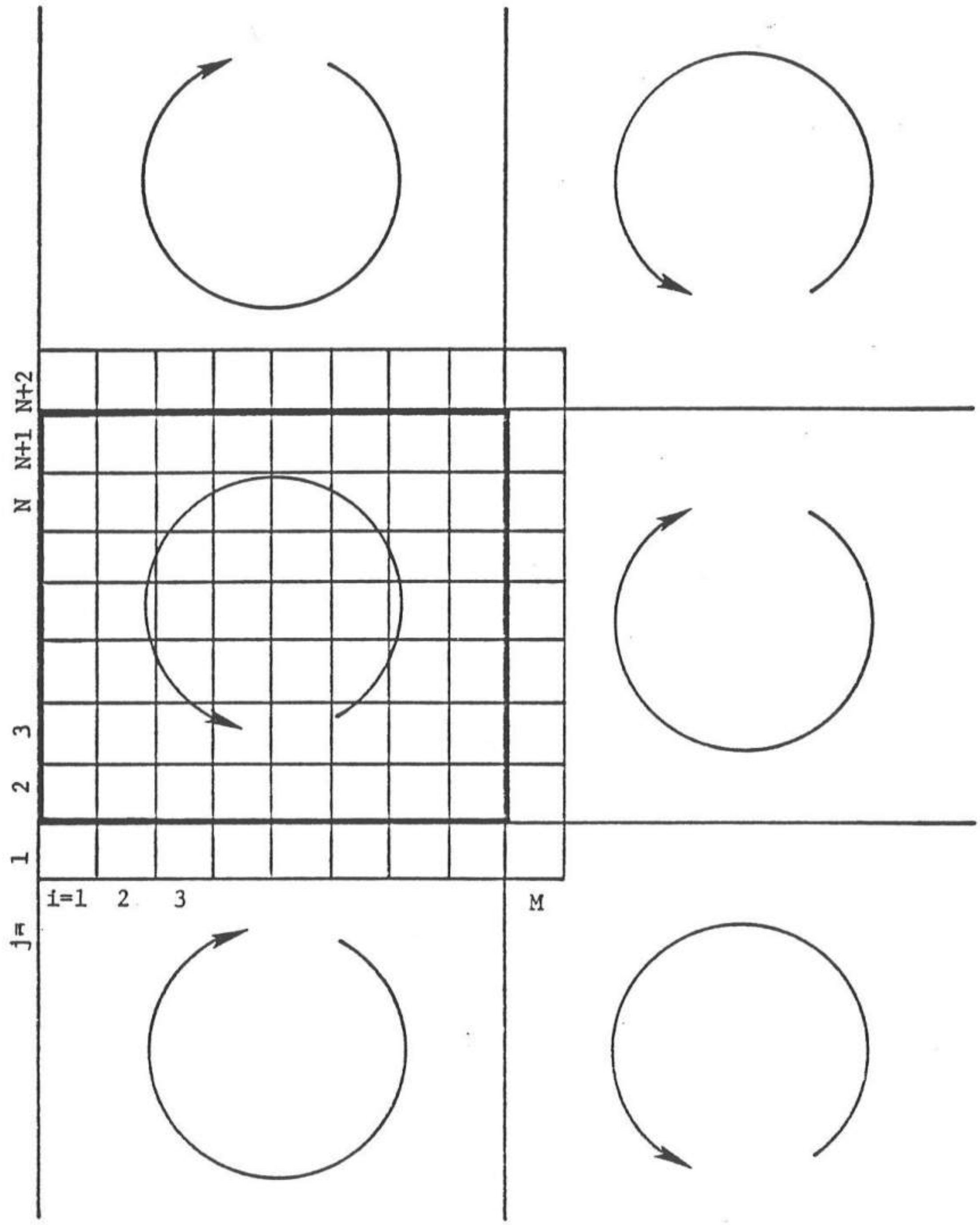

Figure 7 Two-Dimensional Basin Boundary Condition Flow is Reflected Across the Side and End Walls.

to the backwards difference.

$$\frac{\partial Q_{i,2}}{\partial y} = \frac{Q_{i,3}-Q_{i,2}}{\Delta y} \tag{3.28}$$

Although this may not be the most rigorous approach, it allowed a fairly quick testing of the general equations, and as will be shown, provided reasonable results. The procedure also revealed that the numerical scheme can be adopted to various basic configurations.

Since flooding is a very important consequence of wind and wave action, it was included in the program. The procedure is diagrammed in Figure 8 and requires only that the landward most grid row (i=1) remain dry. When the situation shown in Figure 8a occurs, such that the water depth at block (i,j) due to the set-up $\bar{\eta}_{i,j}$ is greater than the depth at grid (i-1,j), a small amount of the difference is moved from (i,j) to (i-1,j) as shown in Figure 8b. Once the block is "wet," it is included in the calculations, and very quickly fills with water. If for some reason, the reverse occurs and the depth at block (i-1,j) becomes less than the original amount placed in it, the program drys the block by moving the remaining water to grid (i,j).

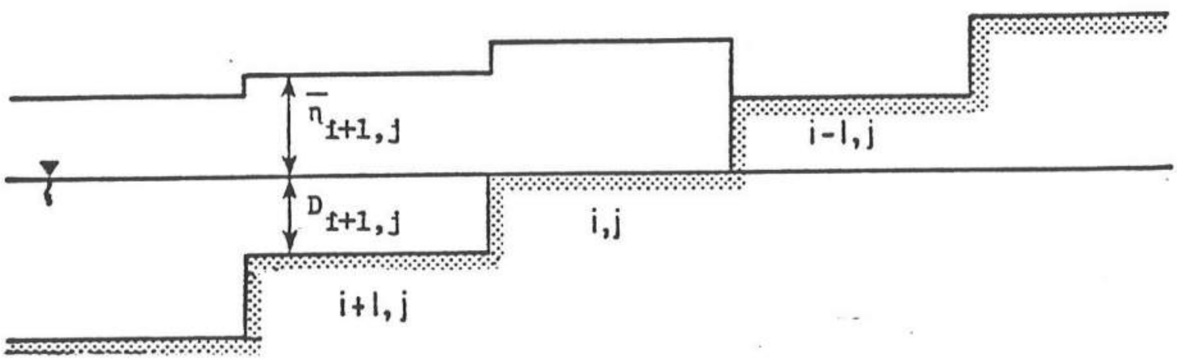

Figure 8a Before Flooding, $\overline{\eta}_{i,j} > -D_{i-1,j}$

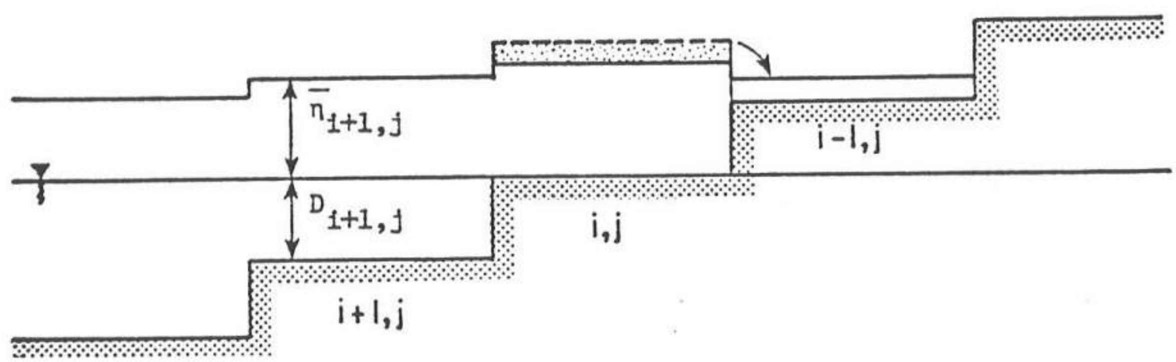

Figure 8b A Small Amount of $\overline{\eta}_{i,j}$ is Moved to Grid (i-1,j) in Order to Flood the "Dry" Block.

FIGURE 8 FLOODING SCHEMATIC

CHAPTER IV

RESULTS

Although three different cases were tested, a number of comments can be made about the program in general. The time dependency while necessary in revealing transient effects is severely limited by the stability criteria, Equations 3.4 and 3.5. It was found for all cases that at least 400 or more time step iterations were needed to arrive at a steady state condition. The implicit scheme was developed in hopes of increasing the allowable time step and to determine the effects of the convective acceleration terms. Although the implicit program produced results similar to the explicit one for the same time step, when the time step was increased, different results were obtained. Though the solution was still stable, large time and grid sizes led to inaccurate results (Abbott, 1967). Because of this and due to the complexity of formulating a two-dimensional implicit model, all subsequent tests were made with the explicit formulation.

It was also found that due to the no-flow boundary condition at row M, when the model was impulsively started up by applying the full wave height field, it developed a high amplitude seiche. To reduce this problem, the deepwater wave height was gradually increased from zero to the desired value during the first 40 to 100 iterations. This did not completely eliminate the seiching and it was found that the period of these oscillations could be accurately predicted knowing only the basin configuration.

Another problem was also revealed by the flooding technique. The refraction program was not able to converge on a solution if there was a mixture of dry and wet grids in the same row. Since this situation does occur when dry grids are flooded, the problem was avoided by not allowing flooding until the water level had set up enough to flood the entire row. Since this problem only occured during the beginning of the run, it had no effect on final results.

In all test cases a friction factor of .01 was used as suggested by Longuet-Higgins (1970) for a sand bottom. It should, of course, be adjusted to fit the bottom conditions and it is common practice to use the coefficient of friction to calibrate the model. This has not been done for the results given here for these tests were made, more to show the validity of the model than to predict actual velocity magnitudes.

4.1 WAVE CHANNEL

This relatively simple case was used to verify the program by using it to predict the experimental values of set-up measured by Bowen et.al. (1968). Their experimental apparatus consisted of a flume 40 meters long, 0.5 meters wide and 0.75 meters deep with a wooden beach at a 1:12 slope. This system was adapted to the program through a 6 x 34 grid system, $\Delta x = 15$ cm, $\Delta y = 10$ cm. Since the problem is one-dimensional, only wave heights were calculated by the refraction program.

Wave-current interaction was included. A deepwater wave height of 6.45 cm and period of T = 1.14 seconds was used. A total of 800 iterations were run, (Δt = .05 sec) with the deepwater wave building up during the first 80.

Figure 9 is a plot of the variations in set-up at the first wet grid over time. The seiching of the tank is clearly evident and has a period of 7.5 seconds. This value is accurately predicted by the formula for first mode sloshing in a rectangular basin, with a sloping bottom (Wilson, 1966).

$$T_s = 1.64 \frac{2\ell}{\sqrt{gh}} = 7.5 \text{ sec} \tag{4.1}$$

where T_s = seiche period

h = deepest depth = 34.4 cm.

ℓ = length of basin = 420 cm.

Figure 10 plots the predicted set-up from the mean water line for both the explicit and implicit schemes for iterations 380 (t = 19 sec.) and 400 (t = 20 sec.). It is evident that except for slight variations offshore of the breaker line, the two solutions are the same. It can be, therefore, theorized that at least in this one-dimensional case, the convective acceleration terms have had little effect. Although no attempt has been made to show this in the two-dimensional models, it is expected that they would be more important.

After 800 iterations (t = 40 sec.) a steady-state result was obtained with the explicit model and is shown in Figure 11. Also

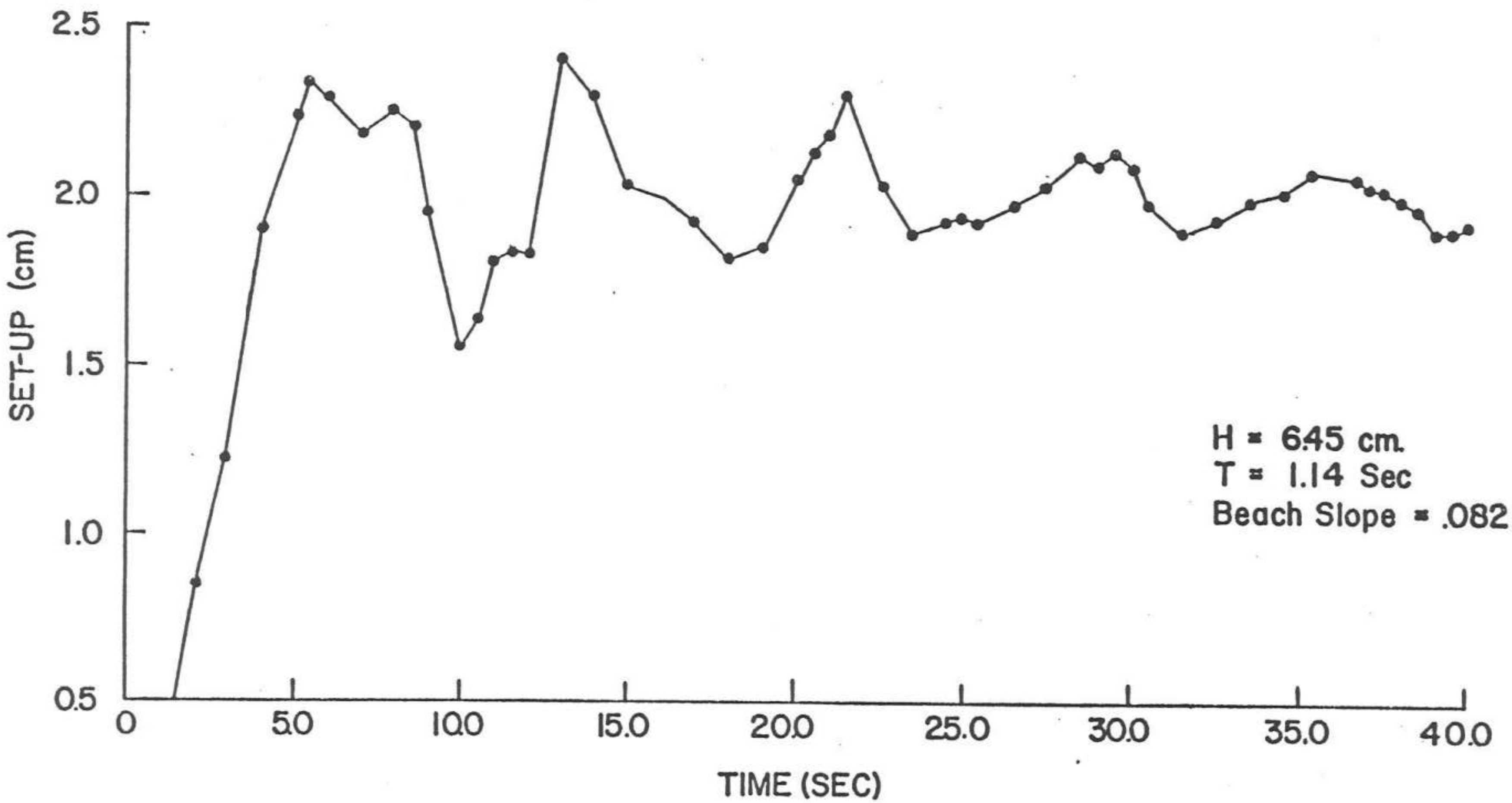

Figure 9 Maximum Set-Up at Beach as a Function of Real Time for the Wave Channel. Δt = .05 sec. Δx = 15 cm.

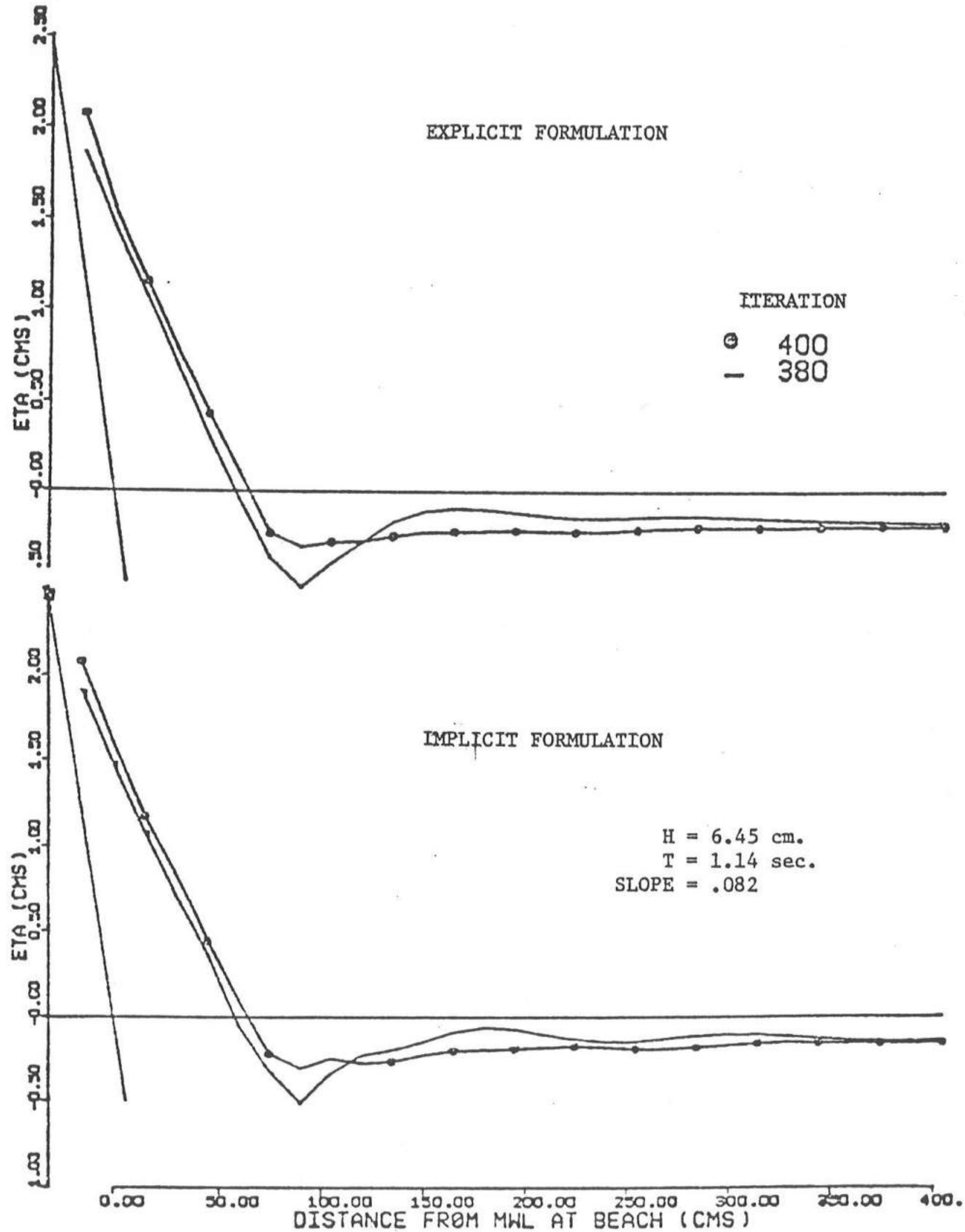

Figure 10 Comparison of Explicit and Implicit Set-Up Results (ETA) for the Same Time Step Iterations

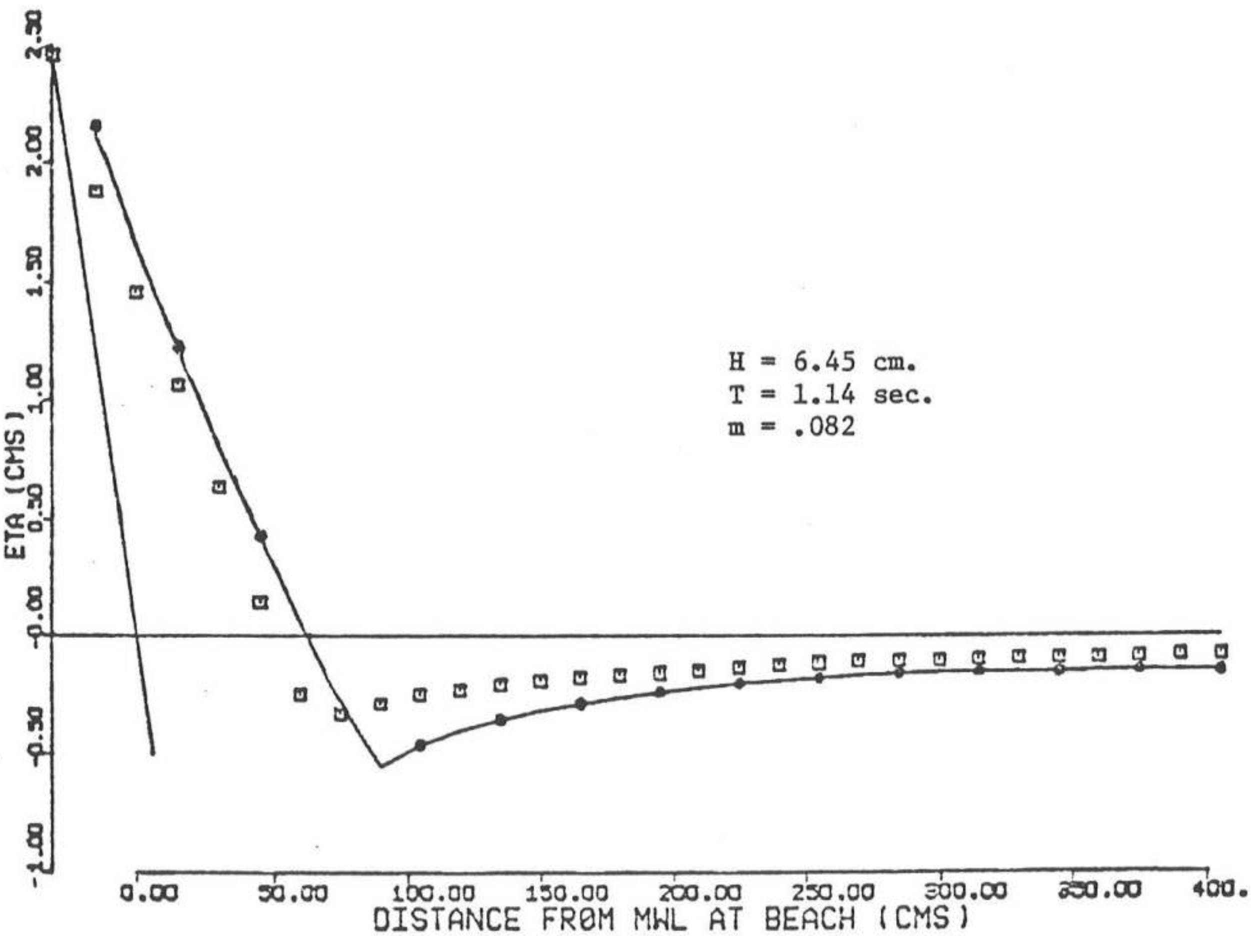

Figure 11 Final Results for Mean Water Level in Wave Channel Test. Squares Correspond to Experimental Data from Bowen et.al. (1968).

plotted are the experimental results of Bowen et.al. (1968). Maximum set-down is at the breaker line, and it was during these runs that it was found that Equation 2.69 approximated the experimental surf zone width better than Equation 2.68. The generally lower set-down offshore calculated by the model is the result of using a shorter tank than Bowen did (4.0m vs. 40m) and the effects of conservation of mass.

Using the results of iteration 800 as a starting point, the effect of a time dependent deepwater wave height was tested. This was done using a sinusoidal variation of the wave height, similar to what would be experienced when groups of waves impinge on a shore.

$$H_o = H_s + A \sin \left(2\pi n \frac{\Delta t}{T_g}\right) \tag{4.2}$$

H_s = starting wave height = 6.45 cm.

A = amplitude of variation = 1.15 cm.

n = iteration number (n = 1, 2, 3, ...)

T_g = period of the wave group = 18 sec.

Figure 12 is a plot of the time variation of both the deepwater wave height and the resulting set-up at the beach. In this run, the set-up lags the wave height by about 2.5 seconds due to the travel time of the wave to shore. Figure 13 shows cross sections of the set-up at maximum and minimum points of Figure 12, t = 10 sec. and t = 15. There is little variation offshore, but the breaking line has moved, a result of the increased breaker height.

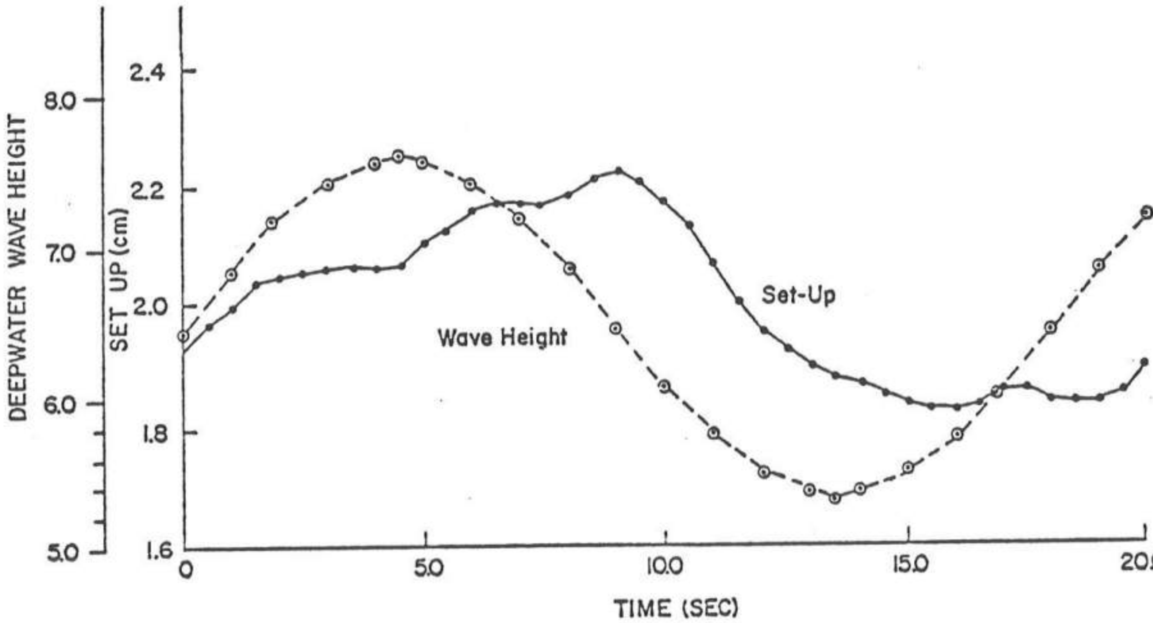

Figure 12 Set-Up at Shoreline in Wave Channel Due to a Wave Group with a Period of 18.0 Seconds.

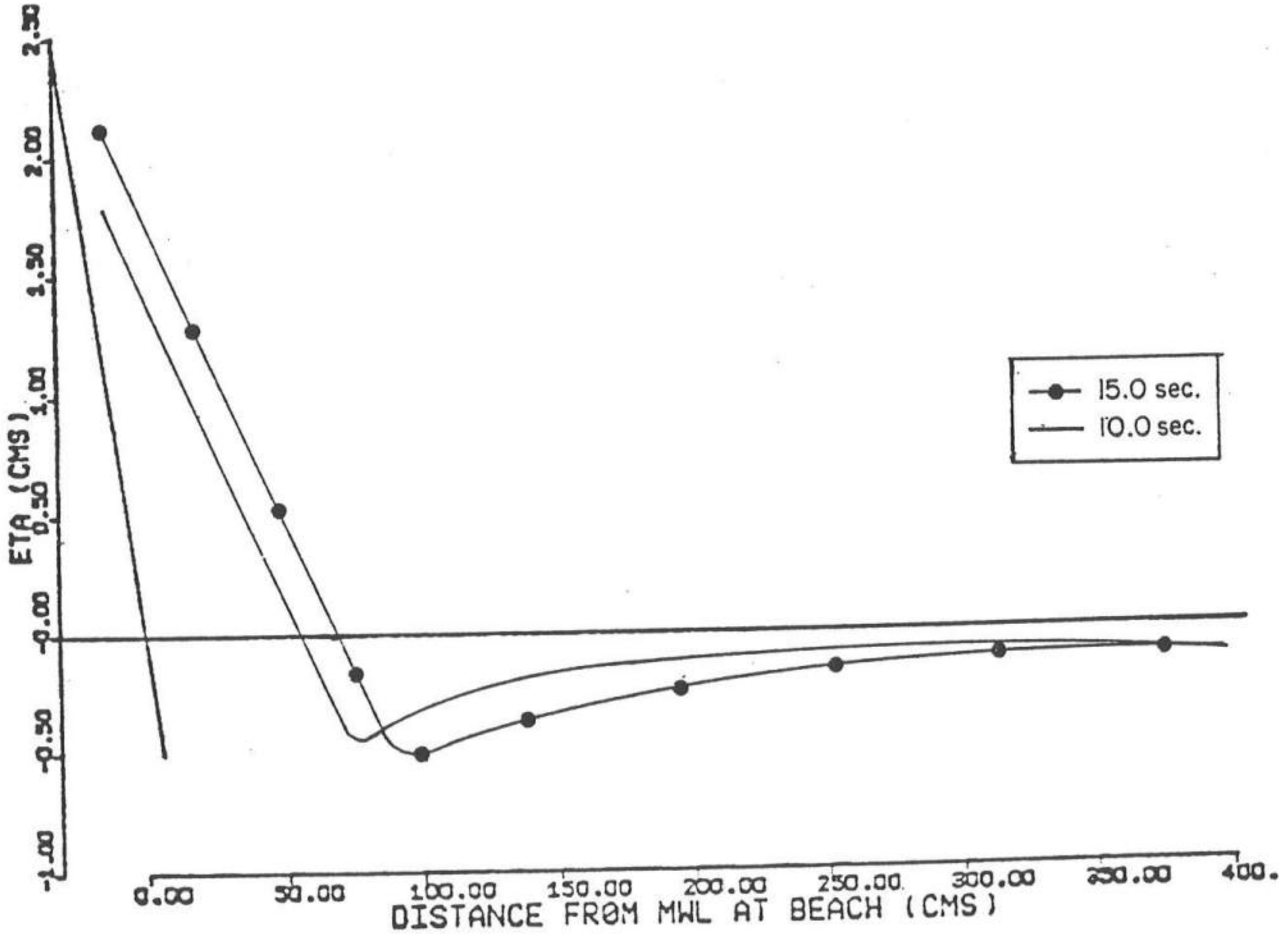

Figure 13 Comparison of Set-Up (ETA) Cross-Sections for the 10 and 15 sec. Points Shown in Figure 12.

An interesting variation of this test was found when the period of the wave group was set equal to the natural period of the basin. Starting at iteration 600 ($t = 30$ sec., Figure 10) a resonant condition was quickly established and the solution became unstable after an additional 300 iterations. The results are shown in Figure 14. A practical aspect of this is possible resonance of a harbor when excited by wave groups at its natural frequency.

4.2 WAVE BASIN

This second test case, though it necessitated a change in boundary conditions, allowed the entire program to be tested on a simple plane beach. Two versions of the experimental wave tank of Dalrymple et.al. (1975) were used. One modeled the basin directly with a 30 x 6 grid system, and the other modeled only half of the length using a 15 x 6 grid. Both cases used the same grid size $\Delta x = 5$ cm., $\Delta y = 10$ cm., and slope (.086). A wave of $H_o = 0.35$ cm., $T = 0.96$ sec., $\theta_o = 204°$ was employed. Runs of 600 iterations were made for both but as a result of different Δt values, real time length differed. The short basin used a $\Delta t = .05$ sec. corresponding to 30 sec. (31 waves) and Δt for the long basin was .03 sec. resulting in a run of 18 sec. (19 waves).

A plot of the set-up at the beach for grid i=3, j=3 is shown in Figure 15. Again as in the wave channel, the basin is seiching. It was also found that due to the oblique forcing due to the waves, standing edge waves were formed. The period of the seiche can be predicted using Equation 4.1, which gives a period of 2.76 sec. for the

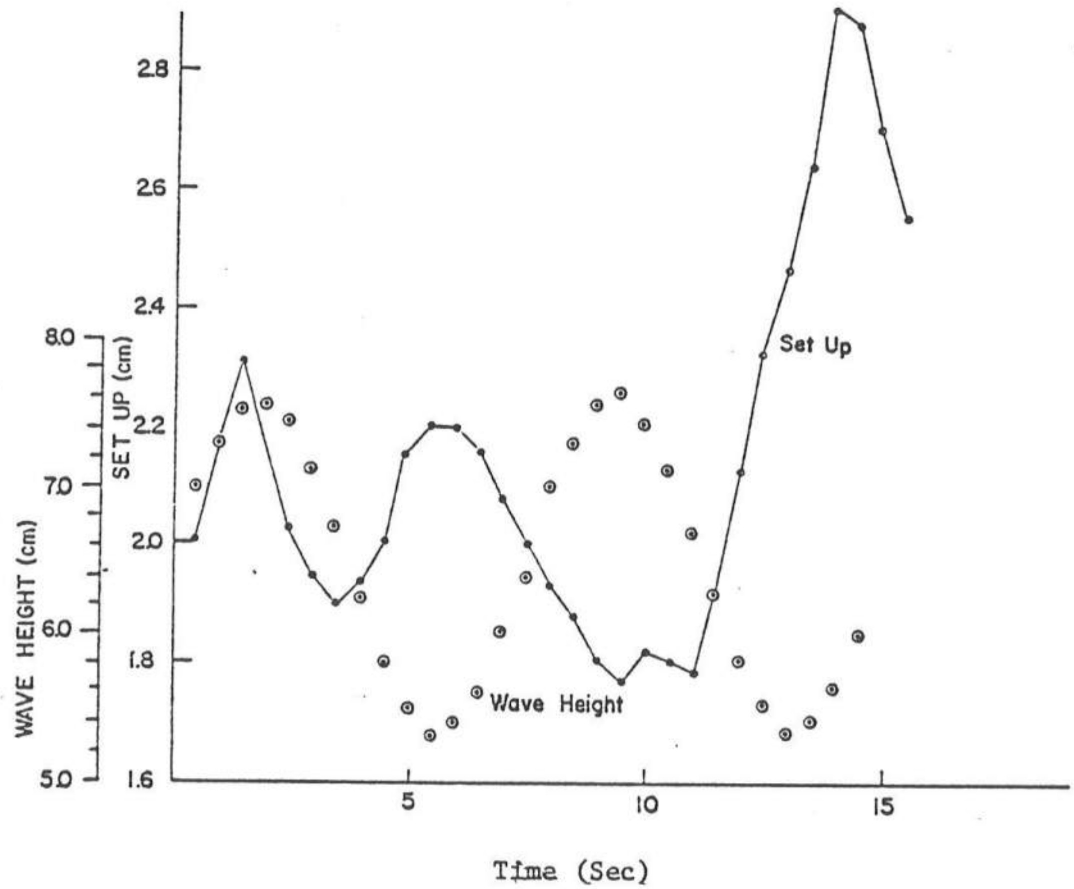

Figure 14 Resonance of Wave Channel When Forcing Function has Same Period as Natural Seiche. Startup After 30 Sec. from Figure 9.

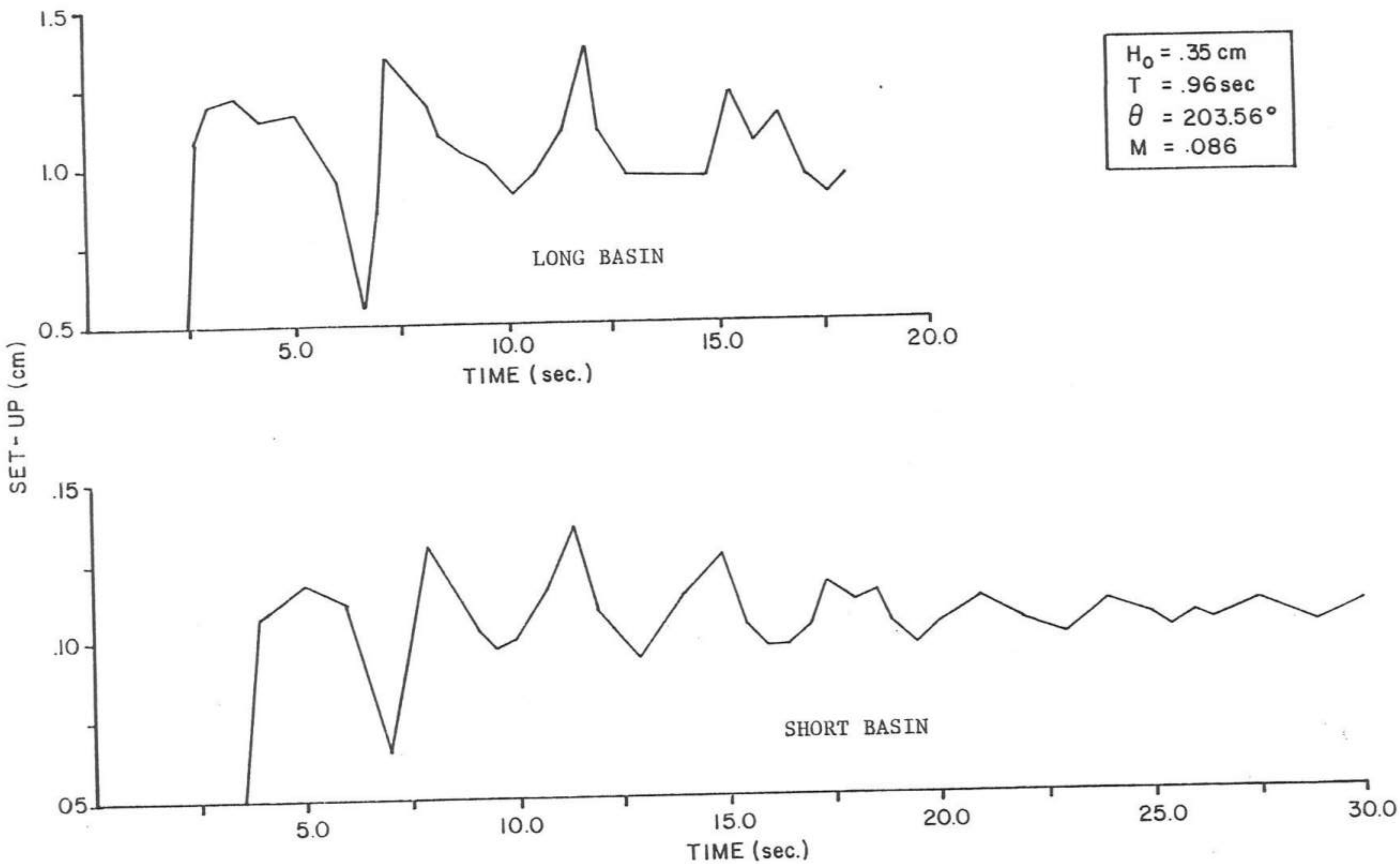

Figure 15 Mean Set-Up at Grid (i=3, j=3) Versus Real Time for Both Long and Short Two-Dimensional Basin Tests.

short basin (ℓ = 60 cm. and h = 5.16 cm.) and 3.9 sec. for the long one (ℓ = 120 cm., h = 10.32 cm.). These compare well with computed values of 2.7 and 3.6 respectively.

Figure 16 plots the velocity vectors in the short basin at the end of the run (t = 31 sec.). A strong longshore current has developed with a maximum value of 6.3 cm/sec. Offshore velocities are small but continue the circular trend. The same pattern is found in Figure 17 which shows the velocity vectors for the long basin. The maximum longshore velocity has been reduced to 5.2 cm/sec., and as found in the experiment, the offshore velocities are negligible but follow the same circular pattern found for the short basin. Both these results compare well with the experimental streamlines shown in Figure 18. This figure was drawn from time exposure photographs of the movements of surface floats in the test basin. Offshore velocities were too small to measure. Measurements were made of the longshore velocity and this is compared to the values predicted by the long basin model in Figure 19. It is obvious that the predicted value is about half the measured one. This underprediction is the result of using a friction factor typical of a sand beach to predict velocities on a smooth plywood board. Figure 19 does, however, show that the predicted change in the longshore velocity between the sidewalls is similar in shape to that of the measured values, indicating that with a lower friction factor, the model could accurately predict both current magnitudes and directions.

Satisfied that the model was working, the next step was to apply it to a regular beach.

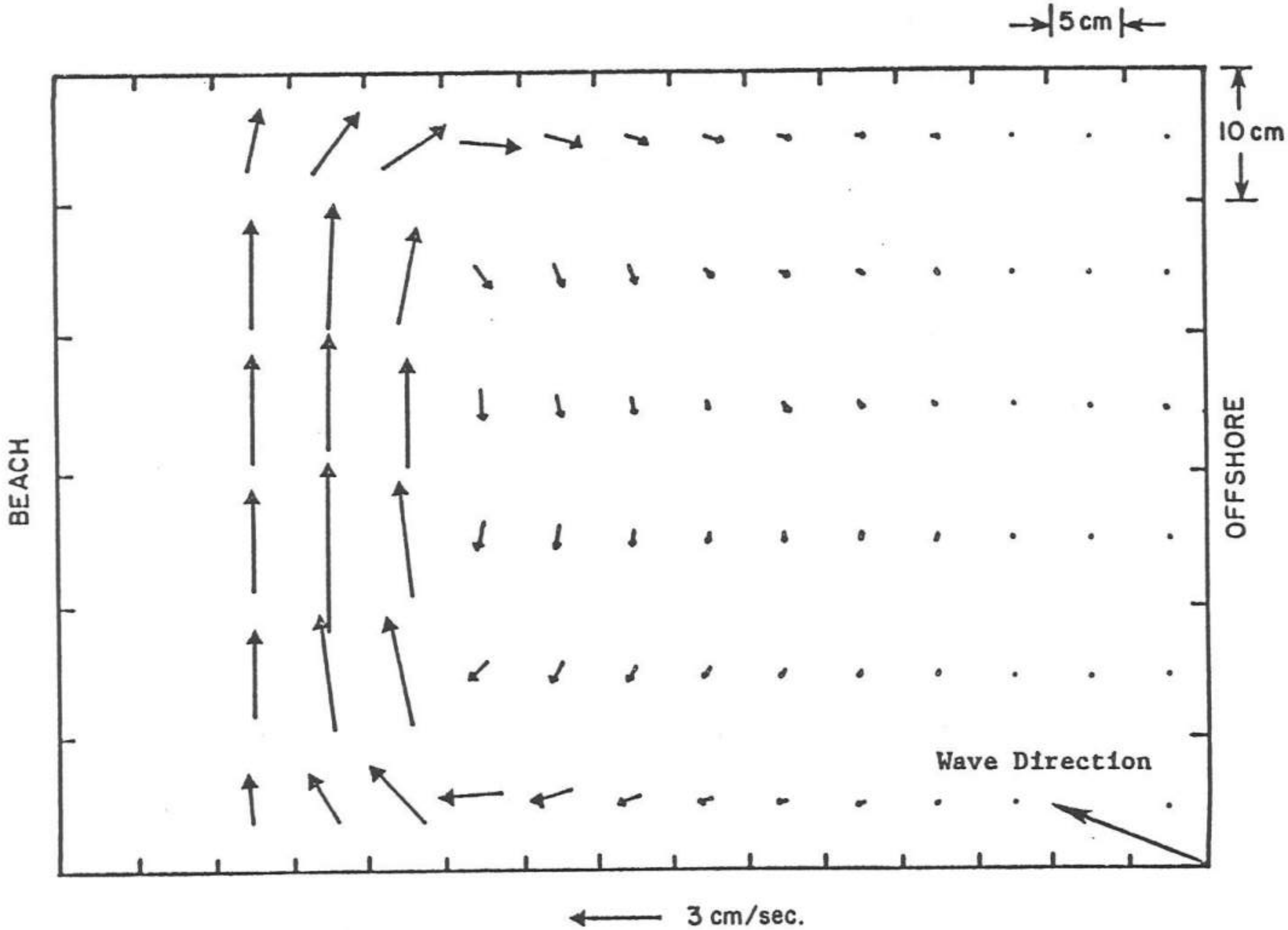

Figure 16 Velocity Vectors for the Short Basin (Not to Scale) After 31 Sec.

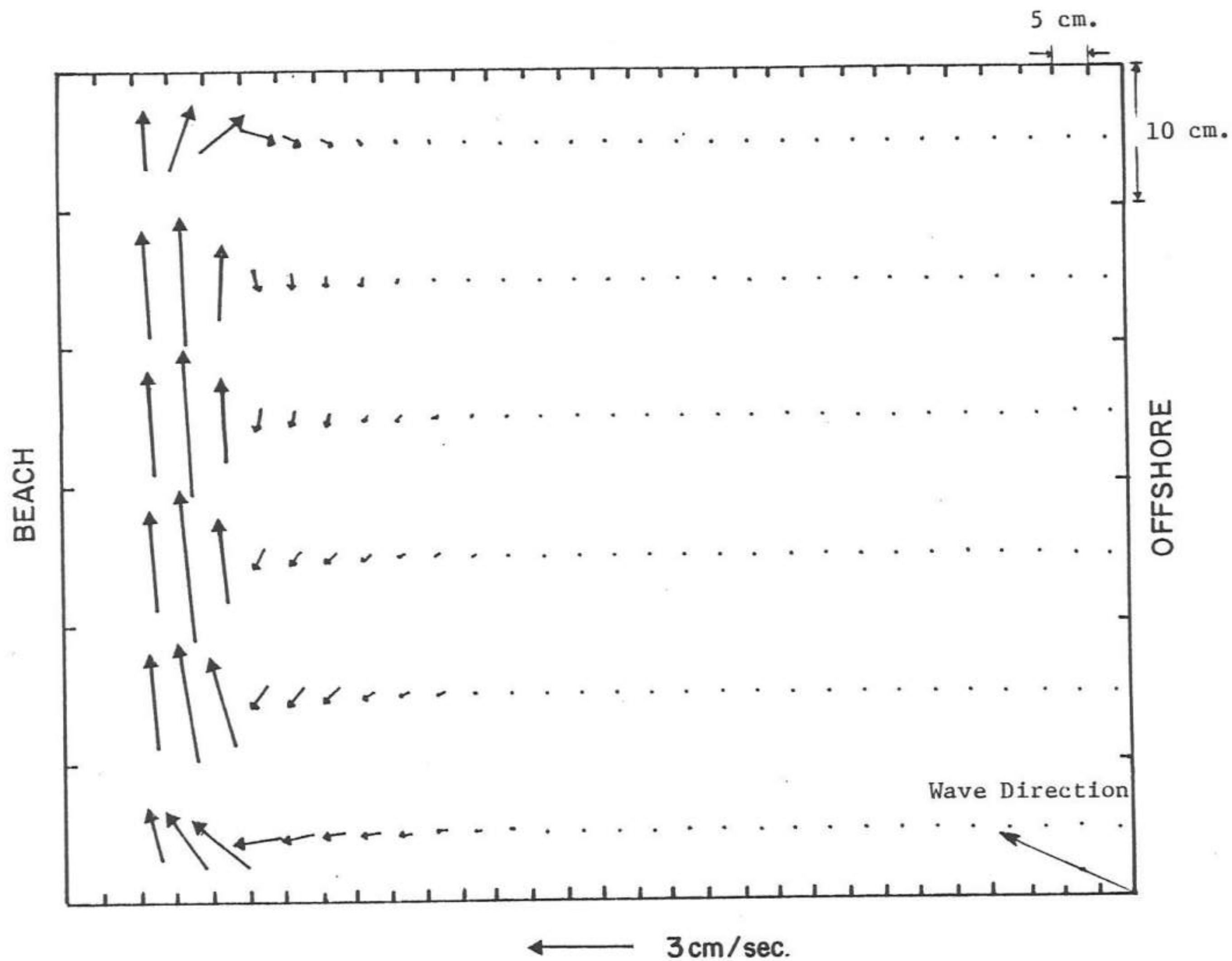

Figure 17 Velocity Vectors for the Long Basin After 16 sec. (Basin Dimensions not to Scale).

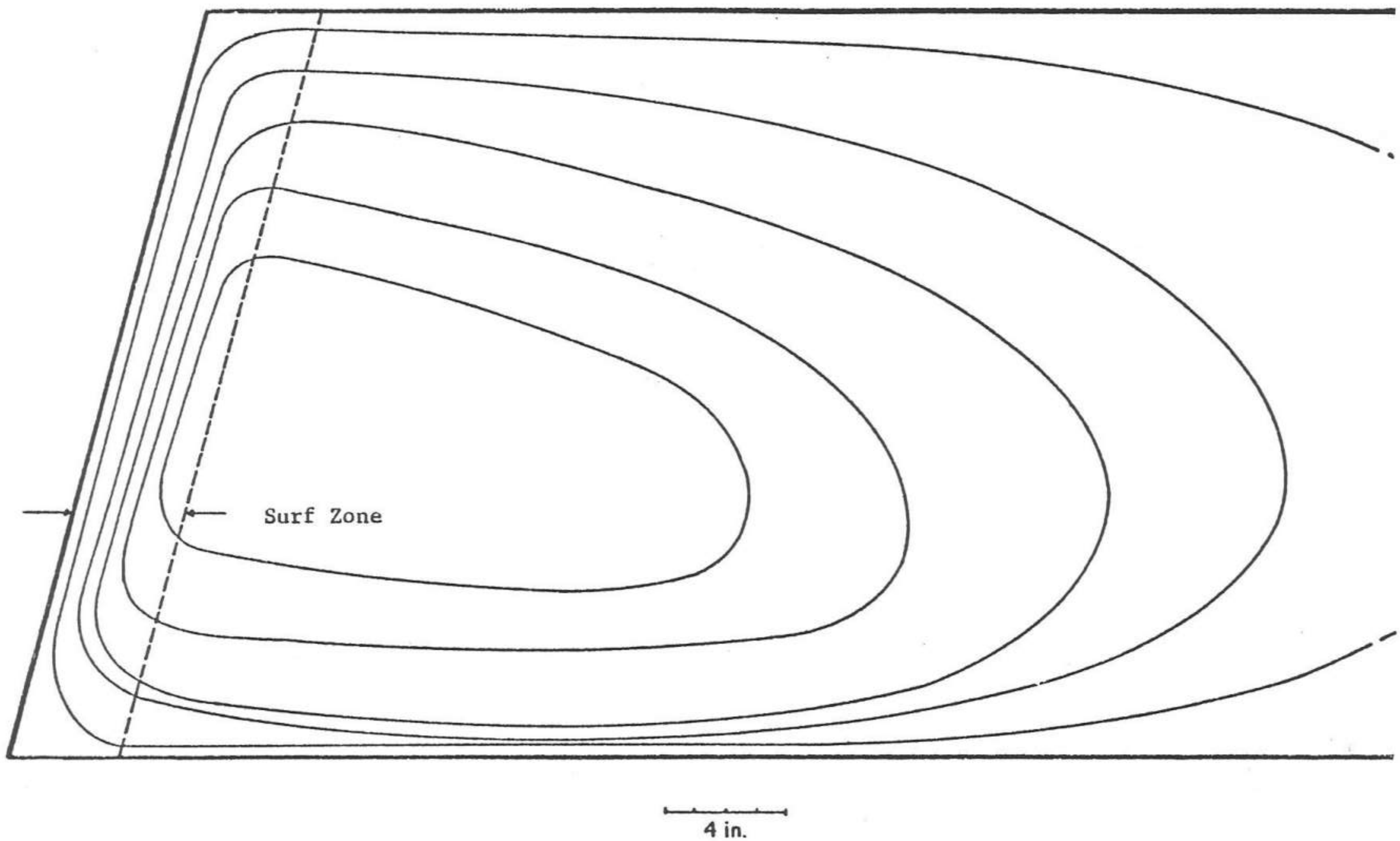

Figure 18 Experimental Streamlines for the Long Basin [From Dalrymple et.al. (1975)].

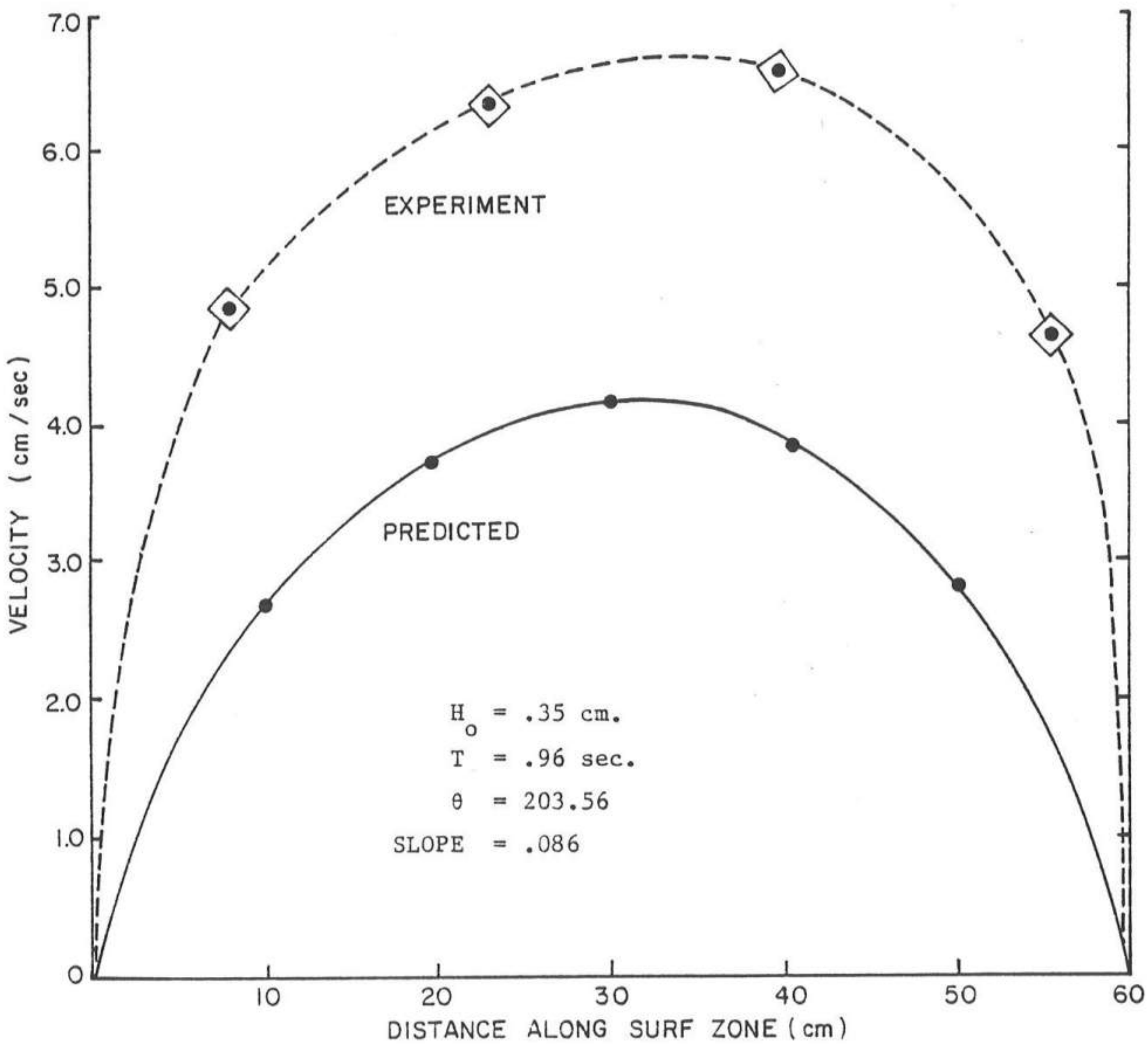

Figure 19 Predicted and Measured Longshore Velocities for the Long Basin Test Case.

4.3 PERIODIC BOTTOM

In applying the model to the open coast, the periodic bottom profile developed by Noda et.al. (1974) was used. The contours are specified by

$$D_{i,j} = \begin{cases} -m(4-i)\Delta x & i = 1, 2, 3, 4 \\ m\Delta x\{1+A \exp\left[-3\left(\frac{x}{20}\right)^{1/3}\right] \sin^{10} \frac{\pi}{\lambda}(y - x \tan\beta)\} & i > 4 \end{cases} \qquad (4.3)$$

where x,y are coordinates of grid (i,j)

m = average beach slope = .025

λ = length of beach period = 70 m.

A = amplitude of bottom variation = 20

β = angle of rip channel to beach normal = 30°

Using a square grid of 10 meters, the bottom contours shown in Figure 20 were calculated. This set-up of N = 8, M = 24 grids was used for all the testing. The major feature of the contours is the large channel running offshore at 30° to the beach normal. The part of the beach which is initially dry is a plane beach of slope m. Offshore of the grid system, the contours once again become uniform to allow Snell's law to be valid in refracting the deepwater wave to the grid system.

It is not necessary to use Equation 4.3 to specify the depth at each grid, depth values could be read in as data with the only criteria being that the bottom be periodic. Equation 4.3 is, however, convenient and the effects of the contours on the circulation can be easily shown by changing A, λ, and β.

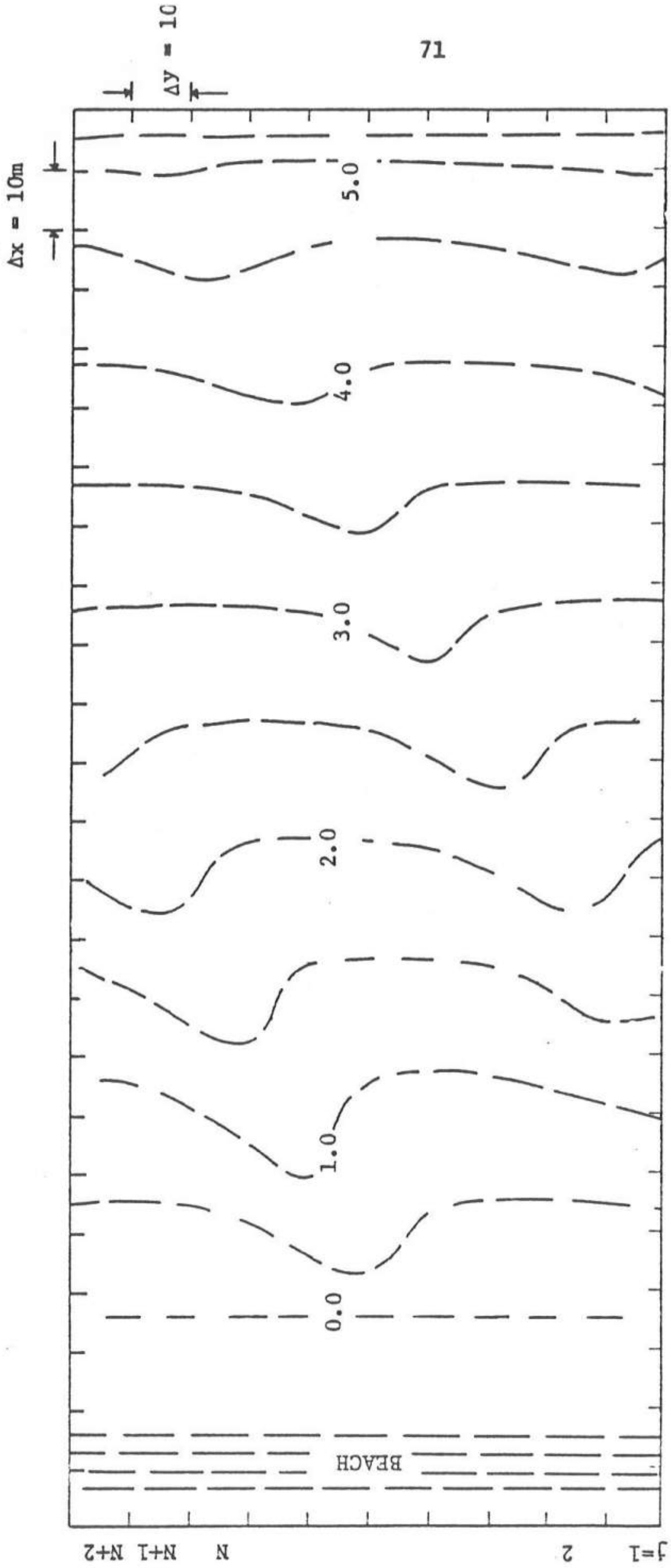

Figure 20 Depth Contours for the Periodic Bottom Tests (Depths in Meters)

Since it was desired to draw some comparisons from the data for a similar topography obtained by Noda et.al. (1974), the same wave field (H_o = 1 m., T = 4 sec., θ = 210°) and friction factor (C_f =0.01) was used. With a time step of 0.9 sec. the model was run for 400 iterations (t = 360 sec.) without wave-current interaction. The calculated velocities were similar to those predicted by Noda et.al. but were higher than values found in the field.

With this loose verification of the model, wave-current interaction was allowed and the program run for 600 iterations (t = 540 sec.). The resulting velocity vectors were found to be significantly lower than those predicted by Noda et.al., even when they allowed 50 percent wave-current interaction,[1] and were, therefore, closer to the field results. The importance of the interaction is shown in Figure 21, which compares the predicted velocity vectors for a section of the surf zone with and without wave-current interaction after identical 400 iteration runs.

The velocity vectors for the entire area are shown in Figure 22 Offshore velocities are not shown due to their small magnitudes. The study area is dominated by a meandering longshore current with the highest velocities (1.9 m/sec) concentrated in the out-going rip current. The rip is surrounded by small eddies and feeder currents which must be a result of the topography since lateral mixing has been neglected. This compares well with the experimental circulation shown in Figure 23 (Noda et.al., 1974).

---

[1] Only 50% of the predicted current was able to be used in the refraction procedure (REFRAC); more than that would lead to numerical instabilities.

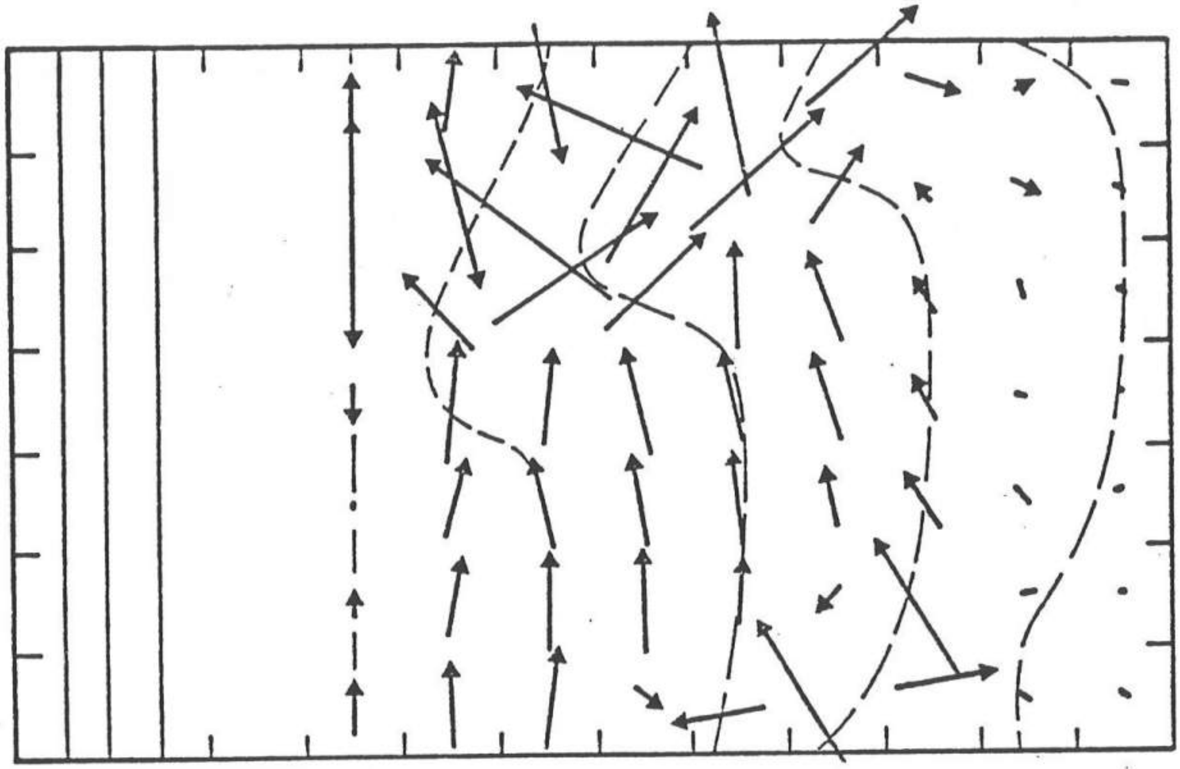

No Wave-Current Interaction

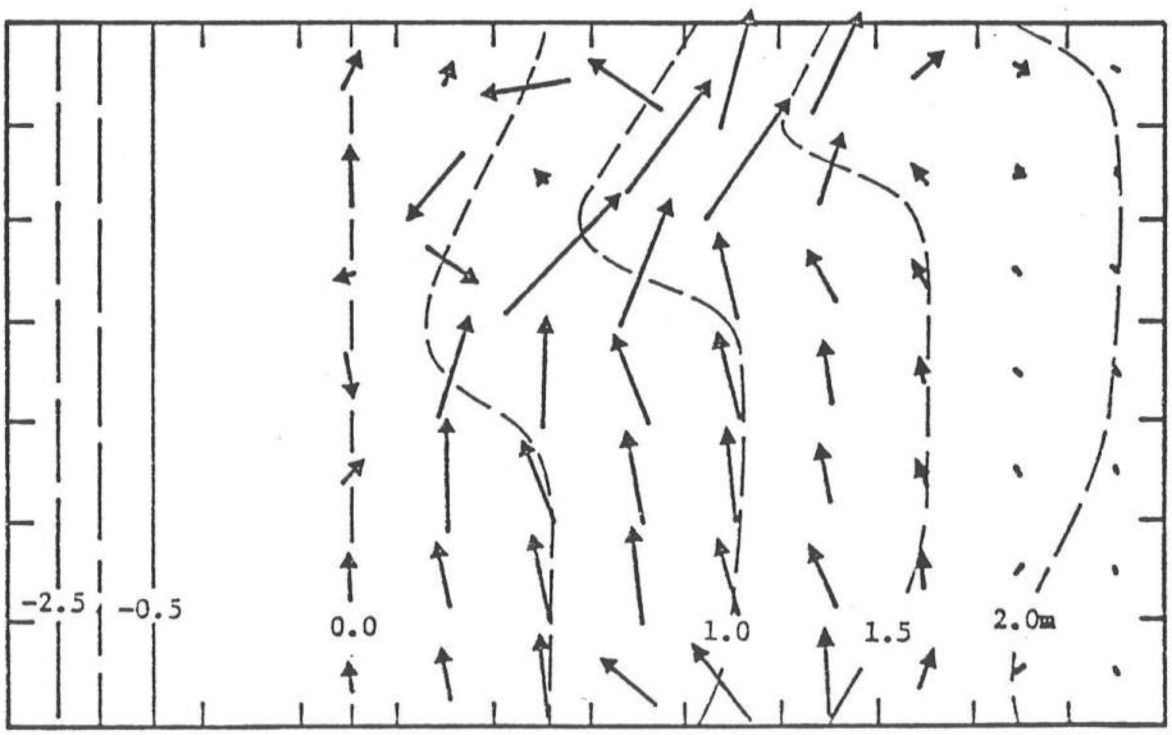

With Wave-Current Interaction

Figure 21 Surf Zone Velocity Vectors Over Trough Showing the Effect of Wave-Current Interaction

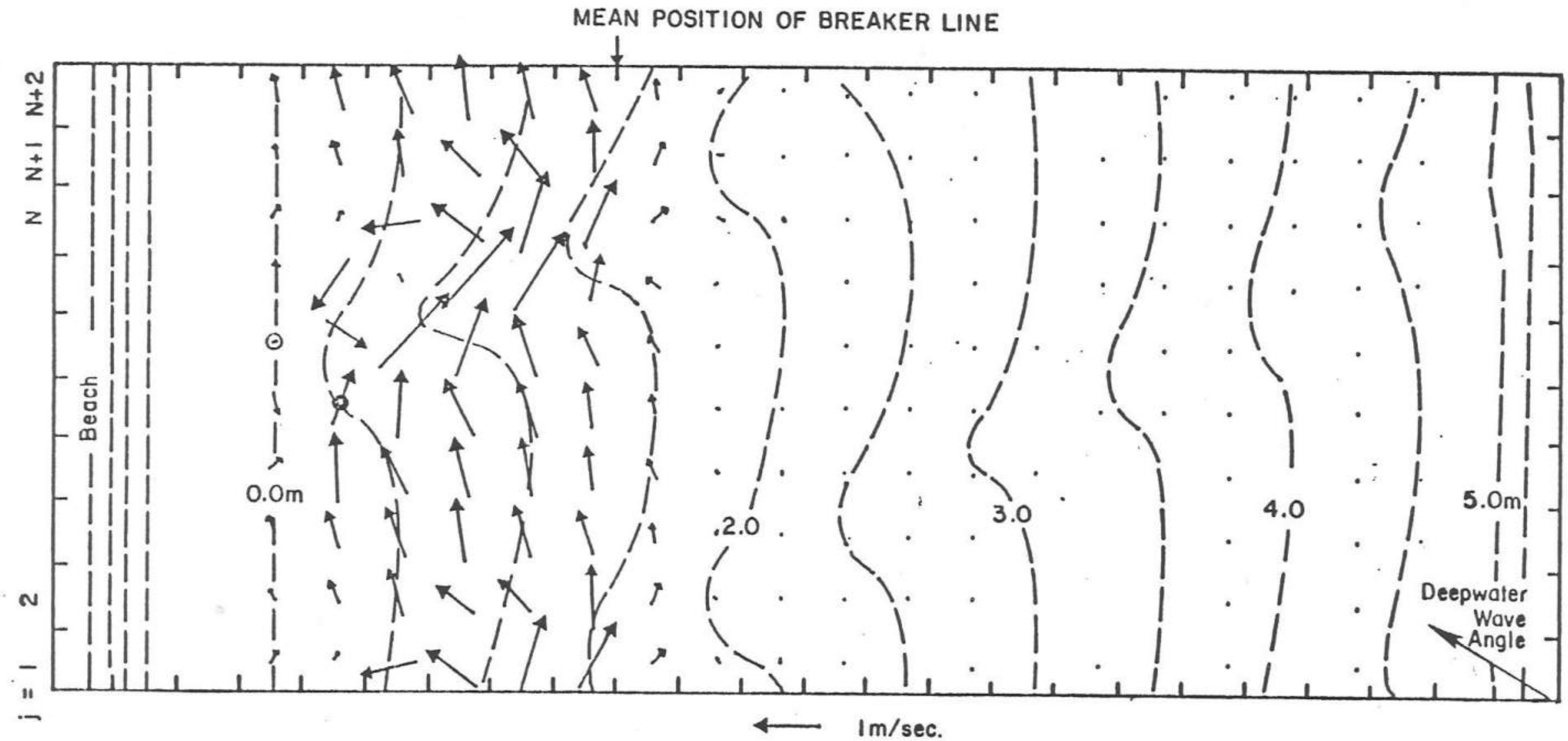

Figure 22 Velocity Vectors Over Periodic Beach After 540 sec. of Wave Action. Note the Presence of a Meandering Longshore Current Due to Oblique Wave Attack. $\Delta x = \Delta y = 10m$
$H_o = 1m$, $T = 4$ sec.

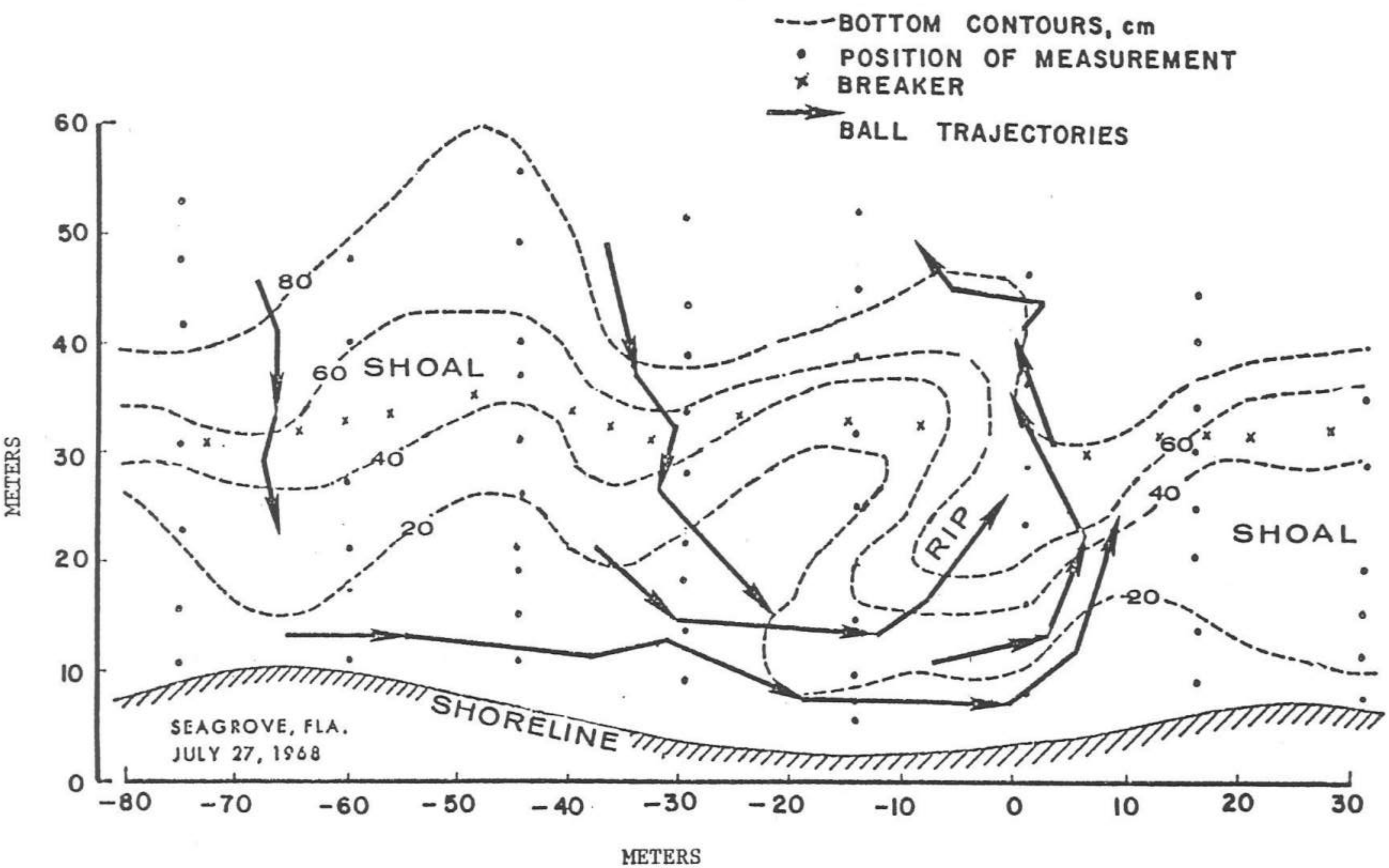

Figure 23 Experimental Data of Sonu Showing Meandering Longshore Current, Rip and Rip Channel [From Noda et.al. (1974)].

Like the previous two cases, the use of a wall at grid M causes a seiche to develop. This is shown in Figure 24 which plots the set-up for grid (i=4, j=6), denoted by a open circle in Figure 22, versus time. Although this seiching is not characteristic of an open coast, its period is predictable by Equation 4.1 which results in a value of 9.1 sec.

Since the variations in set-up and set-down drive the nearshore currents and are affected by the bottom topography, their inclusion in the model is important. This can be seen in Figure 25,which is a contour plot of the values of $\overline{\eta}$ for iteration 600. The effect of the rip channel is obvious with the maximum set-up being found directly in front of it, providing a hydrostatic head to drive the rip current. Figure 26 shows the time variations in longshore velocity for grid (i =5, j =5), marked by a closed circle in Figure 22. It is evident that after 600 iterations (t = 540 sec.) that a steady solution has been obtained.

From this point, in order to see the effects that wind would have on the solution, a 100-knot wind, in the same direction as the waves, was instantaneously applied and the model was run for an additional 200 iterations. This is, of course, an extreme wind speed and startup condition but it does show what might happen under storm conditions. The changes in set-up and velocity are shown in Figures 24 and 26 respectively. There is a significant increase in longshore velocity and in the set-up. The velocity vectors are shown in Figure 27. The wind is clearly the dominate driving force causing an increase in all

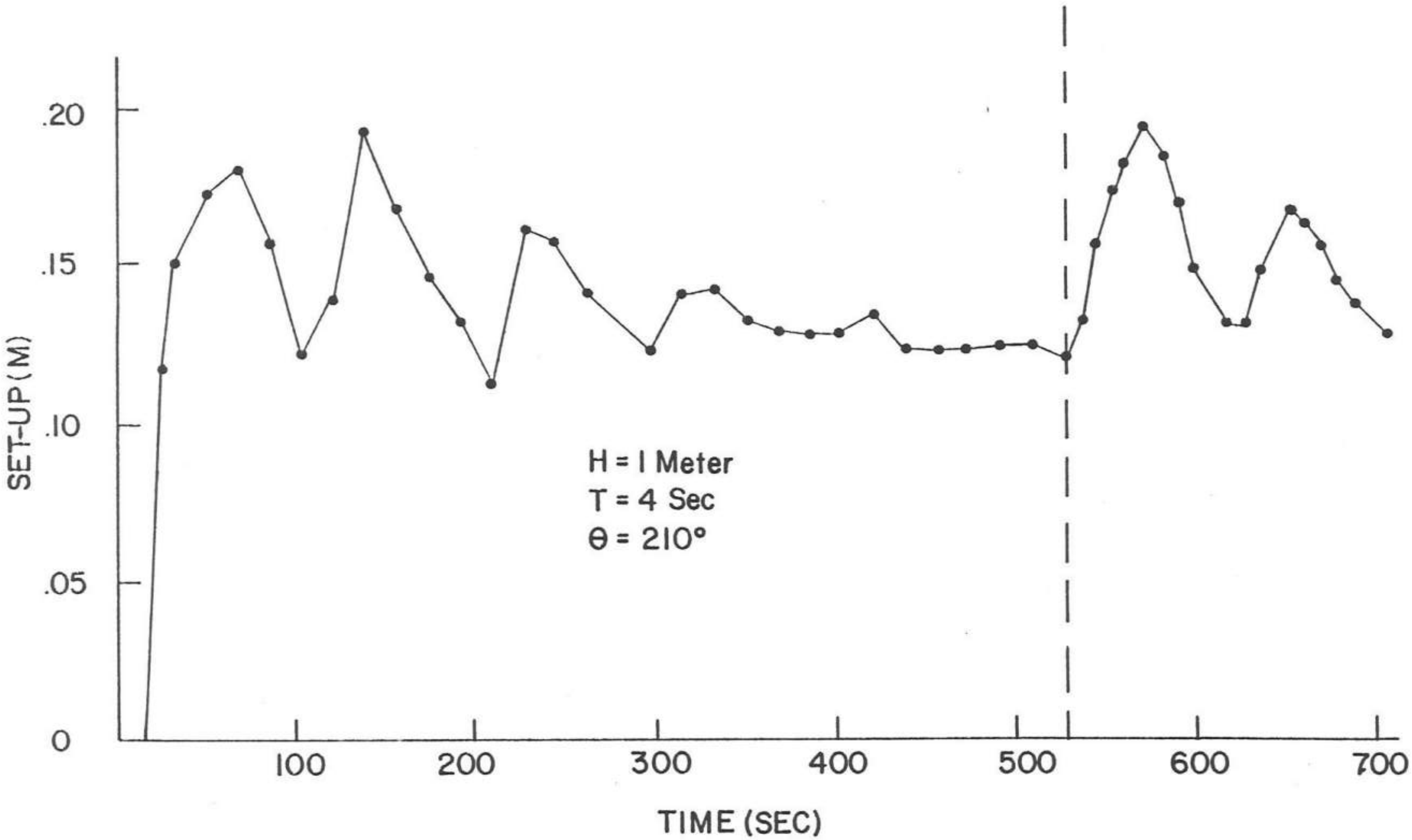

Figure 24 Set-Up at Open Circle in Figures 22 and 27 Versus Real Time. Seiching is the Result of Assumed Offshore Boundary Condition. After 525 sec., A 100 Knot Wind Blowing in the Direction of the Waves was Introduced.

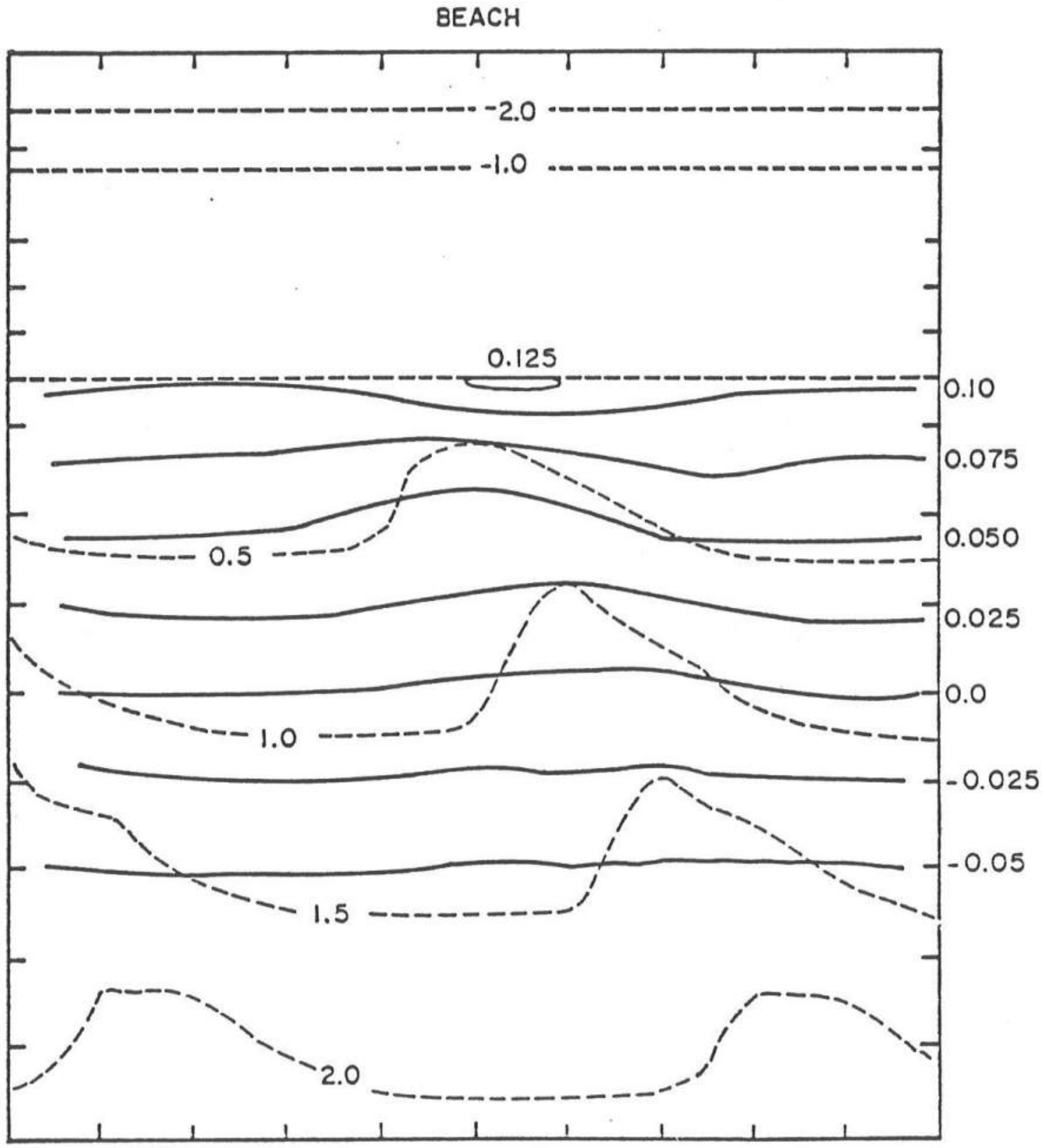

Figure 25 Contour Plot of $\overline{\eta}$ Showing the Effect of the Rip Channel. Dashed Lines are Depth Contours. All Measures in Meters.

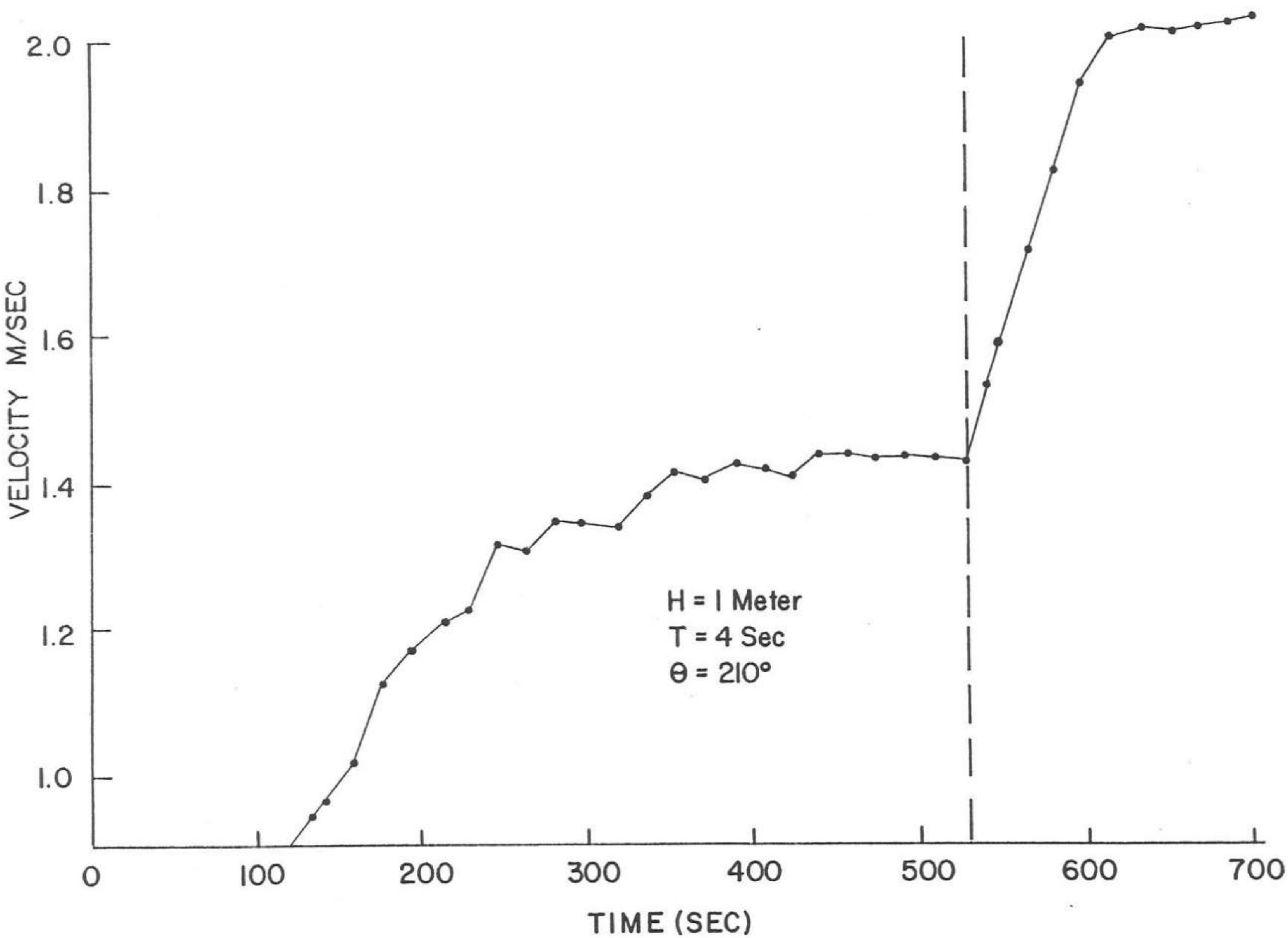

Figure 26 Startup of Longshore Velocity Measured at Solid Circle in Figures 22 and 27. Wind Startup also Shown.

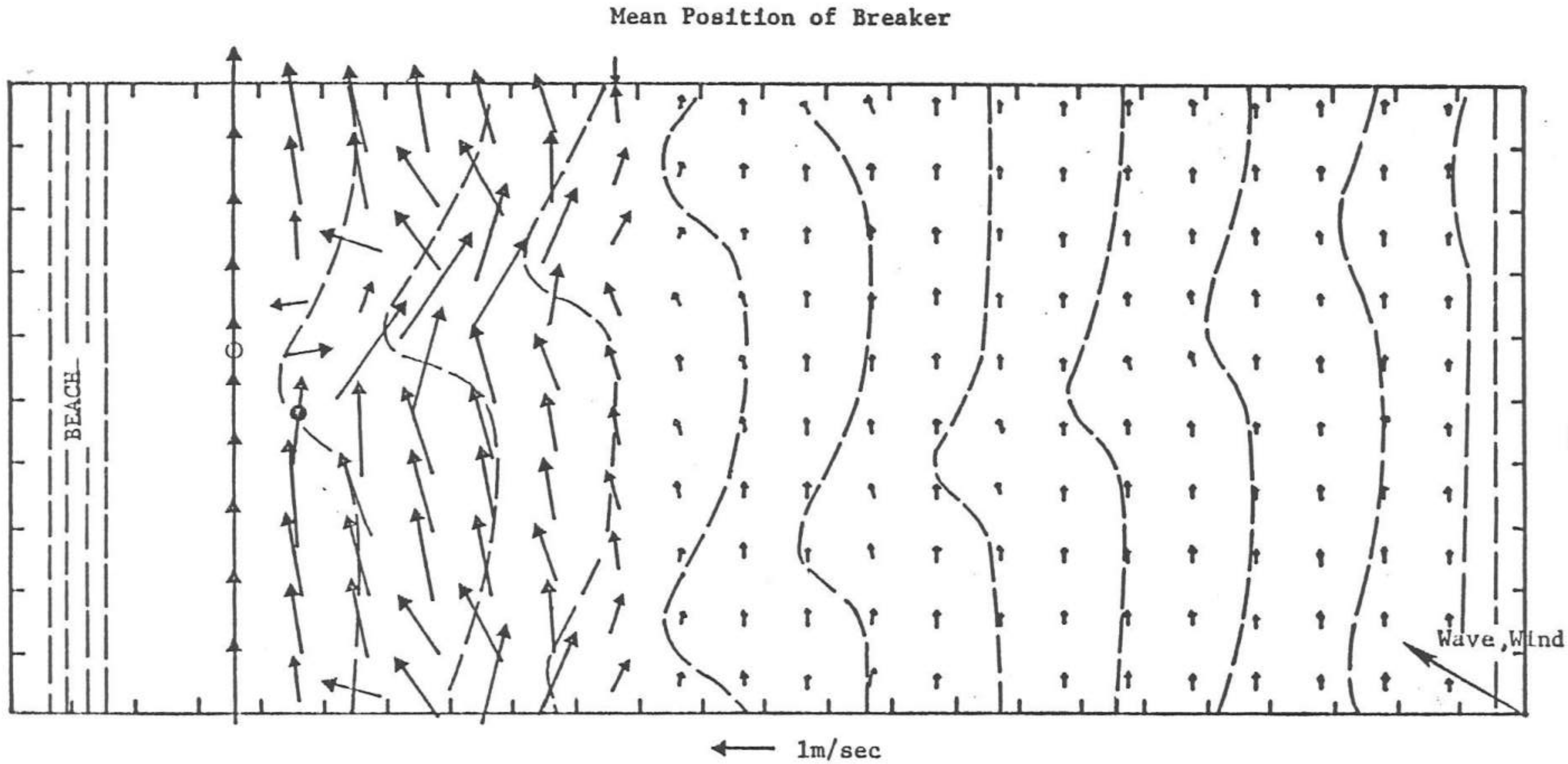

Figure 27 Wave and Wind Induced Circulation Over the Periodic Topography After 180 Sec. of a 100-Knot Wind Blowing in the Direction of the Waves H = 1.0, T = 4 sec., θ = 210°.

velocities. The longshore velocities close to the shore vary from 1.5 to 2 m./sec. The eddies are still evident but bigger, and there are still high velocities in the rip channel.

It should be noted that no provision has been made to allow wave height build up through wind energy input. This is a result of not including the wind stress and bottom friction terms in the energy balance (Equation 2.48) from which the wave height is determined. While this may be a valid procedure for light wind conditions, it is not applicable to storm conditions. Thus to accurately predict the effects of high winds on the velocities, and the set-up, Equation 2.48 will have to be reformulated to include the stress terms.

One conclusion that can be drawn from these results is that once a rip channel is formed in the surf zone, it tends to be self-sustaining. It is also interesting to note that the currents induced by the channel do not go offshore but re-enter the surf zone.

Figure 28 shows the changes that occur in the circulation pattern when the same waves approach normal to the beach. As expected, the magnitude of the longshore current is greatly reduced, and there is now some onshore and offshore velocities. Maximum velocities are again found in the rip channel.

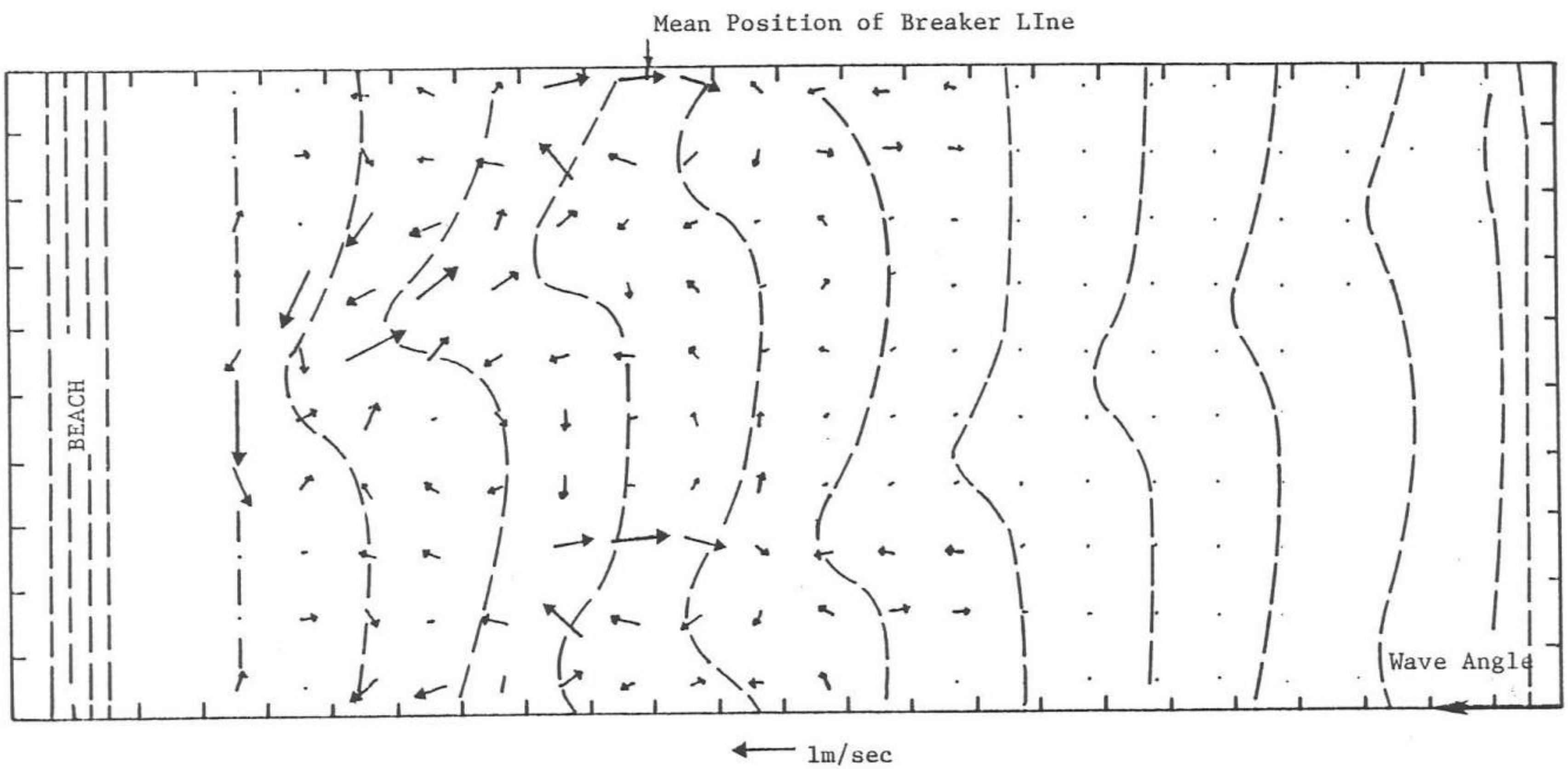

Figure 28 Wave-Induced Circulation Over Periodic Topography. Wave Conditions are the Same as Figures 21 to 27 Except that the Deepwater Wave Angle is Now 180°. Note the Reduction in Strength of the Rip Current and Absence of a Strong Longshore Current.

CHAPTER V

CONCLUSIONS

It has been shown that through numerical modelling it is possible to predict the current field in a study area for a given wave and wind field. The knowledge is very valuable in determining possible beach changes and coastal flooding. The major limitation of the model is that due to the time dependence, initial run times to obtain a steady state solution are long and expensive. However, once the steady state condition has been reached, the response of the system to wave groups, or winds is immediate.

A number of things were included in the formulation due to their direct effect on the circulation pattern. The variations in water elevation as a result of wave-induced set-up produce the hydrostatic head drops that drive longshore or rip currents. This effect can be accentuated by winds which, depending on their direction, increase or decrease the mean velocities. The inclusion of wave-current interaction, while not important in some cases, becomes very important when currents and wave speeds are similar in magnitude and direction. As a first step toward numerically modelling wave spectra, the effect of groups of waves with the same period but varying amplitudes was examined.

Since the major thrust of this study was in developing the program, only a few cases were run to test it. There are now a number of interesting variations that can be run, including different wave conditions for the same beach or slightly different beach configurations for the same wave. The effect of wave groups on the regular beach should also be interesting. With the inclusion of the stress terms in the wave height equations, storm conditions could be studied.

Though the model is useful in its present form, there are a number of further developments that should be made. A major effort should be made to increase the efficiency of the program. There are a number of numerical procedures that can be used. The grid system could be scaled in such a way as to stretch the surf zone, where the detail is needed, and shrink the offshore ones [Liu and Mei (1974)]. This will allow a smaller number of grids to be used thus reducing the computer time needed. It might also be possible to solve the steady state form of the equations and to use the result as a starting point for the time dependency equations. One problem that may be encountered in this procedure is a breakdown in the refraction program due to the wave-current interaction as found by Noda et.al. (1974).

Since it is desirable to include the convective acceleration terms in the two-dimensional problems, further study should be made of the implicit formulation proposed by Abbott (1967). This will guarantee a stable solution and make the formulation more complete. Care will still have to be taken in selecting a grid size and time step that will result in the correct solution. A combination of grid scaling and the implicit scheme should increase the program's efficiency and allow longer time steps.

Besides including the effects of winds and bottom friction in the wave height equation, a more realistic picture would be obtained with the inclusion of:

1. Sediment transport which would allow the beach to adjust itself to the wave field.

2. Varying wave periods to model wave spectra.

3. A diffraction scheme so that the effect of coastal structures on the circulation pattern could be studied.

4. The ability to handle two wave trains of different magnitudes and direction as often found along the coast.

A model of this sophistication is a direct extension of the work discussed here and would be significant aid in predicting beach changes.

APPENDIX A

ANISOTROPIC BOTTOM STRESS

As mentioned in Chapter II, the general form of the bottom friction is

$$\tau_b = \rho C_f |U_t| U_t \qquad \text{(A-1)}$$

where U_t is the total current due to both waves and local currents. This current can be represented as the vector

$$U_t = U_x \hat{i} + U_y \hat{j} = (U_o \cos\theta + U)\hat{i} + (U_o \sin\theta + V)\hat{j} \qquad \text{(A-2)}$$

where U_o is the current due to the orbital wave motion, and U and V are mean currents as defined in Chapter II. The angle θ is as before, the angle of wave approach. If it is assumed that the waves are approaching from a small angle, θ, and that the mean currents are small relative to U_o, then

$$|U_t| = [(U_o \cos\theta + U)^2 + (U_o \sin\theta + V)^2]^{1/2} \quad , \qquad \text{(A-3)}$$

simplifying , $|U_t| = |U_o \cos\theta + U|$ (A-4)

Solving for $\overline{\tau}_{bx}$,

$$\tau_{bx} = C_f \rho |U_t| U_x = C_f \rho |(U_o \cos\theta + U| \; (U_o \cos\theta + U) \qquad \text{(A-5)}$$

expanding and time averaging over a wave period.

$$\overline{\tau}_{bx} = \frac{1}{T}\int_0^T \rho C_f \;|(U_{max}\cos\sigma t)^2 \cos^2\theta + 2U\cos\theta\, U_{max}\cos\sigma t|dt$$

or (A-6)

$$\overline{\tau}_{bx} = \frac{\rho C_f}{T}\int_0^T |(U_{max}\cos\sigma t)^2\cos^2\theta|dt + \frac{\rho C_f}{T}\int_0^T |2U\cos\theta\, U_{max}\cos\sigma t|dt$$

where the U^2 term has been neglected as it is very small relative to the other terms and

$$U_o = U_{max}\cos\sigma t$$

where U_{max} is the maximum orbital velocity from Airy wave theory,

$$U_{max} = \frac{\pi H}{T\sinh(kh)} \tag{A-7}$$

and σ is the wave frequency

$$\sigma = \frac{2\pi}{T} \tag{A-8}$$

To preserve the absolute value, the integral in Equation A-6 must be evaluated in three parts such that,

$$\int_0^T = \int_0^{T/4} - \int_{T/4}^{3T/4} + \int_{3T/4}^{T} \tag{A-9}$$

When this is carried out, the first term of Equation A-6 drops out leaving a final answer of

$$\overline{\tau}_{bx} = \frac{4}{\pi}U_{max}\,U\cos\theta \tag{A-10}$$

Following a similar procedure in the y direction, Equation A-1 becomes,

$$\tau_{by} = \rho C_f|U_t|U_y = \rho C_f|U_o\cos\theta + U|\;(U_o\sin\theta + V) \tag{A-11}$$

Time averaging and expanding,

$$\overline{\tau}_{by} = \frac{1}{T}\int_0^T |C_f \rho U_o{}^2 \sin\theta \cos\theta + U\sin\theta\ U_o + U_o V \cos\sigma|dt \qquad \text{(A-12)}$$

where the term (UV) has been neglected as small. Carrying out this integration, using Equation A-9 as before,

$$\overline{\tau}_{by} = \frac{2\rho C_f}{\pi}\ U\sin\theta\ U_{max} + \frac{2\rho C_f}{\pi} V\cos\theta\ U_{max} \qquad \text{(A-13)}$$

Both Equations A-10 and A-13 can be further simplified using the initial assumption of small angle, (θ) resulting in,

$$\overline{\tau}_{bx} = \frac{4\rho C_f}{\pi}\ U_{max}\ U$$

$$\overline{\tau}_{by} = \frac{4\rho C_f}{\pi}\ U_{max}\ V$$

the final forms employed in this study.

APPENDIX B

IMPLICIT FORMULATION

The one-dimensional (1-D) implicit scheme that was used for set-up in a wave basin followed that of Abbott and Ionescu (1967). Rewriting Equations 2.13 and 2.20 in 1-D, including the convective acceleration term, one obtains:

$$\frac{\partial \bar{\eta}}{\partial t} + \frac{\partial}{\partial x} [U(h+\bar{\eta})] = 0 \tag{B-1}$$

$$\frac{\partial U}{\partial t} + U\frac{\partial U}{\partial x} = -g \frac{\partial \bar{\eta}}{\partial x} - \frac{1}{\rho} (h+\bar{\eta}) \; [\frac{\partial S_{xx}}{\partial x} - \bar{\tau}_s + \bar{\tau}_b] \tag{B-2}$$

The first step is to transpose these equations into a normal form. Multiplying B-1 by U and expanding gives

$$U(h+\bar{\eta}) \frac{\partial U}{\partial x} = -U \frac{\partial \bar{\eta}}{\partial t} - U^2 \frac{\partial (h+\bar{\eta})}{\partial x} \tag{B-3}$$

Multiplying Equation B-2 by $(h+\bar{\eta})$ and substituting in Equation B-3 it becomes

$$(h+\bar{\eta}) \frac{\partial U}{\partial t} - U\frac{\partial \bar{\eta}}{\partial t} - U^2\frac{\partial (h+\bar{\eta})}{\partial x} = -g(h+\bar{\eta}) \frac{\partial \bar{\eta}}{\partial x} - \frac{1}{\rho}(\frac{\partial S_{xx}}{\partial x} + \bar{\tau}_b - \bar{\tau}_s) \tag{B-4}$$

By rearranging the third and fourth term,

$$-U^2 \frac{\partial (h+\bar{\eta})}{\partial x} + g(h+\bar{\eta}) \frac{\partial \bar{\eta}}{\partial x} = -[U^2 - g(h+\bar{\eta})] \frac{\partial (h+\bar{\eta})}{\partial x} - g(h+\bar{\eta}) \frac{\partial h}{\partial x}$$

Equation B-4 can be simplified to

$$(h+\bar{\eta})\ \frac{\partial U}{\partial t} - U\ \frac{\partial \bar{\eta}}{\partial t} - [U^2 - g(h+\bar{\eta})]\ \frac{\partial \bar{\eta}}{\partial x} = F + U^2\ \frac{\partial h}{\partial x} \qquad \text{(B-5)}$$

(B-10)

where

$$F = -\frac{1}{\rho}\ [\frac{\partial S_{xx}}{\partial x} - \bar{\tau}_s + \bar{\tau}_b] \qquad \text{(B-6)}$$

Multiplying Equation B-1 by g and expanding

$$g\frac{\partial \bar{\eta}}{\partial t} + g(h+\bar{\eta})\ \frac{\partial U}{\partial x} + gU\ \frac{\partial h}{\partial x} + gU\ \frac{\partial \bar{\eta}}{\partial x} = 0 \qquad \text{(B-7)}$$

Then multiplying Equation B-2 by U solving for gU $\frac{\partial \bar{\eta}}{\partial x}$ and substituting (B-11)

in Equation B-7 one obtains:

$$g\ \frac{\partial \bar{\eta}}{\partial t} - U\ \frac{\partial U}{\partial t} - [U^2 - g(h+\bar{\eta})]\ \frac{\partial U}{\partial x} = G - gU\ \frac{\partial h}{\partial x} \qquad \text{(B-8)}$$

where

(B-12)

$$G = \frac{U}{\rho(h+\bar{\eta})}\ [\frac{\partial S_{xx}}{\partial x} - \bar{\tau}_s + \bar{\tau}_b] \qquad \text{(B-9)}$$

Equations B-5 and B-8 constitute a normal pair and are next (B-13)

finite differenced using a forward time, forward space scheme with

(B-14)

averaging. Performing the operation on B-5 it becomes:

$$(h+\bar{\eta})\ [\frac{U_i^{n+1} - U_i^n}{\Delta t}] - \frac{U}{2}\ [\frac{\bar{\eta}_i^{n+1} - \bar{\eta}_i^n}{\Delta t} + \frac{\bar{\eta}_{i-1}^{n+1} - \bar{\eta}_{i-1}^n}{\Delta t}] - [\frac{U^2 - g(h+\bar{\eta})}{2}] \qquad \text{(B-15)}$$

$$[\frac{\bar{\eta}_i^{n+1} - \bar{\eta}_{i-1}^{n+1}}{\Delta x} + \frac{\bar{\eta}_i^n - \bar{\eta}_{i-1}^n}{\Delta x}] = F + U^2\ \frac{\partial h}{\partial x} \qquad \text{,(B-8)}$$

Where the subscript is a space step and the superscript denotes a time step. Collecting n+1 terms, this simplifies to

$$\bar{\eta}_i^{n+1} \left\{ -\frac{U}{2\Delta t} - \left[\frac{U^2 - g(h+\bar{\eta})}{2\Delta x}\right] \right\} + U_i^{n+1} \left[\frac{h+\bar{\eta}}{\Delta t}\right] + \bar{\eta}_{i-1}^{n+1} \cdot$$

$$\left\{ -\frac{U}{2\Delta t} + \left[\frac{U^2 - g(h+\bar{\eta})}{2\Delta x}\right] \right\} = D_i \tag{B-10}$$

where

$$D_i = U_i^n \left[\frac{h+\bar{\eta}}{\Delta t}\right] + \bar{\eta}_i^n \left\{ -\frac{U}{2\Delta t} + \left[\frac{U^2 - g(h+\bar{\eta})}{2\Delta x}\right] \right\} +$$

$$\bar{\eta}_{i-1}^n \left\{ -\frac{U}{2\Delta t} - \left[\frac{U^2 - g(h+\bar{\eta})}{2\Delta x}\right] \right\} + F + U^2 \frac{\partial h}{\partial x} \tag{B-11}$$

this is of a form

$$A_i \bar{\eta}_i^{n+1} + B_i U_i^{n+1} + C_i \eta_{i-1}^{n+1} = D_i \tag{B-12}$$

with

$$A_i = -\frac{U}{2\Delta t} - \left[\frac{U^2 - g(h+\bar{\eta})}{2\Delta x}\right] \tag{B-13}$$

$$B_i = \frac{h+\bar{\eta}}{\Delta t} \tag{B-14}$$

$$C_i = -\frac{U}{2\Delta t} + \left[\frac{U^2 - g(h+\bar{\eta})}{2\Delta x}\right] \tag{B-15}$$

Utilizing a similar procedure on the continuity equation, (B-8) becomes

$$g[\frac{\bar{\eta}_i^{n+1} - \bar{\eta}_i^n}{\Delta t}] - \frac{U}{2}[\frac{U_{i+1}^{n+1} - U_{i+1}^n}{\Delta t} + \frac{U_i^{n+1} - U_i^n}{\Delta t}] - [\frac{U^2 - g(h+\bar{\eta})}{2}] \cdot$$

$$[\frac{U_{i+1}^{n+1} - U_i^{n+1}}{\Delta x} + \frac{U_{i+1}^n - U_i^n}{\Delta x}] = G - gU\frac{\partial h}{\partial x}$$

Collecting n+1 terms

$$\eta_i^{n+1}[\frac{g}{\Delta t}] + U_{i+1}^{n+1}\left\{-\frac{U}{2\Delta t} - [\frac{U^2 - g(h+\bar{\eta})}{2\Delta x}]\right\} + U_i^{n+1}\left\{-\frac{U}{2\Delta t} + [\frac{U^2 - g(h+\bar{\eta})}{2\Delta x}]\right\} = D_i^* \quad \text{(B-16)}$$

where

$$D_i^* = \bar{\eta}_i^n[\frac{g}{\Delta t}] + U_{i+1}^n\left\{-\frac{U}{2\Delta t} + [\frac{U^2 - g(h+\bar{\eta})}{2\Delta x}]\right\} + U_i^n\left\{-\frac{U}{2\Delta t} - [\frac{U^2 - g(h+\bar{\eta})}{2\Delta x}]\right\} + G - gU\frac{\partial h}{\partial x} \quad \text{(B-17)}$$

Equation B-16 can then be rewritten as

$$A_i U_{i+1}^{n+1} + B_i^* \bar{\eta}_i^{n+1} + C_i U_i^{n+1} = D_i^* \quad \text{(B-18)}$$

with

$$B_i^* = \frac{g}{\Delta t} \quad \text{(B-19)}$$

The solution to Equations B-12 and B-18 is through two simultaneous tridiagonal algorithms. It is first assumed that U_i^{n+1} and $\bar{\eta}_i^{n+1}$ are related such that

$$\overline{\eta}^{n+1}_{i+1} = E_i U^{n+1}_i + F_i \tag{B-20}$$

$$U^{n+1}_{i+1} = E^*_i \overline{\eta}^{n+1}_i + F^*_i \tag{B-21}$$

Substituting B-20 into B-12 and B-21 into B-18 the following equations are obtained respectively,

$$A_i \left(E_i U^{n+1}_i + F_i\right) + B_i U^{n+1}_i + C_i \overline{\eta}^{n+1}_{i-1} = D_i \tag{B-22}$$

$$A_i \left(E^*_i \overline{\eta}^{n+1}_i + F^*_i\right) + B^*_i \eta^{n+1}_i + C_i U^{n+1}_i = D_i \tag{B-23}$$

Solving B-22 for U^{n+1}_i,

$$U^{n+1}_i = \frac{-C_i \overline{\eta}^{n+1}_{i-1}}{B_i + A_i E_i} + \frac{D_i - A_i F_i}{B_i + A_i E_i} \tag{B-24}$$

and B-23 for $\overline{\eta}^{n+1}_i$,

$$\overline{\eta}^{n+1}_i = \frac{-C_i U^{n+1}_i}{A_i E^*_i + B^*_i} + \frac{D^*_i - A_i F^*_i}{A_i E^*_i + B^*_i} \tag{B-25}$$

It is important to note that by setting $i = i+1$ in Equation B-24, these last two equations are of the form of B-20 and B-21, and thus the following formulas are obtained:

$$E_i = \frac{-C_i}{A_i E^*_i + B^*_i} \tag{B-26}$$

$$F_i = \frac{D^*_i - A_i F^*_i}{A_i E^*_i + B^*_i} \tag{B-27}$$

$$E^*_{i-1} = \frac{-C_i}{B_i+A_iE_i} \tag{B-28}$$

$$F^*_{i-1} = \frac{D_i-A_iF_i}{B_i+A_iE_i} \tag{B-29}$$

By employing the no-flow boundary condition at each end of the wave channel

$$U_i = 0 \quad \text{at} \quad i = 1,M$$

starting values of E^*_i and F^*_i can be found

$$E^*_{i-1} = F^*_{i-1} = 0 \quad \text{at} \quad i = M$$

from Equation B-21. Subsequent values (to i=1) of E, E^*, F, F^* can then be found for the entire grid system through the recursion relationship, Equations B-26 to B-29. Once these quantities are determined, U and $\overline{\eta}$ can be determined from Equations B-20 and B-21 through a reverse sweep from i = 1 to i = M. This double-sweep algorithm results in an unconditionally stable formulation.

The truncation error of the entire formulation is reduced to $0(\Delta x^2, \Delta t^2)$ if the values of U and $\overline{\eta}$ used in determining the constants (A,B,C,D,B^*,D^*) are iterated within a time step. At the beginning of a time step, the first iteration determines new values of U, and $\overline{\eta}$ using constants calculated with the old U and $\overline{\eta}$ values. These constants are then redetermined using an average of U and $\overline{\eta}$ from the preceding time step and first iteration. A second iteration is made and final values of U and $\overline{\eta}$ are determined.

The problem that was encountered in the present testing was that although the solution is stable, a too coarse grid or time step combination will result in an inaccurate solution. This is studied further by Abbott and Ionescu (1967) and the interested reader is referred there.

REFERENCES

Abbott, M. B. and Ionescu, F., "On the Numerical Computation of Nearly Horizontal Flows," Journal of Hydraulic Research, Vol. 5, No. 2, 1967. page 97-117.

Bowen, A. J., Inman, D. L. and Simmons, V. P., "Wave Set-Down and Set-Up," Journal of Geophysical Research, Vol. 73, No. 8, April 15, 1968, pp. 2569-2577.

Brebner, A., and Kamphuis, J. W., "Model Tests on the Relationships Between Deepwaters Wave Characteristics and Longshore Currents," Civil Engineering Department, Report 31, Queens University at Kingston, Ontario, August, 1963.

Dalrymple, R. A., "Coastal Engineering Course Notes." Given at the University of Delaware, 1974.

Dalrymple, R. A., Eubanks, R. and Birkemeier, W., "Wave-Induced Circulation in Shallow Rectangular Basins," Unpublished 1975.

Dean, R. G., "Coastal Engineering Study of Proposed Navarre Pass," Technical Report of the Engineering and Industrial Experiment Station, College of Engineering, University of Florida, 1973.

Divoky, D., LeMehaute, B. and Lin, A., "Breaking Waves on Gentle Slopes," Journal of Geophysical Research, Vol. 75, No. 9, March 20, 1970, pp. 1681-1692.

Galvin, C. J. and Eagleson, P. S., "Experimental Study of Longshore Currents on a Plane Beach," Technical Memorandum No. 10, U. S. Army Coastal Engineering Research Center, 80 p.

Galvin, C. J., "Breaker Travel and Choice of Design Wave Heights," Journal of Waterways and Harbors Division, ASCE, WW2, May, 1969, pp. 175-200.

Gordon, R. and Spaulding, M., "A Bibliography of Numerical Models for Tidal Rivers, Estuaries and Coastal Waters," University of Rhode Island, Technical Report No. 32, 1974, 55 p.

Haltiner, G. J., Numerical Weather Predictions, John Wiley and Sons, Inc., 1971, pp. 90-104.

Hess, K. W. and White, F. M., "A Numerical Tidal Model of Narragansett Bay," University of Rhode Island, Marine Technical Report No. 20, 1974, 141 p.

Huang, L-S. and Divoky, D., "Breaking Wave Setup and Decay on Gentle Slopes," Proceedings of XII Conference on Coastal Engineering, ASCE, 1970, pp. 377-389.

Ippen, A. T., Estuary and Coastline Hydrodynamics, McGraw-Hill Book Co., 1966.

LeBlond, P. H. and Tang, C. L., "On Energy Coupling Between Waves and Rip Currents," Journal of Geophysical Research, Vol. 79, No. 6, February 20, 1974, pp. 811-816.

Liu, P. and Mei, C. C., "Effects of a Breakwater on Nearshore Currents Due to Breaking Waves," Department of Civil Engineering, MIT, Report No. 192, September, 1974.

Longuet-Higgins, M.S., "Longshore Currents Generated by Obliquely Incident Sea Waves," Journal of Geophysical Research, Vol. 75, No. 33, November 20, 1970, pp. 6778-6789.

Longuet-Higgins, M. S., and Stewart, R. W., "A Note on Wave Set-ups," Journal of Marine Research, Vol. 21, 1963, pp. 4-10.

Longuet-Higgins, M. S., and Stewart, R. W., "Radiation Stress and Mass Transport in Gravity Waves, with Application to Surf Beats," Journal of Fluid Mechanics, Vol. 13, 1962, pp. 481-504.

Munk, W. H. and Arthur, R. S., "Wave Intensity Along a Refracted Ray," in Gravity Waves, NBS Circ. 521, 1952, pp. 95-108.

Neumann, G. and Pierson, W. J., Jr., Principles of Physical Oceanography, Englewood Cliffs: Prentice-Hall, Inc., 1966, pp. 362-365.

Noda, E., Sonu, C. J., Rupert, V. C. and Collins, J. I., "Nearshore Circulations Under Sea Breeze Conditions and Wave-Current Interactions in the Surf Zone," Tetra Tech Report TC-149-4, February, 1974.

Pearce, B. R., "Numerical Calculation of the Response of Coastal Waters to Storm Systems with Application to Hurricane Camille of August 17-22, 1969," College of Engineering, University of Florida, Technical Report 12, August, 1972, 149 p.

Phillips, O. M., The Dynamics of the Upper Ocean, Cambridge University Press, 1969, pp. 45-48.

Reid, R. O. and Bodine, B. R., "Numerical Model for Storm Surges in Galveston Bay," Journal of the Waterways and Harbors Division, ASCE, WW1, February, 1968, pp. 33-57.

Roache, P. J., Computational Fluid Dynamics, Albuquerque: Hermosa Publishers, 1972.

Saville, T., "Experimental Determination of Wave Set-up," Proceedings of Second Conference on Hurricanes, 1961, pp. 242-252.

Shore Protection Manual, Corps of Engineers, Vol. 1, Government Printing Office, 1973.

Skovgaard, O., Jonsson, I. G. and Bertelsen, I., "Computation of Wave Heights Due to Refraction and Friction," Journal of Waterways, Harbors and Coastal Engineering, ASCE, WW1, February, 1975, pp. 15-32.

Thornton, E., "Variation of Longshore Current Across the Surf Zone," Proceedings XII Coastal Engineering Conference, 1970, pp. 291-308.

Verma, A. P. and Dean, R. G., "Numerical Modeling of Bay Systems," Proceedings of Civil Engineering in the Oceans II, ASCE Conference, December, 1969, pp. 1069-1087.

Weggel, J. R., "Maximum Breaker Height," Journal of Waterways, Harbors and Coastal Engineering, ASCE, WW4, November, 1972, pp. 529-548.

Wilson, B. W., "Seiche," in Encyclopedia of Oceanography, Reinhold Publishers, New York, 1966.

Wilson, W. S., "A Method for Calculating and Plotting Surface Wave Rays," TM-17, Coastal Engineering Research Center, February, 1966.

Wu, J., "Laboratory Studies of Wind-Wave Interactions," Journal of Fluid Mechanics, Vol. 34, Part 1, 1968, pp. 91-111.

FORTRAN COMPUTER LISTING OF CIRCULATION PROGRAM

```
$RESET FREE
$SET LINEINFO
FILE  3=START,UNIT=DISKPACK,RECORD=25,BLOCKING=30,AREA=30*100
FILE  7=DATA,UNIT=DISKPACK,RECORD=25,BLOCKING=30,AREA=60*1000
FILE  8=FOUT,UNIT=DISKPACK,RECORD=25,BLOCKING=30,AREA=30*100
FILE  9=DEPTH,UNIT=DISKPACK,RECORD=25,BLOCKING=30,AREA=30*100
C     DATA1 MUST HAVE THE LAST VALUES OF ETA,H,U,V ETC TO BE READ IN.
C     BASINE IS THE 2-D BASIN WITH IRREGULAR BOTTOM CONTOURS.
C     DATA2 HOLDS DATA FOR PLOTTING THE VELOCITY VECTORS
C     FOUT HOLDS THE WRITE OUT VALUES OF LAST ETA,H,V,U, ETC.
      COMMON D(50,20),U(50,20),V(50,20),Z(50,20),ST(50,20),CO(50,20),
     1H(50,20),CG(50,20),S(50,20),HBREAK(50,20),TB(50,20),DDDX(50,20)
     2,DDDY(50,20),W(50,20),Y(50,20)
      COMMON/CON/G,PI,PI2,RAD,EPS,DX,DY,DX2,DY2,T,SIGMA,M,N,AM,DD
      COMMON/STRESS/SIGXX(50,20),SIGXY(50,20),SIGYY(50,20),TAUSX(50,20),
     1TAUSY(50,20),  TAUBX(50,20),TAUBY(50,20)
      COMMON /CONST/ RHO,KA(50,20)
      REAL KA
      COMMON/TIME/DT
      COMMON/COM/ETA(50,20),RKAPA,RKK,IN
      DIMENSION YZ(50,20)
C     READ BASIC DATA
      RHO=1000.
C-   RHO IS KILOGRAMS/METER CUBED
      RKAPA =.78
      RKK = .166
      G=9.80
      PI=3.1415927
      PI2=PI *2.0
      RAD=180.0/PI
C     M IS NUMBER OF GRID POINTS PERPENDICULAR TO THE SHORE
C     N IS THE NUMBER OF GRID POINTS PARALLEL TO THE SHORE
C   KSKIP DETERMINES THE FREQUENCY OF WRITTEN ITERATIONS.
C   IF INDEX = 0, PROGRAM CALCULATES ETA1, IF INDEX .NE. 0, READS IN
C IPUN = 0, WRITES OUT LAST ETA VALUE, IF IPUN .NE. 0 LAST ETAS ARE
C   PUNCHED OUT
C INDEX = 1 STARTS PROGRAM FROM STILL WATER
C   IN=0  FLOODING, IN = 1  NO FLOODING
C   MM = 1 ALLOWS ONLY WIND SETUP,MM=0 ALLOWS WAVE SETUP AND IF MM
C   IS SET =2, THE ENTIRE PROGRAM RUNS        AND WRITES
      READ (5,69) T,HO,A,AM
      READ (5,70)M,N,ITA,DX,DY,DT,KSKIP,INDEX,IN,NHIGHT
      READ(5,230) MM,WIND,WINANG,CF,DD
      IF(M.GT.50.OR.N.GT.20) GO TO 140
      WRITE (6,99)M,N,ITA
      WRITE(6,98) DX,DY,DT
      WRITE(6,71) T,HO,A,AM
      WRITE (6,231) WIND, WINANG
      WRITE(6,232) INDEX,IPUN,IN,MM,NHIGHT,DD
      WRITE(6,240) NHIGHT
      WRITE(6,233)CF,DD
      HEIGHT = HO
      IF(INDEX .EQ. 1) AHO = HO/FLOAT(NHIGHT)
      IF(INDEX .EQ. 1) HO = 0.0
      WINANG=WINANG/RAD
      N2=N+2
      DX2=DX*2.0
```

```
7300          DY2=DY*2.0
7400          SIGMA=PI2/T
7500          EPS=0.001
7800          DO 155 I=1,M-4
7900          DO 155 J = 1,N
8000          CALL DEPTH(I,J)
8200      155 CONTINUE
8210          DO 156 II=4,M
8215          DO 156 J=1,N+2
8220          I=M-II+4
8230      156 D(I,J)=D(I-3,J)
8240          DO 154 I=1,3
8250          DO 154 J=1,N+2
8260      154 D(I,J)=-FLOAT(4-I)*DX*AM
8300          DO 151 J=1,N+2
8400          D(M,J) = AM*DX*FLOAT(M-2)
8450          D(1,J)=3.0*D(1,J)
8600      151 CONTINUE
8601          DO 160 I=1,M
8602          D(I,1)=D(I,N)
8603          D(I,N+2)=D(I,3)
8604      160 D(I,N+1)=D(I,2)
8610          WRITE (6,108)
8615          WRITE(6,103)((D(I,J),J=1,N2),I=1,M)
8620 C        WRITE(9,103)((D(I,J),J=1,N2),I=1,M)
8621          LOCK 9
8622          IF(INDEX .EQ. 1) GO TO 3
8640          READ(3,225)((ETA(I,J),J=1,N2),(U(I,J),J=1,N2),(V(I,J),J=1,N
8641         1,J2),(Z(I,J),J=1,N2),(H(I,J),J=1,N2),(D(I,J),J=1,N2),I=1,M)
8650          DO 450 I=1,M
8651          DO 450 J=1,N2
8652          CO(I,J)=COS(Z(I,J))
8653      450 SI(I,J)=SIN(Z(I,J))
8675          WRITE (6,204)
8676          WRITE (6,103) ((U(I,J), J = 1,N2),I=1,M)
8775        4 WRITE (6,206)
8776          WRITE(6,103) ((ETA(I,J), J = 1,N2),I=1,M)
8778          WRITE (6,207)
8779          WRITE(6,103)((D(I,J),J=1,N2),I=1,M)
8800        3  DO 141 IT = 1,ITA
8801          IF(HO.GE.HEIGHT)HO=HEIGHT
8802          IF (HO .EQ. HEIGHT) GO TO 14
8804          IF(INDEX .EQ. 1) HO = HO + AHO
8810       14 K = AMOD(FLOAT(IT),FLOAT(KSKIP))
8820           IF(IPUN .EQ. 4) GO TO 13
8910          CALL DGRAD
9000          CALL REFRAC(A,HO,IT,INDEX,MM,NHIGHT)
9100       13 CALL TAUSW (WIND, WINANG, CF)
9150          CALL UCALC
9160          CALL ETAS
9165          IF(IT .EQ. 1) GO TO 2
9170          IF(K .NE. 0) GO TO 141
9181        2  WRITE (6,220)
9182           WRITE (6,221) IT,HO
9183           WRITE (6,222)
9184          SKIP=2.*FLOAT(KSKIP)
9185          KT=AMOD(FLOAT(IT),SKIP)
9186          IF(KT.NE.0)GO TO 1
9187          WRITE(7,236) IT
9188          WRITE(7,237)((W(I,J),J=1,N2),(Y(I,J),J=1,N2),(ETA(I,J),J=1,N2),
```

```
     1I=1,M)
    1 WRITE(6,223)
      WRITE(6,103)((H(I,J),J=1,N2),I=1,M)
      WRITE(8,225)((ETA(I,J),J=1,N2),(U(I,J),J=1,N2),(V(I
     1,J),J=1,N2),(Z(I,J),J=1,N2),(H(I,J),J=1,N2),(D(I,J),J=1,N2),I
     2=1,M)
      LOCK 8
      WRITE(6,224)
   12 WRITE(6,103)((TB(I,J),J=1,N2),I=1,M)
      DO 401 I=1,M
      DO 401 J=1,N2
  401 ZZ(I,J)=Z(I,J)*RAD
      WRITE(6,241)
      WRITE(6,103)((ZZ(I,J),J=1,N2),I=1,M)
      GO TO 5
   10 WRITE (6,200)
      WRITE(6,103) ((TAUBX(I,J),J = 1,N),I =1,M)
      WRITE (6,201)
      WRITE(6,103) ((TAUBY(I,J),J = 1,N),I =1,M)
      WRITE (6,202)
      WRITE(6,103) ((TAUSX(I,J),J = 1,N),I =1,M)
      WRITE (6,203)
      WRITE(6,103) ((TAUSY(I,J),J = 1,N),I =1,M)
    5 WRITE (6,204)
      WRITE (6,103) ((U(I,J), J = 1,N2),I=1,M)
   11 WRITE (6,205)
      WRITE (6,103) ((V(I,J), J = 1,N2),I=1,M)
      GO TO 6
      WRITE(6,208)
      WRITE(6,103)((SIGXX(I,J),J=1,N2),I=1,M)
      WRITE(6,209)
      WRITE(6,103)((SIGYY(I,J),J=1,N2),I=1,M)
      WRITE (6,210)
      WRITE(6,103)((SIGXY(I,J),J=1,N2),I=1,M)
    6 WRITE (6,206)
      WRITE(6,103) ((ETA(I,J), J = 1,N2),I=1,M)
    7 WRITE (6,207)
      WRITE(6,103)((D(I,J),J=1,N2),I=1,M)
      GO TO 141
  140 WRITE (6,242)
  141 CONTINUE
   69 FORMAT (4F10.5)
   70 FORMAT(3I5,3F10.5,4I5)
   71 FORMAT(1X,'WAVE PARAMETERS',/2X,'PERIOD =',F7.2,'  HEIGHT =',F7
     1.2,3X,7HANGLE =,F7.2,1X,7HDEGREES,4X,12HBEACH SLOPE=,F7.4)
   97 FORMAT (/' THE ORIGINAL MATRIX OF WATER DEPTH IN FEET'/)
   98 FORMAT (//,1X,'DX=',I5,3X,'DY=',I5,3X,3X,'DT=',F5.2)
   99 FORMAT (1X,'M=',I5,3X,'N=',I5,3X,'ITERATIONS =',I5)
  100 FORMAT(2I5)
  101 FORMAT(10X,7F10.1/(8F10.1))
  102 FORMAT (2I5,F6.2)
  103 FORMAT(1X,10F10.4)
  108 FORMAT (//' THE AUGMENTED MATRIX OF WATER DEPTH IN FEET'/)
  200 FORMAT ( 10X, 28HTAUBX - BOTTOM FRICTION GRID)
  201 FORMAT ( 10X, 28HTAUBY - BOTTOM FRICTION GRID)
  202 FORMAT (10X, 29HTAUSX - SURFACE FRICTION GRID)
  203 FORMAT (/,10X, 29HTAUSY - SURFACE FRICTION GRID)
  204 FORMAT ( 10X,12HX - VELOCITY)
  205 FORMAT ( 10X,12HY - VELOCITY)
  206 FORMAT (10X,10HETA VALUES)
```

```
  207 FORMAT (10X,12HDEPTH VALUES)
  208 FORMAT (/,10X,5HSIGYX)
  209 FORMAT(/,10X,'SIGYY')
  210 FORMAT (/,10X,5HSIGXY)
  220 FORMAT('1','**********************************',/)
  221 FORMAT(10X,'ITERATION NUMBER',I6,10X,'WAVE HEIGHT=',F10.5,/)
  222 FORMAT (1X,'**********************************',/)
  223 FORMAT (5X,'WAVE HEIGHTS',/)
  224 FORMAT (5X,'BREAKING INDEX',/)
  225 FORMAT (10F10.5)
  230 FORMAT (I5,4F10.5)
  231 FORMAT (1X,'WIND SPEED =',F7.3,'KNOTS',5X,'WIND ANGLE =',F7.
     13,'DEGREES')
  232 FORMAT(5X,'INDEX =',I5,3X,'IN ='I5,3X,'MM='
     1,I5)
  234 FORMAT(6F8.4,6F9.4,6I2)
  236 FORMAT(F10.5)
  237 FORMAT(10F10.5)
  238 FORMAT(10X,4HCF =,F10.5,5X,4HDD =,F10.5)
  240 FORMAT(10X,'WAVE HEIGHT BUILDS UP FIRST',I6,'ITERATIONS')
  241 FORMAT(2X,"WAVE ANGLE (DEGREES)")
  242 FORMAT(10X,"M OR N TO LARGE, CHANGE ALL DIMENTS")STON STATEMEN
      LOCK 7
      LOCK 3
      STOP
      END
C     *********************
      SUBROUTINE REFRAC(THETAO,HH,ITER,INDEX,MM,NHIGHT)
      COMMON D (50,20),U(50,20),V(50,20),Z(50,20),SI(50,20),CO(50,20),
     1H(50,20),CG(50,20),S(50,20),HBREAK(50,20),IB(50,20),DDMX(50,20)
     2,DDDY(50,20)
      COMMON/CON/G,PI,PI2,RAD,EPS,DX,DY,DX2,DY2,T,SIGMA,M,N,AM,DD
      N2=N+2
      IF(INDEX.NE.1)GO TO 600
      IF(INDEX.EQ.1.AND.ITER.GT.NHIGHT)GO TO 600
      THETA = THETAO
      THETA=THETA/RAD
      THETA=PI2-THETA
      CALL SNELL (THETA,HH,ITER)
  103 FORMAT(1X,10F10.4)
  600 DO 50 I = 1,M
      DO 50 J = 1,N2
      IF(ITER.GT.1) GO TO 51
      IF (INDEX .NE. 1) GO TO 51
      U(I,J)=0.0
      V(I,J)=0.0
   51 CONTINUE
      IF (J.EQ. 1) GO TO 48
      IF (D(I,J-1) .GT. DD) GO TO 50
   52 H(I,J) = 0.0
      Z(I,J)=PI
      SI(I,J)=0.0
      CO(I,J) = -1.0
      GO TO 50
   48 IF(D(I,N-1).LE. DD) GO TO 52
   50 CONTINUE
      IF (MM .NE. 2) GO TO 53
      CALL ANGLE(20)
   53 CALL HEIGHT(10)
      RETURN
```

```
      END
C         ********************
      SUBROUTINE DEPTH(I,J)
      COMMON D (50,20),U(50,20),V(50,20),Z(50,20),SI(50,50),CO(50,20),
     1H(50,20),CG(50,20),SS(50,20),HBREAK(50,20),IB(50,20),DDDX(50,20)
     2,DDDY(50,20)
      COMMON/CON/G,PI,PI2,RAD,EPS,DX,DY,DX2,DY2,T,SIGMA,M,N,AM,DD
      THIRD=1.0/3.0
      B=(20.0**THIRD)/3.0
      FLAMDA=70.0
      A=20.0
      ALPHA=30.0
      ALPHA=ALPHA/RAD
      X=DX*FLOAT(I-1)
      Y=DY*FLOAT(J-1)
      TALPHA=TAN(ALPHA)
      ARG=(Y-X*TALPHA)*PI/FLAMDA
      S=SIN(ARG)
      S9=S**9
      S10=S9*S
      ARGE=-X**THIRD/B
      FF=EXP(ARGE)
      CON=10.0*AM*A*PI*X/FLAMDA
      C=COS(ARG)
      D(I,J)=AM*X*(1.0+A*FF*S10)
      DDDY(I,J)=CON*FF*S9*C
      DDDX(I,J)=AM-DDDY(I,J)*TALPHA+AM*A*FF*S10*(1.0+ARGE/3.0)
      RETURN
      END
C         ********************
      SUBROUTINE GROUP(I,J,DCGDX,DCGDY,FE)
      COMMON D (50,20),W(50,20),Y(50,20),Z(50,20),SI(50,20),CO(50,20),
     1H(50,20),CG(50,20),S(50,20),HBREAK(50,20),IB(50,20),DDDX(50,20)
     2,DDDY(50,20),U(50,20),V(50,20)
      COMMON/CON/G,PI,PI2,RAD,EPS,DX,DY,DX2,DY2,T,SIGMA,M,N,AM
      COMMON /CONST/ RHO,KA(50,20)
      REAL KA
      DUDX(I,J)=(W(I+1,J)-W(I,J))/DX
      DUDY(I,J)=(U(I,J+1)-U(I,J-1))/DY2
      DVDX(I,J)=(V(I+1,J)-V(I-1,J))/DX2
      DVDY(I,J)=(Y(I,J+1)-Y(I,J))/DY
      DTDX(I,J)=(Z(I+1,J)-Z(I-1,J))/DX2
      DTDY(I,J)=(Z(I,J+1)-Z(I,J-1))/DY2
C     DUDX(I,J)=0.0
C     DVDY(I,J)=0.0
      E(I,J)=U(I,J)*COST+V(I,J)*SINI+0.5*A*(1.0+ARG2/SINH2)/RK
      DKDX(I,J)=RK*((U(I,J)*SINI-V(I,J)*COSI)*DTDX(I,J)-(COSI*DUDX(I,J)+
     1SINI*DVDX(I,J))-A*DDDX(I,J-1)/SINH2)/EE
      DKDY(I,J)=RK*((U(I,J)*SINI-V(I,J)*COSI)*DTDY(I,J) -(COSI*DUDY(I,J)
     1 +SINI*DVDY(I,J))-A*DDDY(I,J-1)/SINH2)/EE
      JJ=J-1
      DEP=D(I,JJ)
      COSI=CO(I,J)
      SINI=SI(I,J)
      DCGDX=0.0
      DCGDY=0.0
      FF=0.0
C   CHECK FOR DRY LAND
      IF(DEP.LE.DD) RETURN
      CALL WVNUM(DEP,COSI,SINI,U(I,J),V(I,J),RK,A)
```

```
      *?(I,J) = RK
      TA=TANH(RK*DEP)
      HBREAK(I,J)=0.12*PI2*TA/RK
      COSH1=COSH(RK*DEP)
      SECHSQ=1.0/(COSH1**2)
      ARG2=2.0*RK*DEP
      SINH2=SINH(ARG2)
      COSH2=COSH(ARG2)
      SINHSQ=SINH2**2
      FE=F(I,J)
      C=SQRT(G*TA/RK)
      FF=0.5*(1.0+ARG2/SINH2)
      CG(I,J)=FF*C
      P=C*(SINH2-ARG2*COSH2)/SINHSQ
      DKDDX=RK*DDDX(I,JJ)+DEP*DKDX(I,J)
      DKDDY=RK*DDDY(I,JJ)+DEP*DKDY(I,J)
      Q=0.5*G/(C*RK**2)
      DCDX=Q*(RK*SECHSQ*DKDDX-TA*DKDX(I,J))
      DCDY=Q*(RK*SECHSQ*DKDDY-TA*DKDY(I,J))
      DCGDX=P*DKDDX+FF*DCDX
      DCGDY=P*DKDDY+FF*DCDY
      RETURN
      END
C      ********************
      SUBROUTINE NEWHT(I,J,IFLAG)
      COMMON D (50,20),W(50,20),Y(50,20),Z(50,20),SI(50,20),CO(50,20),
     1H(50,20),CG(50,20),S(50,20),HBREAK(50,20),IB(50,20),DDDX(50,20)
     2,DDDY(50,20),U(50,20),V(50,20)
      COMMON/CON/G,PI,PI2,RAD,EPS,DX,DY,DX2,DY2,T,SIGMA,M,N,AM,DD
      IB(I,J)=1
      N1=N+1
      N2=N+2
      CC1=(V(I,J)+CG(I,J)*SI(I,J))/DY
      CC2=(U(I,J)+CG(I,J)*CO(I,J))/DX
      HNEW= (CC1*H(I,J-1)-CC2*H(I+1,J))/(CC1-CC2-S(I,J)/2.0)
      IF (HNEW .LT. 0.0) GO TO 810
      IF(HNEW.LE.HBREAK(I,J)) GO TO 850
  810 HNEW=HBREAK(I,J)
      IB(I,J)=0
  850 CONTINUE
      IF(ABS(HNEW-H(I,J)).GT.(EPS*ABS(HNEW))) IFLAG=0
      H(I,J)=HNEW
      IF(J.NE.2) GO TO 800
      H(I,N1)=H(I,J)
      IB(I,N1)=IB(I,J)
      GO TO 899
  800 IF(J.NE.3) GO TO 801
      H(I,N2)=H(I,J)
      IB(I,N2)=IB(I,J)
  801 IF(J.NE.N) GO TO 802
      H(I,1)=H(I,J)
      IB(I,1)=IB(I,J)
      GO TO 899
  802 IF(J.NE.N1) GO TO 899 .
      H(I,2)=H(I,J)
      IB(I,2)=IB(I,J)
  899 RETURN
      END
C      ********************
      SUBROUTINE HEIGHT(ITMAX)
```

```
      COMMON U (50,20),W(50,20),Y(50,20),Z(50,20),SI(50,20),CO(50,20),
     1H(50,20),CG(50,20),S(50,20),HBREAK(50,20),TB(50,20),DDDX(50,20)
     2,DDDY(50,20),U(50,20),V(50,20)
      COMMON/CON/G,PI,PI2,RAD,EPS,DX,DY,DX2,DY2,T,SIGMA,M,N,AM,DD
      COMMON/STRESS/SIGX (50,20),SIGXY(50,20),SIGY (50,20),TAUSX(50,20),
     1TAUSY(50,20),   TAUBX(50,20),TAUBY(50,20)
      M1=M-1
      N1=N+1
      N2=N+2
      M2=M-2
C     COMPUTE VALUES OF S(I,J)
      DO 500 I=2,M1
      DO 500 J=2,N1
      IF(D(I,J-1).LE.DD) GO TO 500
      CALL GROUP(I,J,DCGDX,DCGDY,FF)
      DUDX=(W(I+1,J)-W(I,J))/DX
      DUDY=(U(I,J+1)-U(I,J-1))/DY2
      DVDX=(V(I+1,J)-V(I-1,J))/DX2
      DVDY=(Y(I,J+1)-Y(I,J))/DY
C     DUDY=0.0
C     DVDY=0.0
      DTDX=(Z(I+1,J)-Z(I-1,J))/DX2
      DTDY=(Z(I,J+1)-Z(I,J-1))/DY2
  501 SS2=SI(I,J)**2
      CC2=CO(I,J)**2
      SIGXX=(2.0*FF-0.5)*CC2+(FF-0.5)*SS2
      SIGYY=(2.0*FF-0.5)*SS2+(FF-0.5)*CC2
      SIGX(I,J) = SIGXX
      SIGY(I,J) = SIGYY
      TAUXY=FF*SI(I,J)*CO(I,J)
      SIGXY(I,J)=TAUXY
      S(I,J)=CG(I,J)*(SI(I,J)*DTDX-CO(I,J)*DTDY)-(DUDX+DVDY)-(CO(I,J)*DC
     1GDX+SI(I,J)*DCGDY)-(SIGXX*DUDX+TAUXY*DUDY+TAUXY*DVDX+SIGYY*DVDY)
  500 CONTINUE
      DO 510 II=1,M2
      I=M-II
      DO 580 IT=1,ITMAX
      IFLAG=1
      DO 520 J=2,N1
      IF(D(I,J-1) .LE. DD) GO TO 520
      CALL NEWHT(I,J,IFLAG)
  520 CONTINUE
      IF(IFLAG.EQ.1) GO TO 570
  580 CONTINUE
      WRITE(6,540) I,IT
  540 FORMAT(' RELAXATION FOR THE WAVE HEIGHT FAILED TO CONVERGE',
     1'ON ROW',I5,'AFTER',I6,'ITERATIONS')
      WRITE(6,541)(H(I,J),J=1,N2    )
  541 FORMAT('  LAST VALUES OF H ARE'/,10F13.5)
      RETURN
  570 CONTINUE
      GO TO 510
      WRITE(6,542) I,IT
  542 FORMAT(10X,' RELAXATION FOR WAVE HEIGHT CONVERGED ON ROW',I6,3X,'A
     1FTER',I6,'ITERATIONS')
  510 CONTINUE
      RETURN
      END
C       ********************
      SUBROUTINE ANGLE(ITMAX)
```

```
      COMMON D (50,20),W(50,20),Y(50,20),Z(50,20),SI(50,20),CO(50,20),
     1H(50,20),CG(50,20),S(50,20),HBREAK(50,20),IB(50,20),DDDX(50,20)
     2,DDDY(50,20),U(50,20),V(50,20)
      COMMON/CON/G,PI,PI2,RAD,EPS,DX,DY,DX2,DY2,T,SIGMA,M,N,AM,DD
      N1=N+1
      N2=N+2
      M1=M-1
      M2=M-2
      DO 200 IT=1,ITMAX
      IFLAG=1
      DO 210 II=1,M2
      I=M-II
      DO 210 J=2,N1
      IF(D(I,J-1).LE.DD.OR.D(I-1,J-1).LE.DD)GOTO210
      CALL NEWANG(I,J,IFLAG)
  210 CONTINUE
      IF(IFLAG.EQ.1) GO TO 250
  200 CONTINUE
      WRITE(6,220) ITMAX
  220 FORMAT(' RELAXATION FOR THETA FAILED AFTER',I6,3X,'ITERATIONS')
      WRITE(6,221)((Z(I,J),J=1,N2),I=1,M)
  221 FORMAT(10F9.3)
      STOP
C 250 WRITE(6,251) IT,EPS
  250 CONTINUE
  251 FORMAT(1H1,//,10X,'SOLUTION FOR THETA OBTAINED AFTER,'I6,' ITERAT
     1IONS WITH A MAXIMUM RELATIVE ERROR OF',3X,F10.5)
C     WRITE(6,252)((Z(I,J),J=1,N2),I=1,M)
  252 FORMAT(10F10.5)
          RETURN
      END
C        ********************
      SUBROUTINE NEWANG(I,J,IFLAG)
      COMMON D (50,20),W(50,20),Y(50,20),Z(50,20),SI(50,20),CO(50,20),
     1H(50,20),CG(50,20),S(50,20),HBREAK(50,20),IB(50,20),DDDX(50,20)
     2,DDDY(50,20),U(50,20),V(50,20)
      COMMON/CON/G,PI,PI2,RAD,EPS,DX,DY,DX2,DY2,T,SIGMA,M,N,AM,DD
      COMMON/STRESS/SIGXX(50,20),SIGXY(50,20),SIGYY(50,20),TAUSX(50,20),
     1TAUSY(50,20),   TAUBX(50,20),TAUBY(50,20)
C STATEMENT FUNCTIONS
      C(I,J)=0.25*(CO(I+1,J)+CO(I-1,J)+CO(I,J+1)+CO(I,J-1))+0.125*((Z(I
     1+1,J)-Z(I-1,J))*(SI(I+1,J)-SI(I-1,J))+ (Z(I,J+1)-Z(I,J-1))*(SI(I,
     2J+1)-SI(I,J-1)))
      SS(I,J)=0.25*(SI(I+1,J)+SI(I-1,J)+SI(I,J+1)+SI(I,J-1))+0.125*((Z(I
     1+1,J)-Z(I-1,J))*(CO(I-1,J)-CO(I+1,J)) + (Z(I,J+1)-Z(I,J-1))*(CO(I,
     2J-1)-CO(I,J+1)))
      DUDX(I,J)=(W(I+1,J)-W(I,J))/DX
      DUDY(I,J)=(U(I,J+1)-U(I,J-1))/DY2
      DVDX(I,J)=(V(I+1,J)-V(I-1,J))/DX2
      DVDY(I,J)=(Y(I,J+1)-Y(I,J))/DY
C     DUDX(I,J)=0.0
C     DVDY(I,J)=0.0
      F(I,J)=U(I,J)*COST+V(I,J)*SINI + 0.5*A*(1.0 + ARG2/SINH2)/RK
      DKDY(I,J)=(-(COSI*DUDY(I,J) + SINI*DVDY(I,J))-A*DDDY(I,J-1)/SINH2)
     1/FF
      DKDX(I,J)=(-(COSI*DUDX(I,J)+SINI*DVDX(I,J))-A*DDDX(I,J-1)/SINH2)/F
     1F
      FAC(I,J)=U(I,J)*SINI-V(I,J)*COSI
      COSI=C(I,J)
      SINI=SS(I,J)
```

```
      JJ=J
      JJ=J-1
      CALL WVNUM(D(I,JJ),COSI,SINI,U(I,J),V(I,J),RK,A)
      ARG2=2.0*RK*D(I,JJ)
      SINH2=SINH(ARG2)
      FF=F(I,J)
      IF(FF.GT.0.0) GO TO 450
      WRITE(6,451) I,J,D(I,JJ),COSI,SINI,U(I,J),V(I,J),RK,A
  451 FORMAT(10X'FF IS NEGATIVE--OUTPUT I,J,D,COSI,SINI,U,V,RK,A'/,
     12I5,7E13.4)
      RETURN
  450 FACI=FAC(I,J)
      DEN1=(SINI-COSI*FACI/FF)/DY
      DEN2=(COSI+SINI*FACI/FF)/DX
      DEN=DEN1-DEN2
      ZNEW=(COSI*DKDY(I,J)-SINI*DKDX(I,J)+Z(I,J-1)*DEN1-Z(I+1,J)*DEN2)/D
     1EN
      IF(ABS(ZNEW-Z(I,J)).GT.(EPS*ABS(ZNEW))) IFLAG=0
      Z(I,J)=ZNEW
      Z(I,J) = Z(I,J) + 0.7*(ZNEW-Z(I,J))
      CO(I,J)=COS(Z(I,J))
      SI(I,J)=SIN(Z(I,J))
      IF(J.NE.2) GO TO 400
      N1=N+1
      Z(I,N1)=Z(I,2)
      CO(I,N1)=CO(I,J)
      SI(I,N1)=SI(I,J)
      GO TO 499
  400 IF(J.NE.3) GO TO 401
      N2=N+2
      Z(I,N2)=Z(I,J)
      CO(I,N2)=CO(I,J)
      SI(I,N2)=SI(I,J)
      GO TO 499
  401 IF(J.NE.N) GO TO 402
      Z(I,1)=Z(I,N)
      CO(I,1)=CO(I,N)
      SI(I,1)=SI(I,N)
      GO TO 499
  402 N1=N+1
      IF(J.NE.N1) GO TO 499
      Z(I,2)=Z(I,J)
      CO(I,2)=CO(I,J)
      SI(I,2)=SI(I,J)
  499 RETURN
      END
C              *********************
      SUBROUTINE WVNUM(D,COSI,SINI,U,V,RK,A)
C SUBROUTINE COMPUTES THE WAVE NUMBER INCLUDING WAVE-CURRENT INTERATION
      COMMON/CON/G,PI,PI2,RAD,EPS,DX,DY,DX2,DY2,T,SIGMA,M,N,AM,DD
      EPSK=0.001
      RK=PI2/(T*SQRT(G*D))
      DO 100 I=1,50
      A=SIGMA-U*RK*COSI-V*RK*SINI
      A2=A**2
      ARG=RK*D
      F1=EXP(ARG)
      F2=1.0/F1
      SECH=2.0/(F1+F2)
      SECH2=SECH*SECH
```

```
      TT=TANH (ARG)
      FK=G*RK*TT-A2
      FFK=G*(ARG*SECH2+TT)+2.0*(U*COSI+V*SINI)*A
      RKNEW=RK-FK/FFK
      IF(ABS(RKNEW-RK).LE.(ABS(EPSK*RKNEW))) GO TO 110
      RK=RKNEW
  100 CONTINUE
      WRITE(6,101) I,RK,T,D,U,V
  101 FORMAT('  ITERATION FOR K FAILED TO CONVERGE AFTER',I6,3X,5F10.4)
      CALL EXIT
      RETURN
  110 RK=RKNEW
      A=SIGMA-U*RK*COSI-V*RK*SINI
      IF(RK.GT.0.0) GO TO 120
            WRITE(6,130) D,COSI,SINI,U,V,RK,A
  130 FORMAT(10X,'RK IS NEGATIVE--OUTPUT D,COSI,SINI,U,V,RK,A'/,7E12.4)
      CALL EXIT
  120 RETURN
      END
C
C
         ********************
      SUBROUTINE SNELL (THETA0,HH,ITER)
      COMMON D (50,20),U(50,20),V(50,20),Z(50,20),SI(50,20),CO(50,20),
     1H(50,20),CG(50,20),S(50,20),HBREAK(50,20),IB(50,20),DDDX(50,20)
     2,DDDY(50,20)
      COMMON/CON/G,PI,PI2,RAD,EPS,DX,DY,DX2,DY2,T,SIGMA,M,N,AM,DD
      DO 600 J = 2,N+1
      IF(ITER .GT. 1) GO TO 10
      DO 600 II = 1,M
      I = M-II+1
      GO TO 20
   10 I=M
   20 IF (D(I,J-1) .GT. DD)  GO TO 33
      ANG = PI
      WVHT = 0.0
      SS = 0.0
      CC = -1.0
      GO TO 43
   33 CONTINUE
      CALL WVNUM(D(I,J-1),0.0,0.0,0.0,0.0,RK,A)
      AA = RK* D(I,J-1)
      ANG = ARSIN(SIN(THETA0)*TANH(AA))
      ANG = PI-ANG
      ARG = 2.0*AA
      SHOAL = SQRT(1.0/(TANH(AA)*(1.0+ARG/SINH(ARG))))
      REF = SQRT(COS(THETA0)/COS(ANG))
      WVHT = HH*SHOAL*REF
      HB = 0.12*TANH(AA)*PI2/RK
      IF(WVHT .GT. HB) WVHT = HB
      IN = 1
      IF(WVHT .GT. HB) IN = 0
      SS = SIN(ANG)
      CC = COS(ANG)
   43 CONTINUE
      H(I,J) = WVHT
      IB(I,J) = IN
      Z(I,J) = ANG
      SI(I,J) = SS
      CO(I,J) = CC
  600 CONTINUE
```

```
      L = 1
      K = N
      J = 1
   45 DO 60 I = 1,M
      H(I,J) = H(I,K)
      IB (I,J) = IB(I,K)
      Z(I,J)=Z(I,K)
      SI(I,J) = SI(I,K)
   60 CO(I,J) = CO(I,K)
      L = L+1
      IF (L .GT. 3) RETURN
      IF (L .EQ. 3)  GO TO 610
      L = 2
      J = 2
      K = N+ 1
      GO TO 45
  610 J = N+ 2
      K = 3
      GO TO 45
      RETURN
      END
C
C         ********************
      SUBROUTINE TAUSB (WIND, WINANG, CF)
C WIND SPEED MUST BE IN KNOTS
C THIS SUBROUTINE CALCULATES SHEAR STRESS AT THE SURFACE  VAN DORN'S
C METHOD AND AVERAGE BOTTOM STRESS.
      COMMON D (50,20),W(50,20),Y(50,20),Z(50,20),SI(50,20),CO(50,20),
     1H(50,20),CG(50,20),S(50,20),HBREAK(50,20),IB(50,20),DDDX(50,20)
     2,DDDY(50,20),U(50,20),V(50,20)
      COMMON/STRESS/SIGXX(50,20),SIGXY(50,20),SIGYY(50,20),TAUSX(50,20),
     1TAUSY(50,20),  TAUBX(50,20),TAUBY(50,20)
      COMMON/CON/G,PI,PI2,RAD,EPS,DX,DY,DX2,DY2,T,SIGMA,M,N,AM,DD
      REAL KA
      COMMON /CONST/ RHO,KA(50,20)
      COMMON/TIME/DT
      VANCON=1.1E-06
      IF (WIND .GE.14.) VANCON = 1.1E-06+2.5E-06*((1.-14./WIND)**2.)
      IF(G .GE. 980..AND. G.LE. 1000.0) CON2 = 51.4
      IF(G .GE. 9.8 .AND. G .LE. 10.0) CON2 = .514
      IF(G .GE. 32.0.AND. G .LE. 32.2) CON2 = 1.689
      WIN = WIND*CON2
      WINDX = WIN*COS(WINANG)
      WINDY = WIN*SIN(WINANG)
C   NOTE: WINANG IS MEASURED CLOCKWISE FROM THE NEGATIVE X DIRECTION
      CON1   = RHO*VANCON*ABS(WIN)
      DO 20 J = 1,N+2
      DO 20 I = 2, M
      TAUSX(I,J) =- CON1 *WINDX
      TAUSY(I,J) = CON1 *WINDY
   20 CONTINUE
C PROGRAM NOW CALCULATES BOTTOM FRICTION
      DO 40 J = 2,N+1
      K = J-1
      DO 40 I = 2,M
      IF(KA(I,J)*D(I,K) .LE. DD) GO TO 40
      TAUBX(I,J) = (4.*CF*RHO*H(I,J)*U(I,J))/(T*SINH(KA(I,J)*D(I,K)))
      TAUBY(I,J) = (2.*CF*RHO*H(I,J)*V(I,J))/(T*SINH(KA(I,J)*D(I,K)))
C     TAUBX(I,J) = (4.*CF*RHO*H(I,J)*W(I,J))/(T*SINH(KA(I,J)*D(I,K)))
C     TAUBY(I,J) = (2.*CF*RHO*H(I,J)*Y(I,J))/(T*SINH(KA(I,J)*D(I,K)))
```

```
   40 CONTINUE
      DO 100 I = 1,M
      TAUBX(I,1) = TAUBY(I,N)
      TAUBX(I,N+1) = TAUBX( I,2)
      TAUBX(I,N+2) = TAUBX(I,3)
      TAUBY(I,1) = TAUBY(I,N)
      TAUBY(I,N+1) = TAUBY( I,2)
      TAUBY(I,N+2) = TAUBY(I,3)
  100 CONTINUE
      RETURN
      END
C
C        ********************
      SUBROUTINE UCALC
      COMMON D (50,20),U(50,20),V(50,20),Z(50,20),SI(50,20),CD(50,20),
     1H(50,20),CG(50,20),S(50,20),HBREAK(50,20),TB(50,20),DDDX(50,20)
     2,DDDY(50,20),W(50,20),Y(50,20)
      COMMON/CON/G,PT,PI2,RAD,EPS,DX,DY,DX2,DY2,T,SIGMA,M,N,AM,DD
      COMMON/STRESS/SIGXX(50,20),SIGXY(50,20),SIGYY(50,20),TAUSX(50,20),
     1TAUSY(50,20),   TAUBX(50,20),TAUBY(50,20)
      REAL KA
      COMMON /CONST/ RHO,KA(50,20)
      COMMON/COM/ETA(50,20),RKAPA,RKK,IN
      COMMON/TIME/DT
C  COMPUTE HORIZONTAL MEAN VELOCITIES
      DO 50 I = 1,M-1
      DO 20 J = 2,N+1
      E = 0.125*RHO*G*(H(I,J)**2.)
      SIGXX(I,J) = E*SIGXX(I,J)
      SIGYY(I,J) = E*SIGYY(I,J)
      SIGXY(I,J) = E*SIGXY(I,J)
   20 CONTINUE
      SIGXX(I,1) = SIGXX(I,N)
      SIGYY(I,1) = SIGYY(I,N)
      SIGXY(I,1) = SIGXY(I,N)
      SIGXX(I,2) = SIGXX(I,N+1)
      SIGYY(I,2) = SIGYY(I,N+1)
      SIGXY(I,2) = SIGXY(I,N+1)
      SIGXX(I,N+2) = SIGXX(I,3)
      SIGXY(I,N+2) = SIGXY(I,3)
   50 SIGYY(I,N+2) = SIGYY(I,3)
      DO 59 J=1,N+2
   59 SIGXY(M,J)=2.0*SIGXY(M-1,J)-SIGXY(M-2,J)
      DO 21 J = 3,N+1
      K = J-1
      DO 21 I=2,M-1


      IF (D(I,J-1) .LE. DD) GO TO 21
      DBAR = (D(I,K)+D(I-1,K))/2.
      U(I,J) = U(I,J) +DT*((ETA(I-1,J) - ETA(I,J))*G/DX+(SIGXX(I-1,J)-SI
     1GXX(I,J))/(DX*RHO*DBAR )  - (SIGXY(I,J+1)-SIGXY(I,J-1)+SIGXY(I-1,J
     2+1)-SIGXY(I-1,J-1))/(4.*DY*RHO*DBAR)+(TAUSX(I,J)+TAUSX(I-1,J))/(2.
     3*RHO*DBAR)-(TAUBX(I,J)+TAUBX(I-1,J))/(2.*RHO*DBAR))
   56 IF(D(I-1,J-1) .LE. DD) U(I,J) = 0.0
      DBAR = (D(I,K) + D(I,K-1))/2.0
      IF(D(I-1,K).LE.DD.AND.DBAR.LT.0.01) GO TO 23
      V(I,J)=V(I,J) +DT*((ETA(I,J-1)-ETA(I,J))*G/DY-(SIGXY(I+1,J-1)-SIGX
     1Y(I-1,J-1))/(4.*DX*RHO*DBAR)-(SIGXY(I+1,J)-SIGXY(I-1,J))/(4.*DX*RH
     2O*DBAR)+(SIGYY(I,J-1) - SIGYY(I,J))/(DY*RHO*DBAR)+(TAUSY(I,J) + TA
```

```
     3USY(I,J-1))/(2.*RHO*DBAR) - (TAUBY(I,J) + TAUBY(I,J-1))/(2.*RHO*DB
     4AR))
      GO TO 21
C  AT THE SHORE BOUNDRY, A BACKWARDS DIFFERENCE
C   IS USED IN THE CALCULATION OF THE CHANGE IN
C   SXY SINCE THE GRID SIZE IS RELATIVELY COARSE
C   IN THE SURF ZONE AND THE DECAY OF SXY IS UNKNOWN.
   23 V(I,J)=V(I,J) +DT*((ETA(I,J-1)-ETA(I,J))*G/DY-(SIGXY(I,J-1)-SIGX
     1Y(I-1,J-1))/(2.*DX*RHO*DBAR)-(SIGXY(I,J)-SIGXY(I-1,J))/(2.*DX*RH
     2O*DBAR)+(SIGYY(I,J-1) - SIGYY(I,J))/(DY*RHO*DBAR)+(TAUSY(I,J) + TA
     3USY(I,J-1))/(2.*RHO*DBAR) - (TAUBY(I,J) + TAUBY(I,J-1))/(2.*RHO*DB
     4AR))
   21 CONTINUE
      DO 60 I=1,M
      V(I,N+2) = V(I,3)
       U(I,N+2) = U(I,3)
      V(I,2) = V(I,N+1)
       U(I,2) = U(I,N+1)
      V(I,1) = V(I,N)
   60 U(I,1) = U(I,N)
      DO 69 I=1,M-1
      DO 69 J=2,N+1
      U(M,J)=0.0
      W(I,J)=(U(I,J)+U(I+1,J))/2.0
      Y(I,J)=(V(I,J)+V(I,J+1))/2.0
C     W(I,J)=0.0
C     Y(I,J)=0.0
   69 CONTINUE
      DO 79 I=1,M
      Y(I,N+2)=Y(I,3)
      W(I,N+2)=W(I,3)
      Y(I,1)=Y(I,N)
   79 W(I,1)=W(I,N)
      DO 80 J=1,N+2
   80 Y(M,J)=(V(M,J)+V(M,J+1))/2.0
C  80 Y(M,J)=0.0
      RETURN
      END
C
C        *********************
      SUBROUTINE ETAS
      COMMON D (50,20),U(50,20),V(50,20),Z(50,20),SI(50,20),CO(50,20),
     1H(50,20),CG(50,20),S(50,20),HBREAK(50,20),IB(50,20),DDDX(50,20)
     2,DDDY(50,20)
      COMMON/CON/G,PI,PI2,RAD,EPS,DX,DY,DX2,DY2,T,SIGMA,M,N,AM,DD
      COMMON/TIME/DT
      COMMON/COM/ETA(50,20),RKAPA,RKK,IN
      DIMENSION DFLD(50,20)
      DO 20 J = 2,N+1
      K = J-1
   16 DO 17 I = 1,M
      IF (D(I,K) .GT. DD) GO TO 18
   17 CONTINUE
   18 IL1 = I
      IL = IL1-1
C  IL DENOTES THE I VALUE OF THE LAST DRY GRID POINT
   19 DO 20 I=IL1,M-1
      ETAOLD = ETA(I,J)
      ETA(I,J) = 0.0
C     IF (D(I,J-1) .LT. DD) GO TO 90
```

```
      IF(K .EQ. 1) GO TO 21
      ETA(I,J)=ETAOLD+DT*(U(I,J)*(D(I,K)+D(I-1,K))/(2.*DX)      - U(I+1,J)
     1*(D(I,K)+D(I+1,K))/(2.*DX)+V(I,J)*(D(I,K-1)+D(I,K))/(2.*DY) - V(I,
     2J+1)*(D(I,K+1)+D(I,K))/(2.*DY))
      GO TO 22
   21 ETA(I,J)=ETAOLD+DT*(U(I,J)*(D(I,K)+D(I-1,K))/(2.*DX)      - U(I+1,J)
     1*(D(I,K)+D(I+1,K))/(2.*DX)-V(I,J+1)*(D(I,K+1)+D(I,K))/(2.*DY))
   22 D(I,K) = D(I,K) - ETAOLD + ETA(I,J)
C  CHECK FOR FLOODING
      IF (IN .EQ. 1) GO TO 50
      IFLAG=1
      DO 400 J=2,N+1
      K=J-1
      IF(ETA(IL1,K)+D(IL,K).LE.ABS(.01+0.3*D(IL,K)))IFLAG=0
  400 CONTINUE
      IF(IFLAG.EQ.0) GO TO 50
      DO 50  J=2,N+1
      K=J-1
      FLOOD = ETA(IL1,J) + D (IL,K)
      IF (FLOOD .LE. 0.0) GO TO 25
      DFLOOD = FLOOD/10.0
      DFLD(IL,K) = DFLOOD
      ETA(IL,J) = -D(IL,K) + DFLOOD
      D(IL,K) = DFLOOD
      ETA(IL1,J) = ETA(IL1,J) - DFLOOD
      D(IL1,K) = D(IL1,K)-DFLOOD
C  CHECK FOR DRYING
   25 FLOOD = D(IL1,K) - DFLD(IL1,K)
   26 IF(FLOOD .GE. 0.0) GO TO 50
      D(IL+2,K) = D(IL+2,K) + D(IL1,K)
      ETA(IL+2,J) = ETA(IL+2,J) + D(IL1,K)
      D(IL1,K) = -ETA(IL1,J) + D(IL1,K)
      ETA(IL1,J) = 0.0
   50 CONTINUE
      DO 60 I = 1,M
      D(I,N+2) = D(I,3)
       D(I,N+1) = D(I,2)
      D(I,1) = D(I,N)
      ETA(I,N+2) = ETA(I,3)
      ETA(I,2) = ETA(I,N+1)
   60 ETA(I,1) = ETA(I,N)
      RETURN
      GO TO 26
      END
C     ***************
      SUBROUTINE DGRAD
      COMMON D (50,20),U(50,20),V(50,20),Z(50,20),SI(50,20),CO(50,20),
     1H(50,20),CG(50,20),S(50,20),HBREAK(50,20),IB(50,20),DDDX(50,20)
     2,DDDY(50,20)
      COMMON/CON/G,PI,PI2,RAD,EPS,DX,DY,DX2,DY2,T,SIGMA,M,N,AM,DD
      DO 60 I = 2,M-1
      DO 60 J = 2,N+1
      DDDX(I,J) =-(D(I-1,J)-D(I+1,J))/(2.*DX)
      DDDY(I,J) =-(D(I,J-1)-D(I,J+1))/(2.*DY)
   60  CONTINUE
      DO 70 I = 1,M
      DDDX(I,1) = DDDX(I,N)
      DDDY(I,1) = DDDY(I,N)
      DDDX(I,N+2) = DDDY(I,3)
      DDDY(I,N+2) = DDDY(I,3)
```

```
66900      70 CONTINUE
67000         RETURN
67100         END
```

Security Classification

DOCUMENT CONTROL DATA - R & D

(Security classification of title, body of abstract and indexing annotation must be entered when the overall report is classified)

1. ORIGINATING ACTIVITY (Corporate author) Department of Civil Engineering University of Delaware Newark, DE 19711	2a. REPORT SECURITY CLASSIFICATION Unclassified 2b. GROUP Unclassified

3. REPORT TITLE

Numerical Models for the Predictions of Wave Set-Ups and Nearshore Circulation

4. DESCRIPTIVE NOTES (Type of report and inclusive dates)

Technical Report

5. AUTHOR(S) (First name, middle initial, last name)

William A. Birkemeier and Robert A. Dalrymple

6. REPORT DATE	7a. TOTAL NO. OF PAGES	7b. NO. OF REFS
January, 1976	127	35

8a. CONTRACT OR GRANT NO. N0014-76-C-0342 b. PROJECT NO.	9a. ORIGINATOR'S REPORT NUMBER(S) Technical Report No. 1
c. d.	9b. OTHER REPORT NO(S) (Any other numbers that may be assigned this report) Ocean Engineering Report No. 3

10. DISTRIBUTION STATEMENT

Distribution of this document is unlimited

11. SUPPLEMENTARY NOTES	12. SPONSORING MILITARY ACTIVITY
	Geography Branch Office of Naval Research Arlington, VA 22217

13. ABSTRACT

A finite difference model for predicting time-dependent, wave-induced nearshore circulation is discussed. The formulation includes wave refraction, wave-current interaction, an anistropic bottom friction, wave set-up, wind effects and coastal flooding. Results are shown for three cases including: set-up in a wave channel due to steady waves and wave groups, circulation in a rectangular wave tank under oblique wave attack, and for wave and wind induced circulation on a longshore periodic beach. Important results are that tuned wave groups can incite seiching in an enclosed basin and harbors and that rip currents will be induced or maintained by the presence of surf zone channels.

DD FORM 1 NOV 65 1473 (PAGE 1)

S/N 0101-807-6811

Unclassified

Security Classification

A-31408

Unclassified

Security Classification

14. KEY WORDS	LINK A		LINK B		LINK C	
	ROLE	WT	ROLE	WT	ROLE	WT
Nearshore Circulation Wave Set-Up Rip Currents						

DD FORM 1 NOV 65 1473 (BACK)

S/N 0101-807-6821

Unclassified

Security Classification

A-31409